HETEROGENEOUS SHALLOW-SHELF CARBONATE BUILDUPS IN THE PARADOX BASIN, UTAH AND COLORADO: TARGETS FOR INCREASED OIL PRODUCTION AND RESERVES USING HORIZONTAL DRILLING TECHNIQUES

(Contract No. DE-2600BC15128)

DELIVERABLE 1.2.5
THIN SECTION EPIFLUORESCENCE: CHEROKEE AND BUG FIELDS, SAN JUAN COUNTY, UTAH

Submitted by

Utah Geological Survey
Salt Lake City, Utah 84114
April 2005

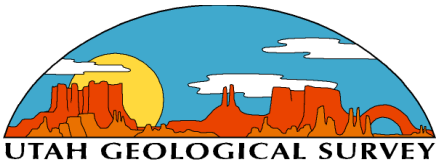

Contracting Officer's Representative

Virginia Weyland, Contract Manager
U.S. Department of Energy
National Petroleum Technology Office
1 West 3rd Street
Tulsa, OK 74103-3532

DISCLAIMER

This report was prepared as an account of work sponsored by an agency of the United States Government. Neither the United States Government nor any agency thereof, nor any of their employees, makes any warranty, express or implied, or assumes any legal liability or responsibility for the accuracy, completeness, or usefulness of any information, apparatus, product, or process disclosed, or represents that its use would not infringe privately owned rights. Reference herein to any specific commercial product, process, or service by trade name, trademark, manufacturer, or otherwise does not necessarily constitute or imply its endorsement, recommendation, or favoring by the United States Government or any agency thereof. The views and opinions of authors expressed herein do not necessarily state or reflect those of the United States Government or any agency thereof.

Although this product represents the work of professional scientists, the Utah Department of Natural Resources, Utah Geological Survey, makes no warranty, express or implied, regarding its suitability for a particular use. The Utah Department of Natural Resources, Utah Geological Survey, shall not be liable under any circumstances for any direct, indirect, special, incidental, or consequential damages with respect to claims by users of this product.

HETEROGENEOUS SHALLOW-SHELF CARBONATE BUILDUPS IN THE PARADOX BASIN, UTAH AND COLORADO: TARGETS FOR INCREASED OIL PRODUCTION AND RESERVES USING HORIZONTAL DRILLING TECHNIQUES

(Contract No. DE-2600BC15128)

DELIVERABLE 1.2.5
THIN SECTION EPIFLUORESCENCE: CHEROKEE AND BUG FIELDS, SAN JUAN COUNTY, UTAH

Submitted by

Utah Geological Survey
Salt Lake City, Utah 84114
April 2005

by

David E. Eby, Eby Petrography & Consulting, Inc.
and
Thomas C. Chidsey, Jr., Principal Investigator/Program Manager, Utah Geological Survey

CONTENTS

FIGURES

INTRODUCTION

Over 400 million barrels (64 million m^3) of oil have been produced from the shallow-shelf carbonate reservoirs in the Pennsylvanian (Desmoinesian) Paradox Formation in the Paradox Basin, Utah and Colorado. With the exception of the giant Greater Aneth field, the other 100 plus oil fields in the basin typically contain 2 to 10 million barrels (0.3-1.6 million m^3) of original oil in place. Most of these fields are characterized by high initial production rates followed by a very short productive life (primary), and hence premature abandonment. Only 15 to 25 percent of the original oil in place is recoverable during primary production from conventional vertical wells.

An extensive and successful horizontal drilling program has been conducted in the giant Greater Aneth field. However, to date, only two horizontal wells have been drilled in small Ismay and Desert Creek fields. The results from these wells were disappointing due to poor understanding of the carbonate facies and diagenetic fabrics that create reservoir heterogeneity. These small fields, and similar fields in the basin, are at high risk of premature abandonment. At least 200 million barrels (31.8 million m^3) of oil will be left behind in these small fields because current development practices leave compartments of the heterogeneous reservoirs undrained. Through proper geological evaluation of the reservoirs, production may be increased by 20 to 50 percent through the drilling of low-cost single or multilateral horizontal legs from existing vertical development wells. In addition, horizontal drilling from existing wells minimizes surface disturbances and costs for field development, particularly in the environmentally sensitive areas of southeastern Utah and southwestern Colorado.

GEOLOGIC SETTING

The Paradox Basin is located mainly in southeastern Utah and southwestern Colorado with a small portion in northeastern Arizona and the northwestern most corner of New Mexico (figure 1). The Paradox Basin is an elongate, northwest-southeast trending evaporitic basin that predominately developed during the Pennsylvanian (Desmoinesian), about 330 to 310 million years ago (Ma). During the Pennsylvanian, a pattern of basins and fault-bounded uplifts developed from Utah to Oklahoma as a result of the collision of South America, Africa, and southeastern North America (Kluth and Coney, 1981; Kluth, 1986), or from a smaller scale collision of a microcontinent with south-central North America (Harry and Mickus, 1998). One result of this tectonic event was the uplift of the Ancestral Rockies in the western United States. The Uncompahgre Highlands in eastern Utah and western Colorado initially formed as the westernmost range of the Ancestral Rockies during this ancient mountain-building period. The Uncompahgre Highlands (uplift) is bounded along the southwestern flank by a large basement-involved, high-angle reverse fault identified from geophysical seismic surveys and exploration drilling. As the highlands rose, an accompanying depression, or foreland basin, formed to the southwest — the Paradox Basin. Rapid subsidence, particularly during the Pennsylvanian and then continuing into the Permian, accommodated large volumes of evaporitic and marine sediments that intertongue with non-marine arkosic material shed from the highland area to the northeast (Hintze, 1993). The Paradox Basin is surrounded by other uplifts and basins that formed during the Late Cretaceous-early Tertiary Laramide orogeny (figure 1).

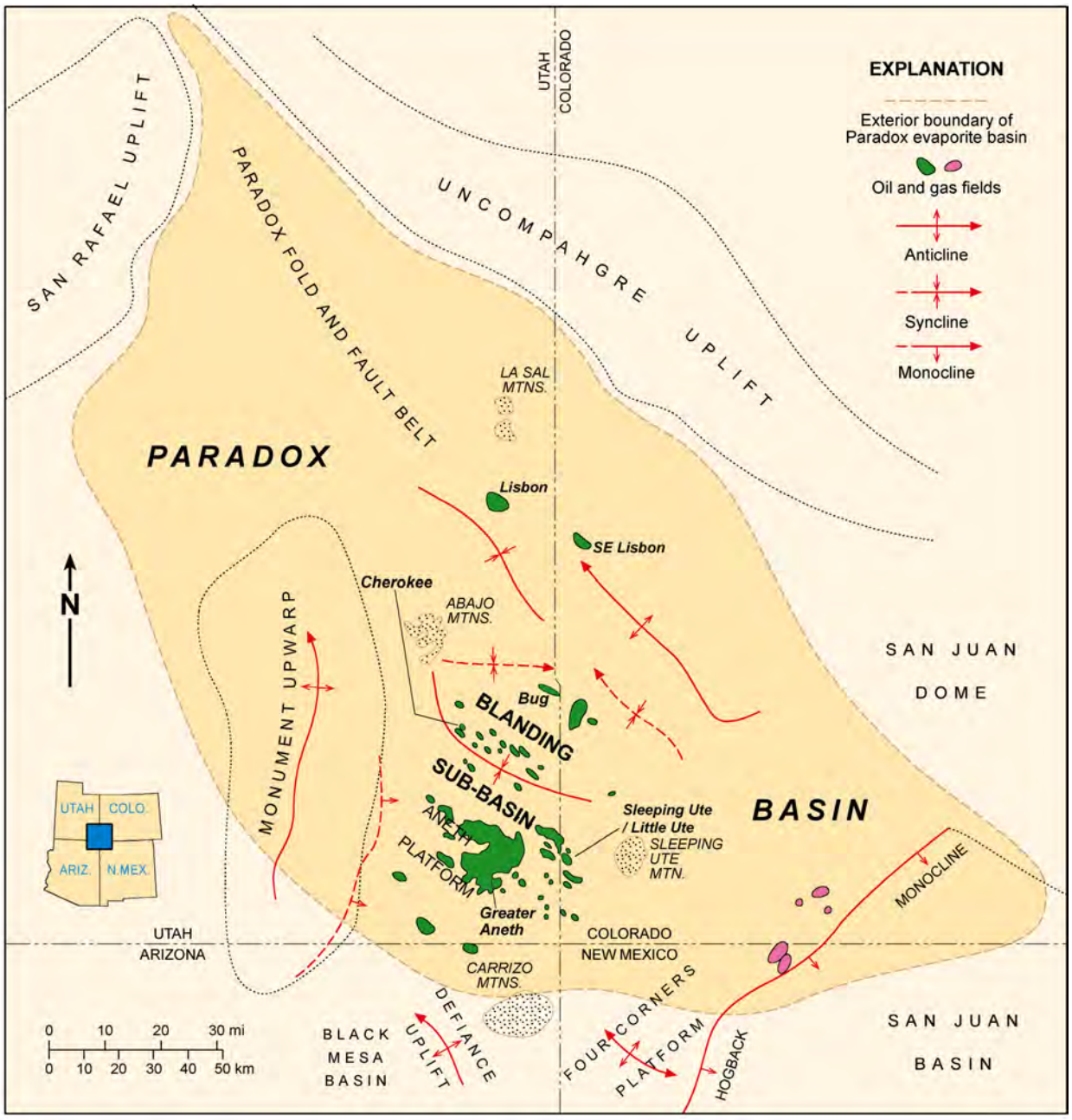

Figure 1. Location map of the Paradox Basin, Utah, Colorado, Arizona, and New Mexico showing producing oil and gas fields, the Paradox fold and fault belt, and Blanding sub-basin as well as surrounding Laramide basins and uplifts (modified from Harr, 1996).

The Paradox Basin can generally be divided into two areas: the Paradox fold and fault belt in the north, and the Blanding sub-basin in the south-southwest (figure 1). Most oil production comes from the Blanding sub-basin. The source of the oil is several black, organic-rich shales within the Paradox Formation (Hite and others, 1984; Nuccio and Condon, 1996). The relatively undeformed Blanding sub-basin developed on a shallow-marine shelf which locally contained algal-mound and other carbonate buildups in a subtropical climate.

The two main producing zones of the Paradox Formation are informally named the Ismay and the Desert Creek (figure 2). The Ismay zone is dominantly limestone comprising equant buildups of phylloid-algal material with locally variable small-scale subfacies (figure 3A) and capped by anhydrite. The Ismay produces oil from fields in the southern Blanding sub-basin (figure 4). The Desert Creek zone is dominantly dolomite comprising regional nearshore shoreline trends with highly aligned, linear facies tracts (figure 3B). The Desert Creek produces oil in fields in the central Blanding sub-basin (figure 4). Both the Ismay and Desert Creek buildups generally trend northwest-southeast. Various facies changes and extensive diagenesis have created complex reservoir heterogeneity within these two diverse zones.

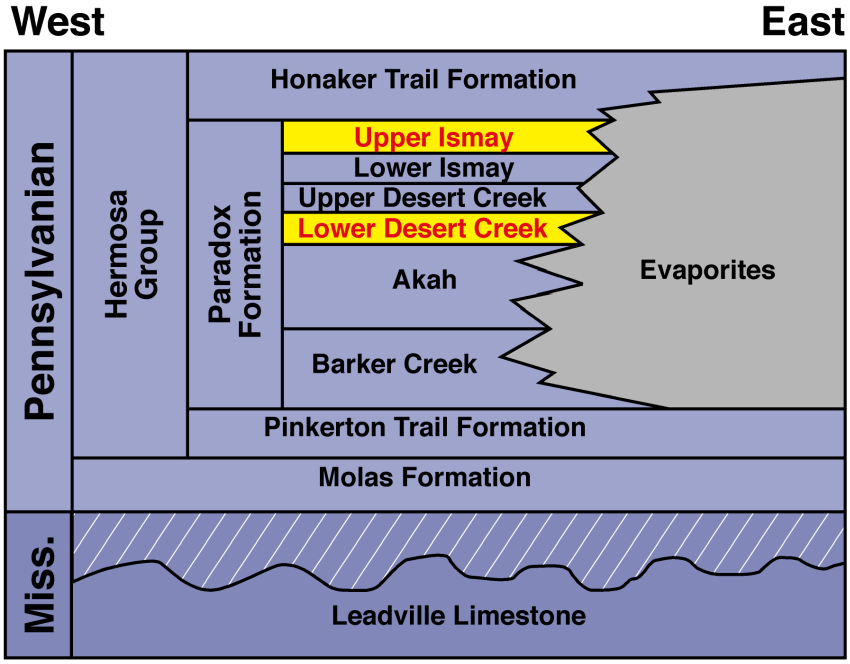

Figure 2. Pennsylvanian stratigraphy of the southern Paradox Basin including informal zones of the Paradox Formation; the Ismay and Desert Creek zones productive in the case-study fields described in this report are highlighted.

CASE-STUDY FIELDS

Two Utah fields were selected for local-scale evaluation and geological characterization: Cherokee in the Ismay trend and Bug in the Desert Creek trend (figure 4). The diagenetic evaluation summarized in this report included blue-light epifluorescence microscopy of selected samples from wells in these fields.

The geological characterization focused on reservoir diagenesis, heterogeneity, quality, and lateral continuity, as well as possible compartmentalization within the fields. From these evaluations, untested or under-produced compartments can be identified as targets for horizontal drilling. The models resulting from the geological and reservoir characterization of these fields can be applied to similar fields in the basin (and other basins as well) where data might be limited. Modification of rock fabrics and porosity within the lower Desert Creek and upper Ismay zones of the Blanding sub-basin study area is quite complex. Diagenesis played a major role in the development of reservoir heterogeneity in Bug and Cherokee fields as well as throughout the all of the Paradox Formation fields. Diagenetic processes started during deposition and continued throughout burial history (figure 5). A complete discussion on the diagenetic history based upon visual core examination and thin section petrography is contained in separate deliverables already completed for this project.

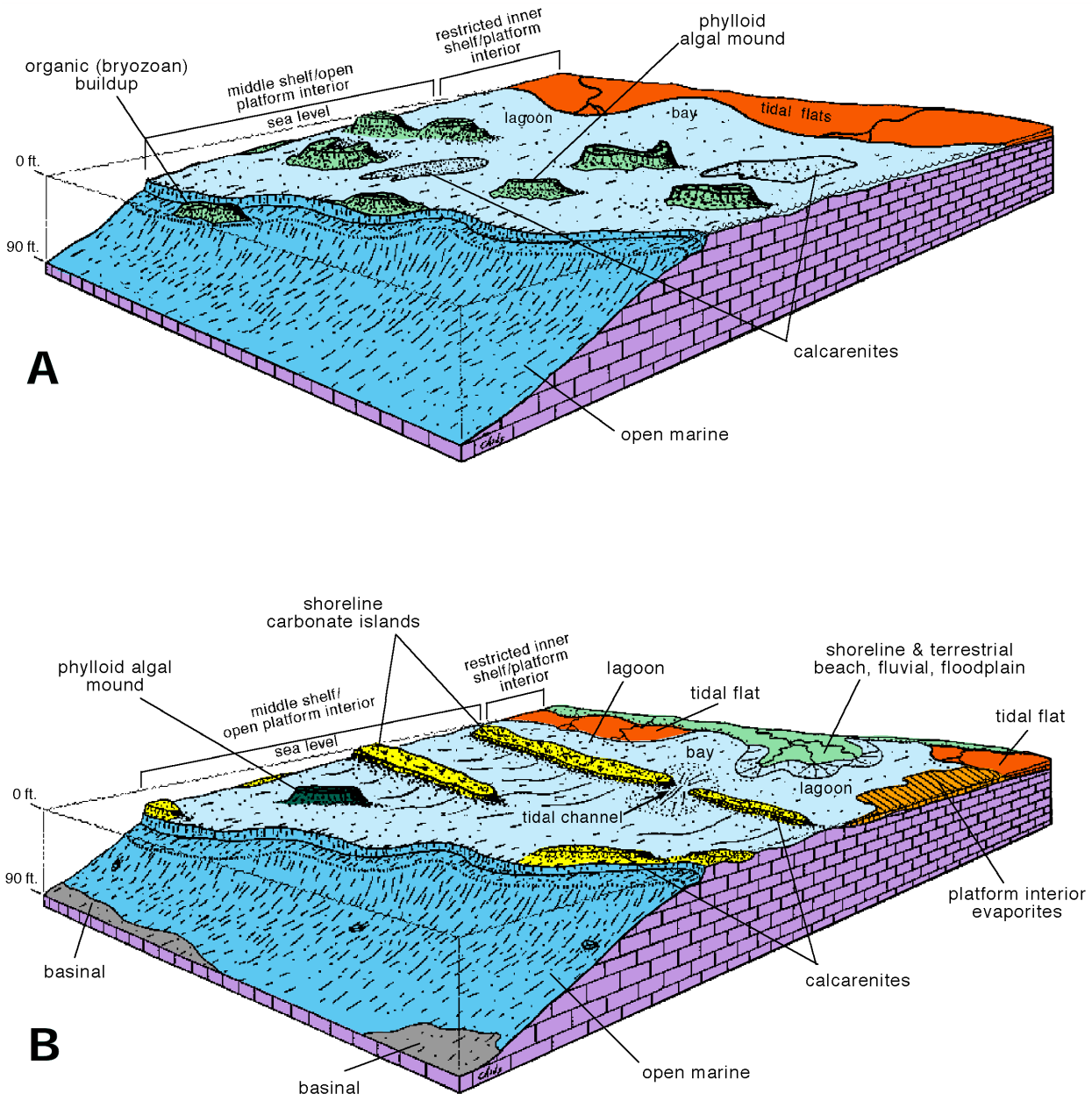

Figure 3. Block diagrams displaying major depositional facies, as determined from core, for the Ismay (A) and Desert Creek (B) zones, Pennsylvanian Paradox Formation, Utah and Colorado.

Cherokee Field

Cherokee field (figure 4) is a phylloid-algal buildup capped by anhydrite that produces from porous algal limestone and dolomite in the upper Ismay zone. The net reservoir thickness is 27 feet (8.2 m), which extends over a 320-acre (130 ha) area. Porosity averages 12 percent with 8 millidarcies (mD) of permeability in vuggy and intercrystalline pore systems. Water saturation is 38.1 percent (Crawley-Stewart and Riley, 1993).

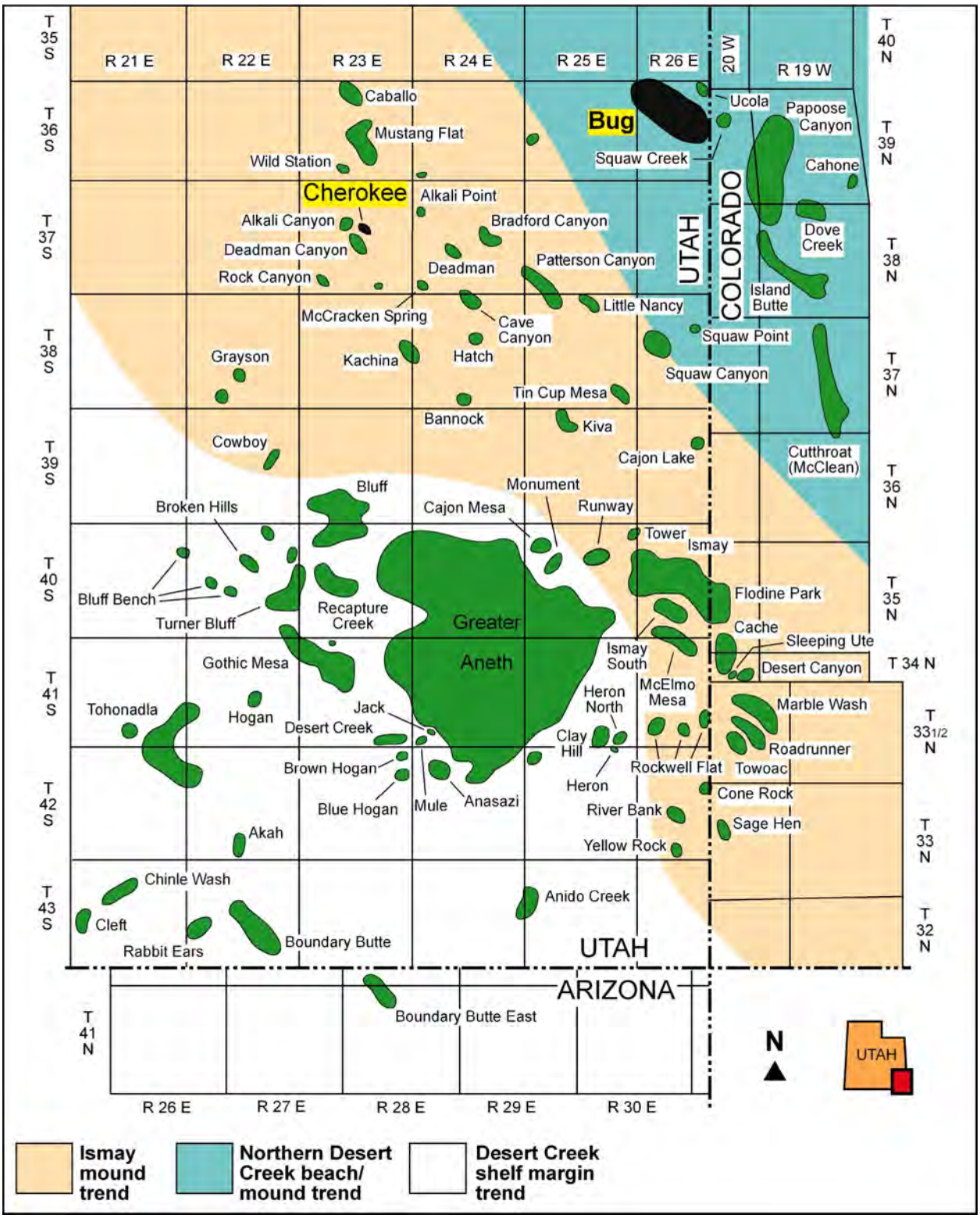

Figure 4. Map showing the project study area and fields (case-study fields in black) within the Ismay and Desert Creek producing trends in the Blanding sub-basin, Utah and Colorado.

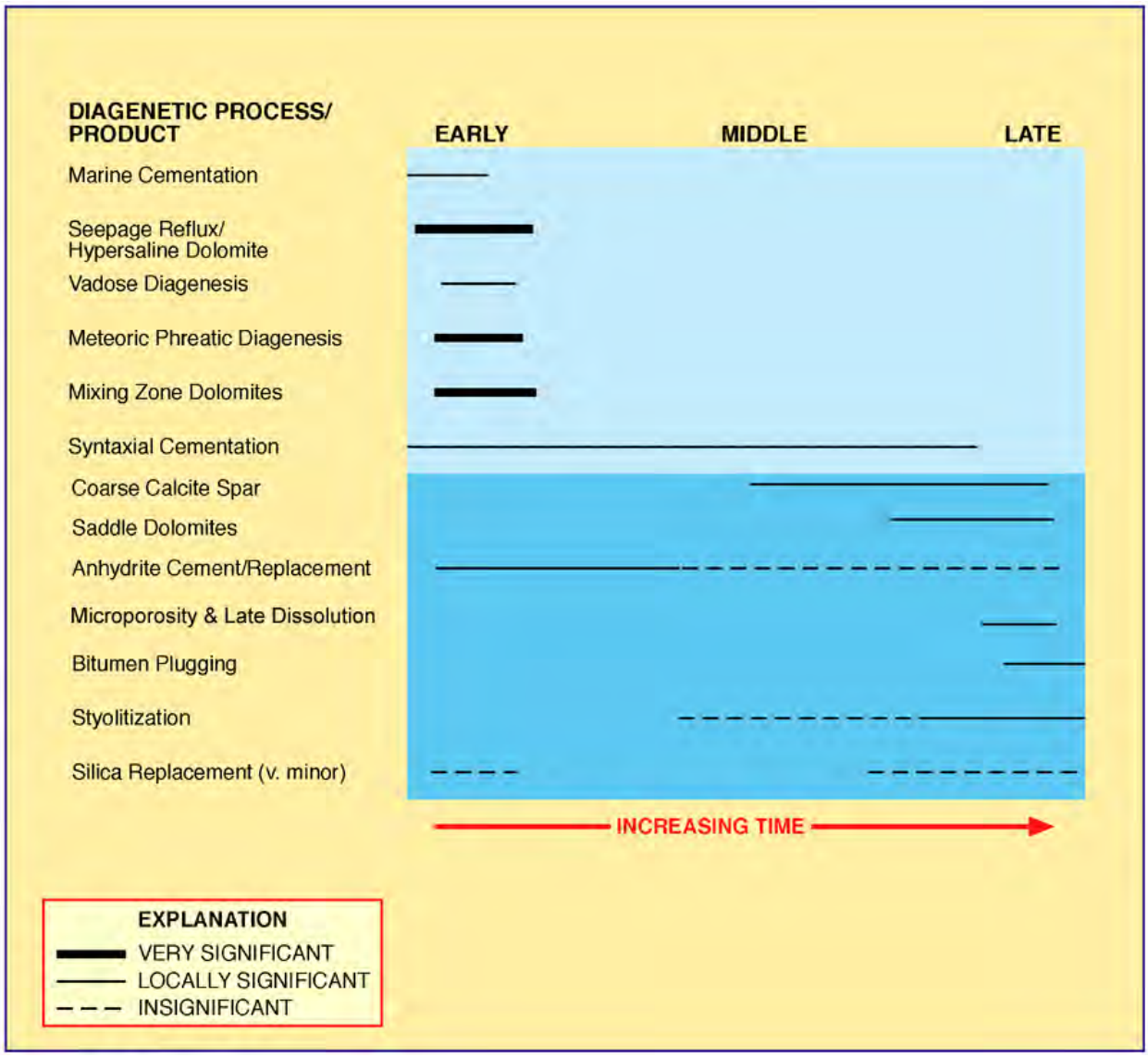

Figure 5. Ideal diagenetic sequence through time based on thin section analysis, Ismay and Desert Creek zones, Cherokee and Bug fields.

Cherokee field was discovered in 1987 with the completion of the Meridian Oil Company Cherokee Federal 11-14, NE1/4NW1/4 section 14, T. 37 S., R. 23 E., Salt Lake Base Line and Meridian (SLBL&M); initial flowing potential (IFP) was 53 barrels of oil per day (BOPD) (8.4 m^3), 990 thousand cubic feet of gas per day (MCFGPD) (28 MCMPD), and 26 barrels of water (4.1 m^3). There are currently four producing (or shut-in) wells and two dry holes in the field. The well spacing is 80 acres (32 ha). The present field reservoir pressure is estimated at 150 pounds per square inch (psi) (1034 kPa). Cumulative production as of December 1, 2004, was 182,901 barrels of oil (29,081 m^3), 3.68 billion cubic feet of gas (BCFG) (0.1 BCMG), and 3358 barrels of water (534 m^3) (Utah Division of Oil, Gas and Mining, 2004). The original estimated primary recovery is 172,000 barrels of oil (27,348 m^3) and 3.28 BCFG (0.09 BCMG) (Crawley-Stewart and Riley, 1993). The fact that both these estimates have been surpassed suggests significant additional reserves could remain.

Bug Field

Bug field (figure 4) is an elongate, northwest-trending carbonate buildup in the lower Desert Creek zone. The producing units vary from porous dolomitized bafflestone to packstone and wackestone. The trapping mechanism is an updip porosity pinchout. The net reservoir thickness is 15 feet (4.6 m) over a 2600-acre (1,052 ha) area. Porosity averages 11 percent in moldic, vuggy, and intercrystalline networks. Permeability averages 25 to 30 mD, but ranges from less than 1 to 500 mD. Water saturation is 32 percent (Martin, 1983; Oline, 1996).

Bug field was discovered in 1980 with the completion of the Wexpro Bug No. 1, NE1/ SE1/4 section 12, T. 36 S., R. 25 E., SLBL&M, for an IFP of 608 BOPD (96.7 m^3), 1128 MCFGPD (32 MCMPD), and 180 barrels of water (28.6 m^3). There are currently eight producing (or shut-in) wells, five abandoned producers, and two dry holes in the field. The well spacing is 160 acres (65 ha). The present reservoir field pressure is 3550 psi (24,477 kPa). Cumulative production as of December 1, 2004, was 1,622,863 barrels of oil (258,035 m^3), 4.49 BCFG (0.13 BCMG), and 3,181,467 barrels of water (505,853 m^3) (Utah Division of Oil, Gas and Mining, 2004). Estimated primary recovery is 1,600,000 bbls (254,400 m^3) of oil and 4 BCFG (0.1 BCMG) (Oline, 1996). Again, since the original reserve estimates have been surpassed and the field is still producing, significant additional reserves likely remain.

EPIFLUORESCENCE

Epifluorescence (EF) microscopy is a technique that has been used successfully in recent years to provide additional information on diagenesis, pores, and organic matter (including "live" hydrocarbons) within sedimentary rocks. It is a rapid, non-destructive procedure that can be done using a high-quality petrographic (polarizing) microscope equipped with reflected light capabilities. The basic principles and equipment for EF were largely developed in the 1960s and 1970s for applications in coal petrology and palynology (see reviews by van Gijzel, 1967; Teichmuller and Wolf, 1977). All applications depend upon the emission of light (by a material capable of producing fluorescence) that continues only during absorption of the excitation-generating light beam (Rost, 1992; Scholle and Ulmer-Scholle, 2003).

Epifluorescence techniques have been used within industry and research for three objectives. Firstly, EF microscopy has been used extensively for enhancing petrographic observations, including the recognition of depositional and diagenetic fabrics within recrystallized limestone and massive dolomite (see, for instance, Dravis and Yurowicz, 1985; Cercone and Pedone, 1987; Dravis, 1991; LaFlamme, 1992). Secondly, the study of pore structures, microfractures, and microporosity within both carbonates and sandstones has been greatly facilitated by impregnating these voids with epoxy spiked with fluorescing dyes (Yanguas and Dravis, 1985; Gies, 1987; Cather and others, 1989a, 1989b; Soeder, 1990; and Dravis, 1991). Thirdly, the evaluation of "oil shows" (Eby and Hager, 1986; Kirby and Tinker, 1992), determination of the gravity or type cements and minerals, and identification of fluid inclusions within carbonate cements has been facilitated by EF microscopy (Burruss, 1981, 1991; Burruss and others, 1986; Guihaumou and others, 1990; Lavoie and others, 2001). Only the first two objectives were pursued in this study. Also, fluid inclusions were not evaluated in this project.

Previous Work

There is no known published use of EF microscopy on the upper Ismay and lower Desert Creek subsurface rocks of the Blanding sub-basin. However, the published work cited above, applications to carbonate reservoirs listed in Eby and Hager (1986) for a study done within a Permian Basin carbonate field, and case studies documented by Dravis (1988, 1992) provided incentives to apply EF petrography to Paradox Formation reservoir rocks within the Cherokee and Bug case-study fields.

Methodology

Epifluorescence petrography for this project used incident (reflected) blue light fluorescence microscopy employing the general procedures outlined by Dravis and Yurewicz (1985), including the use of the modified "white card" technique outlined by Folk (1987) and Dravis (1991). Ultraviolet (UV) fluorescence did not effectively add any textural or pore structure information that could not otherwise be seen under blue-light excitation, even though some workers utilize UV fluorescence for evaluating fluid inclusions and compositional zoning within dolomite crystals (see Scholle and Ulmer-Scholle, 2003). Fluorescence data and observations collected for this study utilized a Jena (now part of Carl Zeiss) research-grade combination polarizing-reflected light microscope equipped with a high-pressure mercury vapor lamp for EF excitation, a Zeiss IIIRS EF nosepiece, and a 35-mm camera system. Magnification ranges for examination and photo-documentation were between ~130 and 320x. The EF optical configuration used is similar to that shown in figure 6.

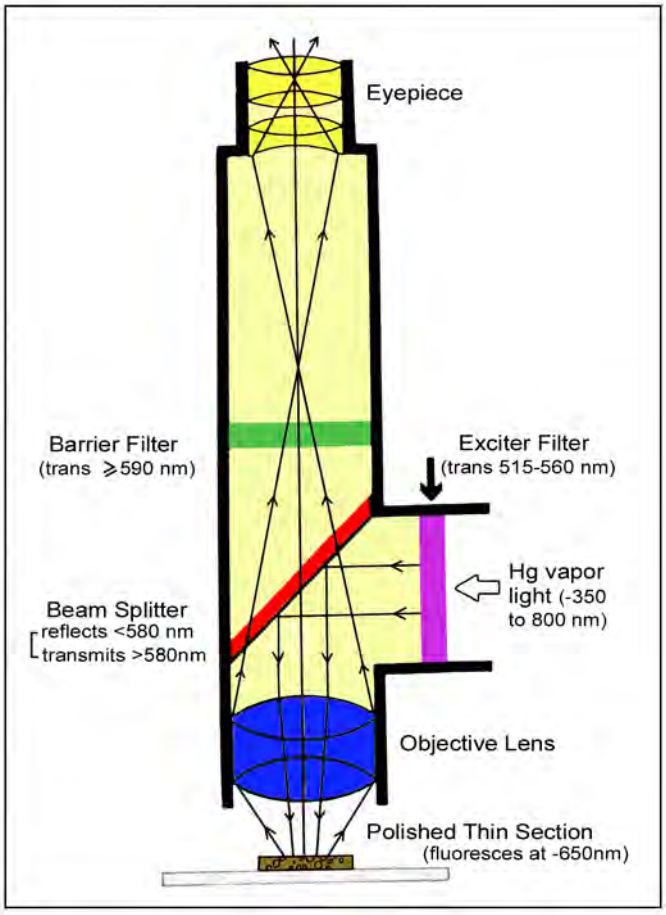

Figure 6. Generalized microscope optical configuration for observing fluorescence under incident light (modified from Soeder, 1990).

The light pathways and mechanics of the EF used in this study have been generally described by Soeder (1990). As described by Burruss (1991), "these excitation wavelengths are reflected to the microscope objective and sample by a dichroic beamsplitter which has a dielectric coating that reflects a specific short wavelength range. Fluorescence emission and reflected short wavelength excitation light is collected by the objective. The dichroic

beamsplitter transmits the long wavelength fluorescence emission, but reflects the short wavelengths back toward the light source. The fluorescence emission passes through a barrier filter which removes any remaining short wavelength excitation light." Blue light (~420-490 nm exciter filter/520 nm barrier filter) was used to excite the cuttings and core-chip samples. We have found broad-band, blue-light EF to be the most helpful in observational work on dolomite, although some workers report applications using UV light (330-380 nm exciter filter/420 nm barrier filter) or narrow-band, blue-violet light (400-440 nm exciter filter/480 nm barrier filter). Finally, the greater depth of investigation into a sample by the reflected fluorescence technique than by transmitted polarized light or other forms of reflected light make it possible to resolve grain boundary and compositional features that are normally not appreciated in cutting or thin-section petrography.

Sample preparation is inexpensive and rapid, involving standard thin section preparation techniques. Thin sections were prepared from 12 samples - four from representative upper Ismay fabrics in Cherokee field and eight from lower Desert Creek dolomites in Bug field. These thin sections were vacuum- and pressure-impregnated with blue-dyed epoxy (see Gardner, 1980) that was spiked with a fluorescing compound. Microscopy used only uncovered polished surfaces. Examination for each thin section area of interest included photo-documentation under EF and plane-polarized light at the same magnification. Photomicrography of the compositional, textural, and pore structure attributes was done using high-speed film (ISO 800 and 1600) with some bracketing of exposures as camera metering systems do not always reliably read these high-contrast images in the yellow and green light spectrum. Since the image brightness is directly proportional to magnification, the best images are obtained at relatively high magnifications (such as greater than 100x). Low-power fluorescence is often too dim to effectively record on film. These techniques are applicable to thin sections from both core and cuttings samples.

Epifluorescence Petrography of Upper Ismay Thin Sections

Blue-light, EF microscopy was completed on eight core samples for a variety of rock textures and diagenetic phases from upper Ismay zone limestone and dolomite within Cherokee field (figure 4). These samples were selected to be representative of compositional, diagenetic, and pore types encountered within the two cored wells (Cherokee Federal No. 22-14 and Cherokee Federal No. 33-14). A detailed description and interpretation of the fluorescence petrography of each sample follows below. The Appendix contains photomicrographs representative views under both blue-light EF and plane-polarized light. Short descriptive captions for these photomicrographs are included with each photo pair.

Cherokee Federal No. 22-14 Well

5768.7 feet: Blue-light, EF microscopy nicely shows pore spaces and structures that are not readily seen under transmitted, plane-polarized lighting. Black bitumen linings and interlocking, dolomite, crystalline aggregates mask clear definition of the blue-dyed epoxy that has been impregnated into the open pore spaces. However, the reddish fluorescence of the epoxy makes it possible to image pores in cross section very nicely. Despite the significant amount of open porosity visible under EF, many of these voids appear to be completely surrounded by a micro-box-work of dolomite crystals. Much of the dolomite has a dull- to

bright-yellow fluorescence, due in part to the presence of live-oil films around many of the tight intercrystalline spaces. There are no identifiable remnants of the original depositional fabric of this carbonate sediment, although the appearance of probable micro-moldic and slightly larger dissolution pores suggests that there were original detrital carbonate grains present. Where anhydrite has secondarily plugged earlier intercrystalline pores, the differences in fluorescence between oil-impregated dolomite and very massive anhydrite cement are easy to see.

5778.1 feet: Blue-light, EF microscopy assists with the identification of fossil fragments and peloids that populate this massive, partially dolomitized limestone. Under plane polarized lighting, this interval appears dense and muddy. However, the fluorescence petrography reveals depositional textures that range from a fine grainstone to packstone. In addition, the distribution and types of pores are difficult to identify without examination under fluorescence. Abundant open micropores with some bitumen linings are much easier to see under EF microscopy than trying to resolve the blue-dyed epoxy that has been impregnated into the sample.

5783.5 feet: This sample displays considerable heterogeneity of porosity and permeability. The EF petrography nicely shows the location and distribution of pores in cross sections and provides good visual discrimination boundaries. Areas of low porosity and permeability show up particularly well because fluorescent live oil is trapped in the tighter (low-permeability) portions of this sample. In addition, this sample displays some relatively large dolomite crystals (>100 μm across) that have replaced the finer carbonate matrix. Without EF, the size variation of dolomite crystals and some of the related intercrystalline pore space would be nearly impossible to resolve.

5801.3 feet: This sample also displays significant heterogeneity in porosity distribution. Blue-light EF made it possible to image the quantity and quality of microporosity throughout the sample. "Micro-sucrosic" dolomite appears to dominate this sample with an excellent micro-intercrystalline pore structure that could not be resolved without fluorescence microscopy. Low-amplitude stylolites act as significant vertical permeability barriers between different layers of well-developed matrix microporosity. Replacement of the matrix rock by dolomite and the development of micro-intercrystalline porosity appears to be greatly reduced in areas immediately adjoining the stylolites.

5864.1 feet: Epifluorescence of a very dense limestone containing abundant, closely spaced, wispy, stylolite seams reveals some very interesting textural and porosity information. Under plane transmitted light, this sample appears to be a dense lime mudstone, whereas fluorescence examination clearly shows distinct grain-supported peloids. More importantly, EF reveals small compartments of good porosity separated from much tighter rocks by subhorizontal stylolitic seams. Hence, some of the stylolites and wispy seams with concentrations of insoluble residues act as barriers to vertical fluid flow between the porous compartments. Epifluorescence also suggests that the origin of the porosity may be related to dissolution of the peloidal limestone matrix after the formation of the stylolites.

Cherokee Federal No. 33-14 Well

Epifluorescence microscopy of the sample from 5773.9 feet (1759.8 m) of slightly dolomitic limestone shows high amounts of microporosity and solution-enlarged pores that are difficult to image under plane-polarized lighting. Blue-light EF images nicely show the open pores and their shapes despite the presences of variable amounts of black bitumen lining pore walls. In addition, EF nicely shows remnants of fossils and non-skeletal grains (peloids and possibly ooids), as well as excellent examples of zoned, replacement, dolomite crystals.

Epifluorescence Petrography of Lower Desert Creek Thin Sections

Blue-light EF microscopy was completed on four samples for a variety of rock textures and diagenetic phases in core samples from oil-productive, lower Desert Creek zone dolomites within Bug field. These samples were selected to be representative of the compositional, diagenetic, pore, and fracture types encountered within the three cored wells (Bug Nos. 7, 10, and 16 [two samples]) from Bug field. A detailed description and interpretation of the fluorescence petrography of each sample follows below. A total of 32 photomicrographs have been included in the Appendix to show representative views under both blue-light EF and plane-polarized light. Short descriptive captions are included for each photomicrograph pair.

Bug No. 7 Well

Blue-light EF microscopy of the sample from 6359.3 feet (1938.2 m) shows very tight dolomites with fairly uniform oil saturation throughout. Much of the dolomite fluoresces a dull to bright yellow, due in part to the presence of live oil films around many of the tight inter-crystalline spaces. Non-fluorescent areas (which appear red to black in the photomicrographs) indicate extremely tight places where oil could not penetrate. In places, fluorescence petrography makes it possible to see outlines of carbonate grains as well as occasional larger dolomite rhombs. Perhaps the best application of EF in this sample is to determine open, oil-bearing fractures and “stylo-fractures” from healed fractures and tight microstylolites.

Bug No. 10 Well

Epifluorescence examination of the sample from 6327.9 feet (1928.6 m) aids in two very important aspects of the Bug dolomite oil reservoir. Firstly, the definition of open, crystal-lined microfractures within dense portions of this dolomite is aided considerably with EF. Secondly, this sample displays well-developed micro-box-works of dolomite crystal aggregates that serve to isolate a number of the open pores within some of the most porous parts of this sample. While some pore throats are wide and open, other megascopic pores are “blind” and dead end into dolomite partitions. Only EF petrography techniques allow visual definition of this type of reservoir heterogeneity, as standard plane light (Pl) petrography does not image the micro-box-work patterns very well.

Bug No. 16 Well

6299.3 feet: This sample shows fine- to medium-sized, interlocking crystals in a sucrosic dolomite that displays some intercrystalline porosity. Epifluorescence examination nicely shows that many of these types of rhombic, sucrosic, dolomite crystals display internal zonation with occasional ghosts of the original replaced carbonate grains. As in other Bug field samples, the definition of pore to matrix boundaries, especially where there are bitumen linings, can be seen much more clearly under EF.

6300.5 feet: Excellent examples of rhombic dolomite crystals and crystal aggregates are imaged from this sample under EF. Fluorescence photomicrographs show sharp contacts between the dolomite crystals and the intercrystalline pores. This thin section is probably representative of a cross sectional view of a typical sucrosic dolomite from the lower Desert Creek interval at Bug field. In addition, this sample also contains complex networks of micro-box-work structure. Many of the pores within this network appear to be isolated or "blind." Therefore, drainage of oil from this type of pore system may be inefficient. Under high magnification, EF imaging makes it easy to see highly corroded or scalloped margins of many dolomite crystals in this sample. The corroded dolomite rhomb contacts indicate that there has been some partial dissolution of dolomite rhombs.

SUMMARY

1. Epifluorescence petrography makes it possible to clearly identify grain types and shapes, within both limestone and dolomite reservoir intervals in upper Ismay zone thin sections from cores examined in this study. In particular, identification of peloids, skeletal grain types, and coated grains are easy to see in rocks where these grains have been poorly preserved, partially leached, or completely dolomitized.

2. Depositional textures that are frequently occult or poorly preserved can often be clearly distinguished using blue-light EF microscopy. In many of the microporous limestones and finely crystalline dolomites of the upper Ismay reservoir at Cherokee field, the differences between muddy and calcarenitic fabrics can only be clearly appreciated with fluorescence lighting.

3. Epifluorescence petrography clearly and rapidly images pore spaces that cannot otherwise be seen in standard viewing under transmitted polarized lighting. In addition, the cross-sectional size and shape of pores are easy to determine.

4. Much of the upper Ismay zone porosity is very heterogeneous and poorly connected as viewed under EF. In particular, microporosity within some of the upper Ismay reservoir section in Cherokee field can be resolved much more clearly than with transmitted polarized lighting. The EF examination helps in seeing the dissolution origin of most types of the microporosity. Transmitted polarized lighting does not image microporosity in carbonate samples very well, even though blue-dyed epoxy can be impregnated into even very small pores. This porosity does not show up very well because the pores are much smaller than the thickness of the thin section, and hence carbonate crystallites on either side of

micropores are seen rather than the pores. In addition, opaque bitumen linings prevent light from passing through some of the pores to the observer. Without the aid of the EF view, the amount of visible open pore space would be underestimated in the plane-light image.

5. Where dolomitization has occurred, EF petrography often shows the crystal size, shape, and zonation far better than transmitted plane or polarized lighting. This information is often very useful when considering the origin and timing of dolomitization as well as evaluating the quality of the pore system within the dolomite.

6. Permeability differences within these dolomite and limestone samples are also easy to image because of the differential oil saturations between the tighter areas and the more permeable lithologies. Low-permeability carbonates from this study area show bright yellow fluorescence due to trapped live oil that is retained within tighter parts of the reservoir system. More permeable rocks show red fluorescence due to the epoxy fluorescence where oil has almost completely drained from the better quality portions of the reservoir.

7. Fluorescence of dense, "muddy" limestone and dolomite containing abundant, closely spaced, wispy stylolite seams often reveals some very interesting textural and porosity information. Under plane transmitted light, these types of samples appear to be a dense lime mudstone whereas EF examination clearly shows distinct grain-supported peloids. More importantly, EF frequently reveals small compartments of good porosity separated from much tighter rocks by subhorizontal stylolitic seams. Hence, some of the stylolites and wispy seams with concentrations of insoluble residues act as barriers to vertical fluid flow between the porous compartments. Epifluorescence also suggests that the origin of the porosity may be related to dissolution of the peloidal limestone matrix after the formation of the stylolites.

ACKNOWLEDGEMENTS

Core and petrophysical data were provided by Burlington Resources, Seeley Oil Company, and Wexpro Company. James Parker and Cheryl Gustin of the Utah Geological Survey (UGS) drafted the figures. The report was reviewed by David Tabet and Michael Hylland of the UGS. Cheryl Gustin, UGS, formatted the manuscript for publication.

REFERENCES

Burruss, R.C., 1981, Hydrocarbon fluid inclusions in studies of sedimentary diagenesis, *in* Hollister, L.S., and Crawford, M.L., editors, Fluid inclusions - applications in petrology: Mineralogical Association of Canada Short Course Notes, v. 6, p. 138-156.

---1991, Practical aspects of fluorescent microscopy of petroleum fluid inclusions, *in* Barker, C. E., and Kopp, O.C., editors, Luminescence microscopy - quantitative and qualitative aspects: Society for Sedimentary Geology (SEPM) Short Course 25 Notes, p. 1-7.

Burruss, R.C., Cercone, K.R., and Harris, P.M., 1986, Timing of hydrocarbon migration: evidenced from fluid inclusions in calcite cements, tectonics and burial history, *in* Schneidermann, Nahum, and Harris, P.M., editors, Carbonate cements: Society for Sedimentary Geology (SEPM) Special Publication 36, p. 277-289.

Cather, M.E., Morrow, N.R., Brower, K.R., and Buckley, J.S., 1989a, Uses of epi-fluorescent microscopy in evaluation of Mesaverde tight gas sands [abs.]: American Association of Petroleum Geologists Bulletin, v. 73, p. 1150-1151.

Cather, M.E., Morrow, N.R., and Klich, I., 1989b, Applications of fluorescent dye staining techniques to reservoir studies of tight gas sands, Measverde Group, southwestern Colorado [abs.]: American Association of Petroleum Geologists Bulletin, v. 73, p. 342.

Cercone, K.R., and Pedone, V.A., 1987, Fluorescence (photoluminescence) of carbonate rocks - instrumental and analytical sources of observational error: Journal of Sedimentary Petrology, v. 57, p. 780-782.

Crawley-Stewart, C.L., and Riley, K.F., 1993, Cherokee, *in* Hill, B.G., and Bereskin, S.R., editors, Oil and gas fields of Utah: Utah Geological Association Publication 22, non-paginated.

Dravis, J.J., 1988, Deep-burial microporosity in Upper Jurassic Haynesville oolitic grainstones, East Texas: Sedimentary Geology, v. 63, p. 325-341.

---1991, Carbonate petrography – update on new techniques and applications: Journal of Sedimentary Petrology, v. 61, p. 626-628.

---1992, Burial dissolution in limestones and dolomites – criteria for recognition and discussion of controls: a case study approach (Pt. 1: Upper Jurassic Haynesville limestones, East Texas; Pt. 2: Devonian Upper Elk Point dolomites, western Canada): American Association of Petroleum Geologists Bulletin/Canadian Society of Petroleum Geologists Short Course Notes, Subsurface dissolution porosity in carbonates.

Dravis, J J., and Yurewicz, D.A., 1985, Enhanced carbonate petrography using fluorescence microscopy: Journal of Sedimentary Petrology, v. 55, p. 795-804.

Eby, D.E., and Hager, R.C., 1986, Fluorescence petrology of San Andres dolomites – H.O. Mahoney lease, Wasson field, Yoakum County, Texas: Permian Basin Section, Society for Sedimentary Geology (SEPM) Publication 86-26, p. 37-38.

Folk, R.L., 1987, Detection of organic matter in thin sections of carbonate rocks using a white card: Sedimentary Geology, v. 54, p. 193-200.

Gardner, K.L., 1980, Impregnation technique using colored epoxy to define porosity in petrographic thin sections: Canadian Journal of Earth Sciences, v. 17, p. 1104-1107.

Gies, R.M., 1987, An improved method for viewing micropore systems in rocks with the polarizing microscope: Society of Petroleum Engineers Formation Evaluation, v. 2, p. 209-214.

Guihaumou, N., Szydlowskii, N., and Padier, B., 1990, Characterization of hydrocarbon fluid inclusions by infra-red and fluorescence microspectrometry: Mineralogical Magazine, v. 54, p. 311-324.

Harr, C.L., 1996, Paradox oil and gas potential of the Ute Mountain Ute Indian Reservation, *in* Huffman, A.C., Jr., Lund, W.R., and Godwin, L.H., editors, Geology of the Paradox Basin: Utah Geological Association Publication 25, p. 13-28.

Harry, D.L., and Mickus, K.L., 1998, Gravity constraints on lithospheric flexure and the structure of the late Paleozoic Ouachita orogen in Arkansas and Oklahoma, south-central North America: Tectonics, v. 17, no. 2, p. 187-202.

Hintze, L.F., 1993, Geologic history of Utah: Brigham Young University Geology Studies Special Publication 7, 202 p.

Hite, R.J., Anders, D.E., and Ging, T.G., 1984, Organic-rich source rocks of Pennsylvanian age in the Paradox Basin of Utah and Colorado, *in* Woodward, Jane, Meissner, F.F., and Clayton, J.L., editors, Hydrocarbon source rocks of the greater Rocky Mountain region: Rocky Mountain Association of Geologists Guidebook, p. 255-274.

Kirby, K.C., and Tinker, S.W., 1992, The Keg River/Winnipegosis petroleum system in northeast Alberta [abs.]: American Association of Petroleum Geologists Annual Convention, Official Program with Abstracts, v. 1, p. A66.

Kluth, C.F., 1986, Plate tectonics of the Ancestral Rocky Mountains: American Association of Petroleum Geologists Memoir 41, p. 353-369.

Kluth, C.F., and Coney, P.J., 1981, Plate tectonics of the Ancestral Rocky Mountains: Geology, v. 9, p. 10-15.

LaFlamme, A.K., 1992, Replacement dolomitization in the Upper Devonian Leduc and Swan Hills Formations, Caroline area, Alberta, Canada [abs.]: American Association of Petroleum Geologists Annual Convention, Official Program with Abstracts, v. 1, p. A70.

LaVoie, D., Chi G., and Fowler, M.G., 2001, The Lower Devonian Upper Gaspe Limestones in eastern Gaspe - carbonate diagenesis and reservoir potential: Bulletin of Canadian Petroleum Geology, v. 49, p. 346-365.

Martin, G.W., 1983, Bug, *in* Fassett, J.E., editor, Oil and gas fields of the Four Corners area, volume III: Four Corners Geological Society, p. 1073-1077.

Nuccio, V.F., and Condon, S.M., 1996, Burial and thermal history of the Paradox Basin, Utah and Colorado, and petroleum potential of the Middle Pennsylvanian Paradox Formation, *in* Huffman, A.C., Jr., Lund, W.R., and Godwin, L.H., editors, Geology of the Paradox Basin: Utah Geological Association Publication 25, p. 57-76.

Oline, W.F., 1996, Bug, *in* Hill, B.G., and Bereskin, S.R., editors, Oil and gas fields of Utah: Utah Geological Association Publication 22 Addendum, non-paginated.

Rost, F.W.D., 1992, Fluorescence microscopy, v. 1: New York, Cambridge University Press, 253 p.

Scholle, P.A., and Ulmer-Scholle, D.S., 2003, A color guide to the petrography of carbonate rocks: American Association of Petroleum Geologists Bulletin Memoir 77, p. 427-440.

Soeder, D.J., 1990, Applications of fluorescent microscopy to study of pores in tight rocks: American Association of Petroleum Geologists Bulletin, v. 74, p. 30-40.

Teichmuller, M., and Wolf, M., 1977, Application of fluorescence microscopy in coal petrology and oil exploration: Journal of Microscopy, v. 109, p. 49-73.

Utah Division of Oil, Gas and Mining, 2004, Oil and gas production report, November: non-paginated.

van Gijzel, P., 1967, Palynology and fluorescence microscopy: Reviews of Paleobotany and Palynology, v. 1, p. 49-79.

Yanguas, J.E., and Dravis, J.J., 1985, Blue fluorescent dye technique for recognition of microporosity in sedimentary rocks: Journal of Sedimentary Petrology, v. 55, p. 600-602.

APPENDIX

THIN SECTION EPIFLUORESCENCE AND DESCRIPTIONS, CHEROKEE AND BUG FIELDS, SAN JUAN COUNTY, UTAH

CHEROKEE FEDERAL NO. 22-14 WELL, CHEROKEE FIELD

5768.7 feet

Top Photomicrograph

Epifluorescence under moderate magnification of a representative area of microporosity shows outlines of small dolomite crystals (fluorescing yellow here due to oil staining). The reddish areas are pores with abundant bitumen linings and plugging (see below). Fluorescence petrography makes it possible to clearly see the dolomite crystals versus the pore space. Occasionally, very small rhombic outlines of dolomite crystals can be resolved (see, for instance, E-9, G-4, and N-1). Most of the pores appear in cross section to be poorly size-sorted and of dissolution origin. Many of these pores appear to be completely surrounded by an interlocking network of dolomite crystals (see, for instance, H-3, H-6.5, and J-4).

Bottom Photomicrograph

The same field of view as above is shown under Pl at the same magnification. Note that the black (and opaque) areas composed of bitumen mask the crystal boundaries of the dolomite as well as individual pore outlines. The white and gray areas are remnants of the dolomite matrix that are not masked by the bitumen. Only a small amount of pore space (blue-dyed areas) can be seen in this view compared to the fluorescence photomicrograph above.

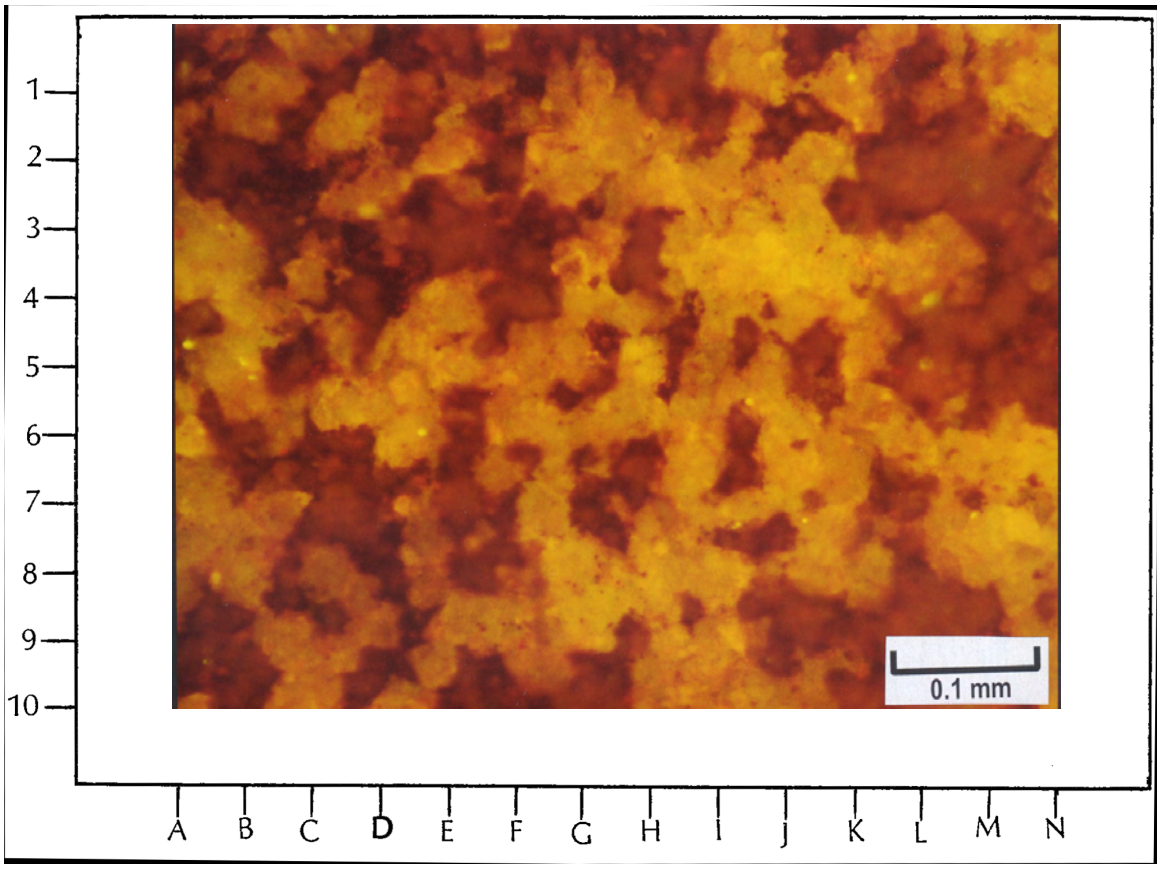
1
2
3
4
5
6
7
8
9
10
A B C D E F G H I J K L M N
0.1 mm

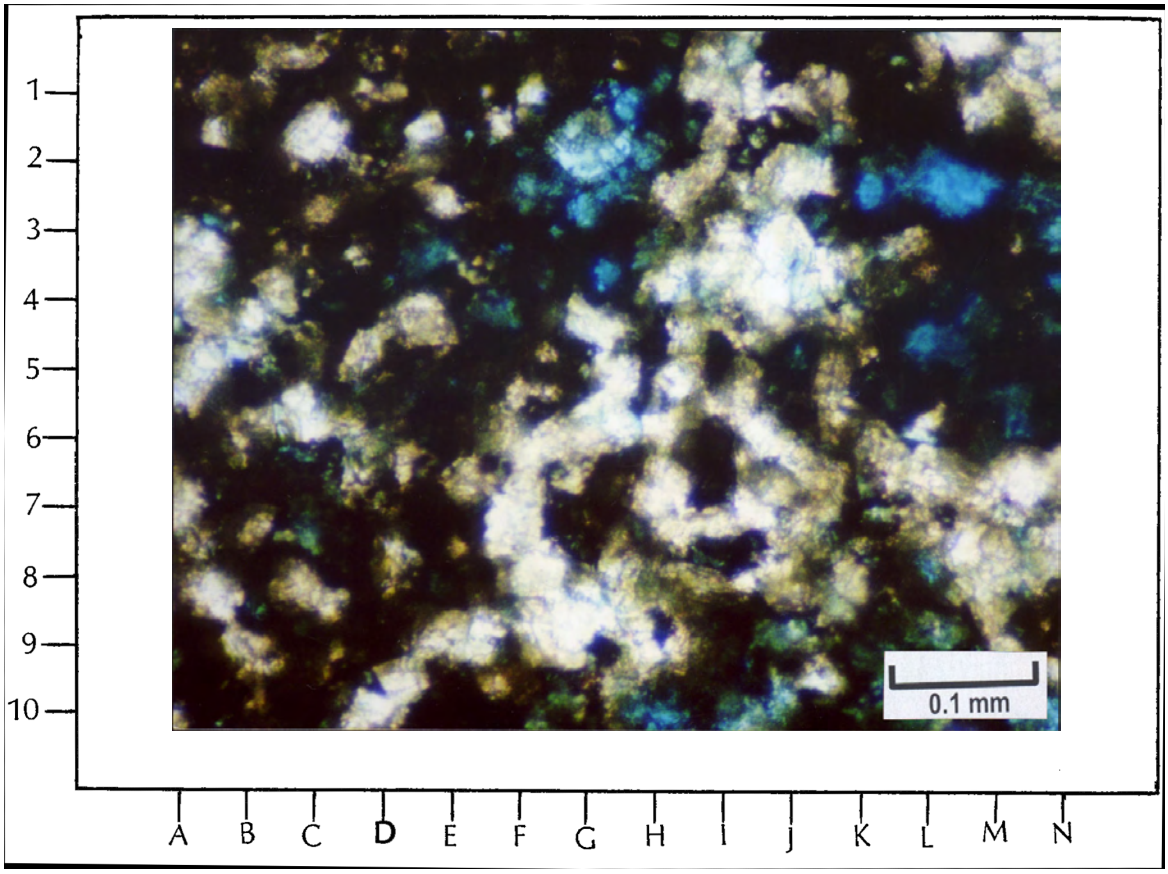
1
2
3
4
5
6
7
8
9
10
A B C D E F G H I J K L M N
0.1 mm

5768.7 feet

Top Photomicrograph

High-magnification EF of a bitumen-rich portion of this thin section shows quite distinct dolomite crystal outlines (in the dim to moderate yellow shades) among the interlocking dolomite network. Most of the pores (red in this view) are not well connected. Most of this microporosity appears to be of dissolution origin and micromoldic in type. (The bright yellow spot at C-2 is a surface contamination.)

Bottom Photomicrograph

The same field of view as above is shown under Pl at the same magnification. Black bitumen within this sample makes it difficult to image the large amount of pore space that can be observed under EF (see photomicrograph above). Hence, this standard transmitted light view provides a significant underestimate of available pore space within this dolomite.

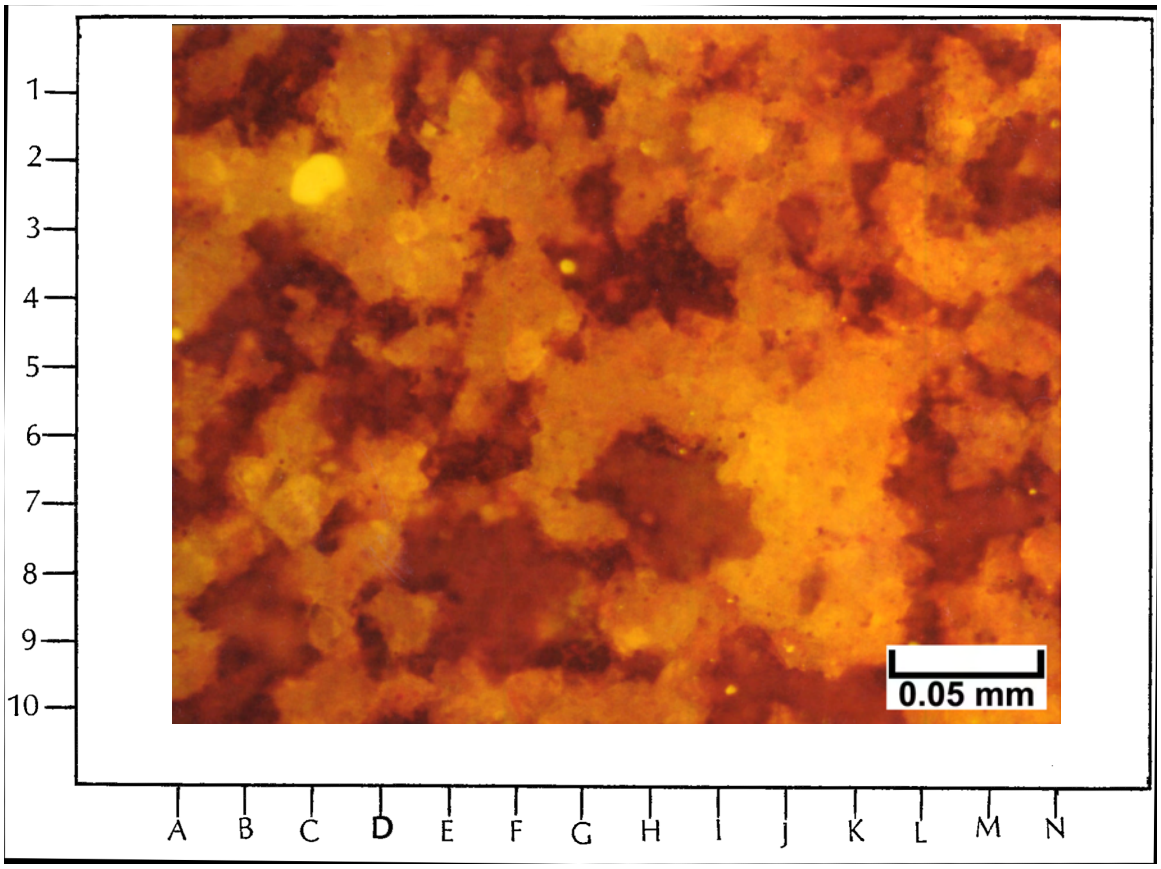
1
2
3
4
5
6
7
8
9
10
A B C D E F G H I J K L M N
0.05 mm

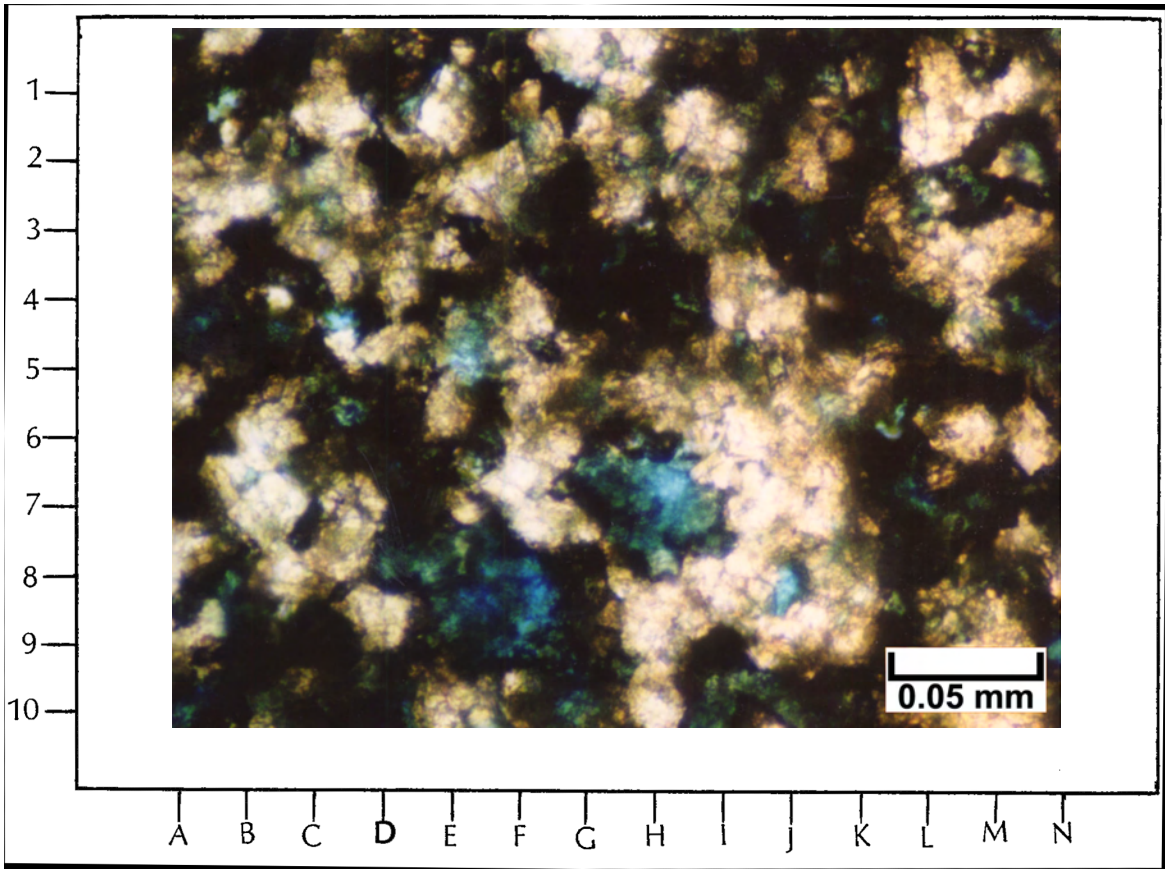
1
2
3
4
5
6
7
8
9
10
A B C D E F G H I J K L M N
0.05 mm

5768.7 feet

Top Photomicrograph

This EF image under moderate magnification of a representative area shows the patchiness of porosity in this dolomite. The masses of generally tight, interlocking dolomite are identifiable as the dull yellowish and greenish shades. Most of the open pore space appears dark red in this view, although a few pores in the areas of tighter, interlocking dolomite are bright yellow due to live oil that has bled into these isolated spaces (see, for instance, C-2, D-7.5, I-7.5, and M-6).

Bottom Photomicrograph

The same field of view as above is shown under Pl at the same moderate magnification. The blue areas show open pores where they have not been plugged or lined with black bitumen. Note that the amount of blue is far less than the pore spaces imaged above under EF.

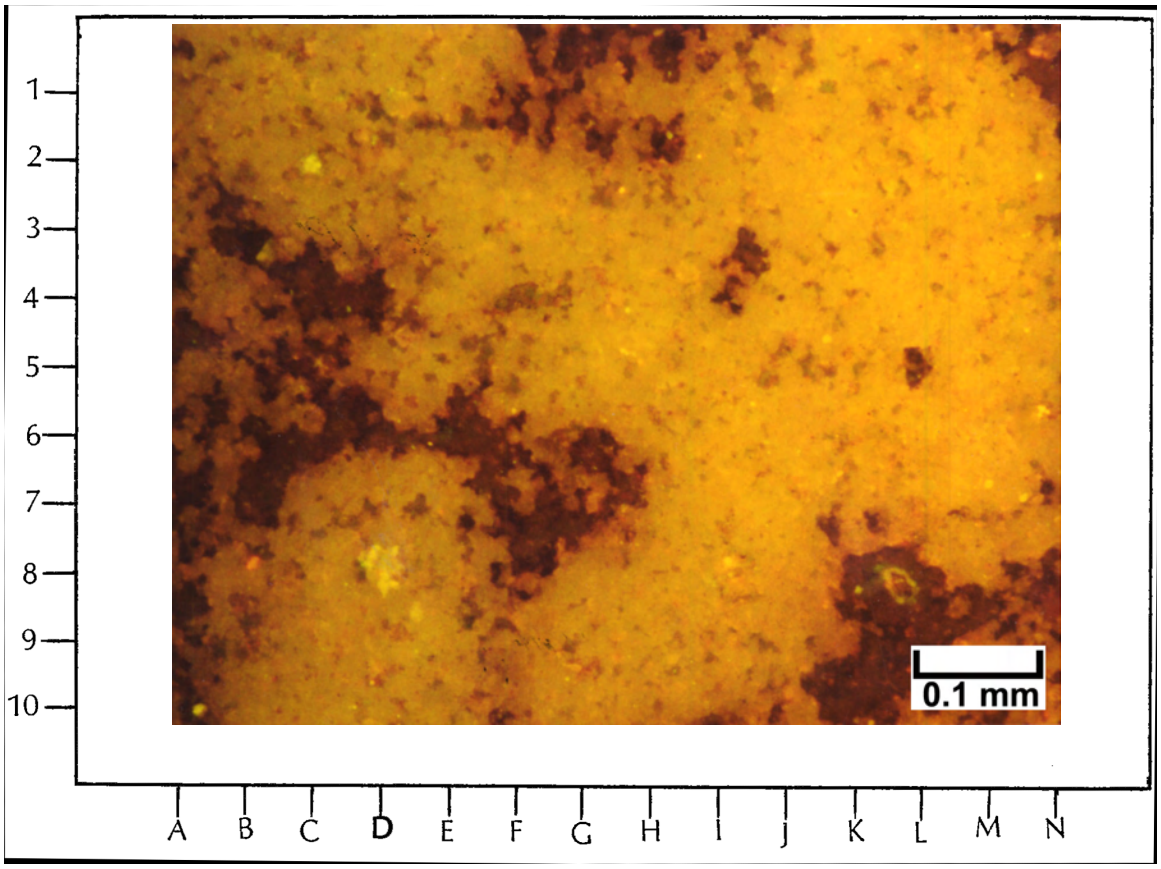
1
2
3
4
5
6
7
8
9
10
A B C D E F G H I J K L M N
0.1 mm

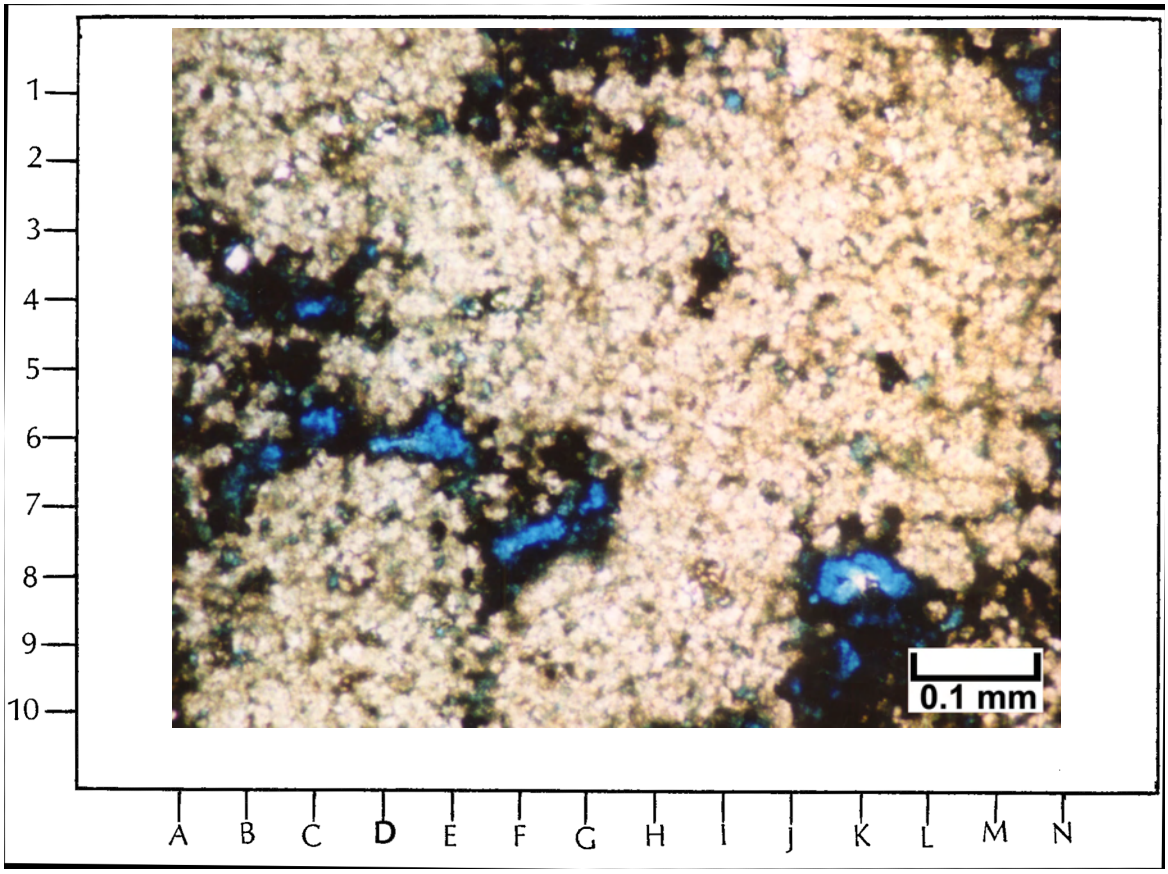
1
2
3
4
5
6
7
8
9
10
A B C D E F G H I J K L M N
0.1 mm

5768.7 feet

Top Photomicrograph

This area of the sample shows a dolomite matrix (fluorescing yellow due to probable saturation with live oil) that has been cemented with anhydrite (displaying greenish fluorescence). Most of the anhydrite resides where earlier pore space existed. The dark reddish areas are open pores lined with variable amount of black bitumen.

Bottom Photomicrograph

The same field of view as above is shown under Pl at the same magnification. In this area of anhydritic dolomite, there is no visible porosity that would be recognizable with the blue-dyed epoxy that has been impregnated into open pores. The black bitumen masks some of the pore space that EF images above.

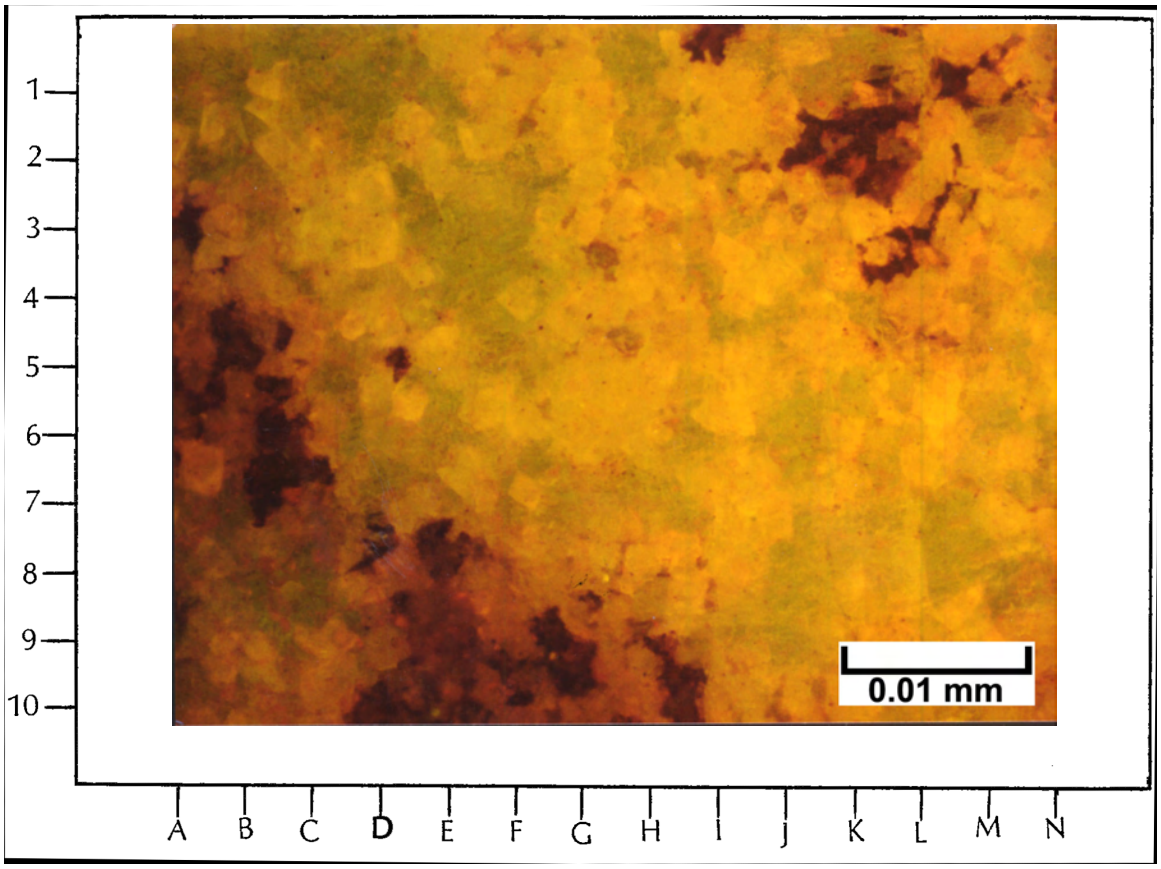
1
2
3
4
5
6
7
8
9
10
A B C D E F G H I J K L M N
0.01 mm

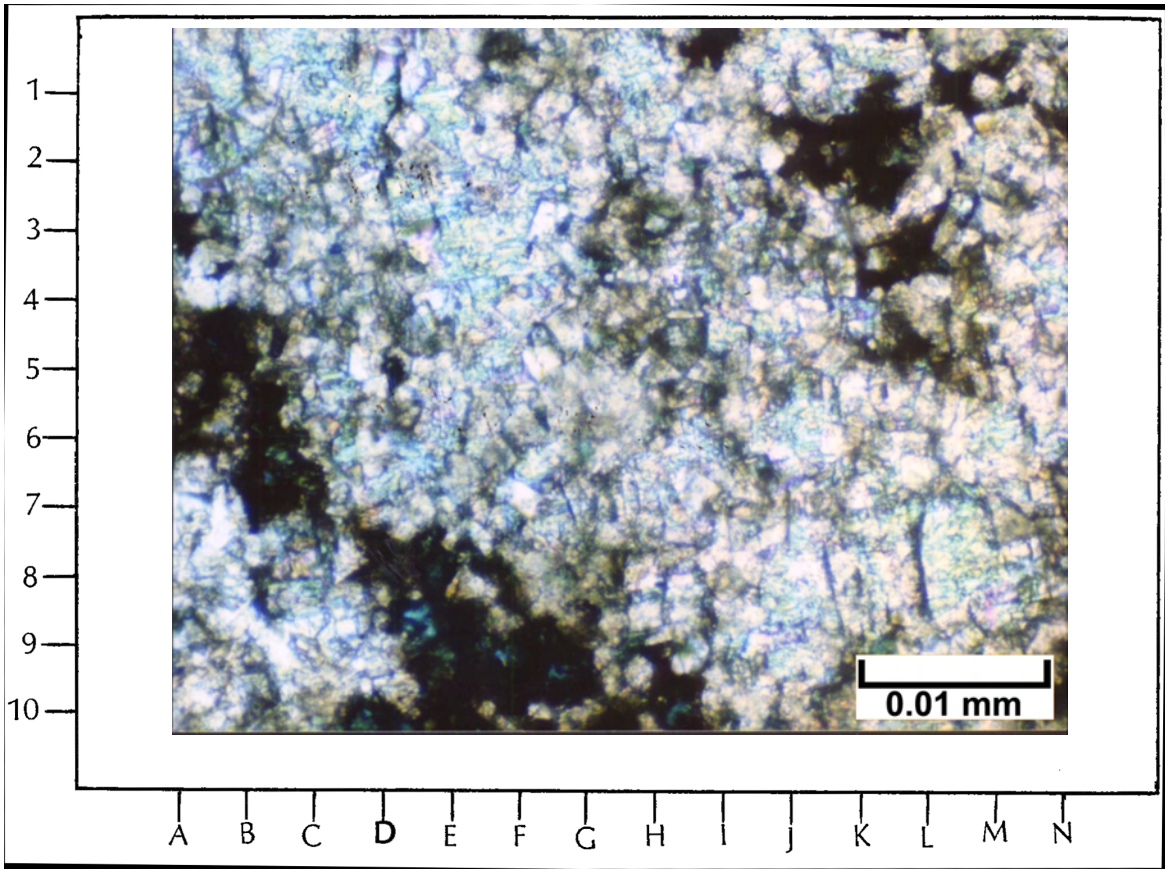
1
2
3
4
5
6
7
8
9
10
A B C D E F G H I J K L M N
0.01 mm

5778.1 feet

Top Photomicrograph

A representative EF photomicrograph of a dense dolomitic limestone under moderate magnification distinguishes porosity from oil-stained matrix. The reddish areas represent the epoxy-impregnated pores within this sample. The yellow areas are the oil-stained carbonate mineral matrix. Note that the fluorescence image helps to identify occult carbonate grains such as probable fossils (for example G-2, H-2, and J-9), small peloids (for example C-1, I-5, K-8, and so forth) that are not visible in the Pl image below. This dense limestone was deposited as a bioclastic-peloidal grainstone to packstone.

Bottom Photomicrograph

The same field of view as above is shown under Pl at the same magnification. This portion of the sample has been artificially stained with Alizarin Red-S solution. The pink areas are calcite while the white and gray areas are mostly dolomite. The indistinct black patches are indicative of some bitumen plugging within microporous spaces. The bluish areas within this view are due to the impregnation of blue-dyed epoxy into the micropores. However, it is impossible to see any of the carbonate components, the depositional texture, or the open pores without use of EF lighting as shown above.

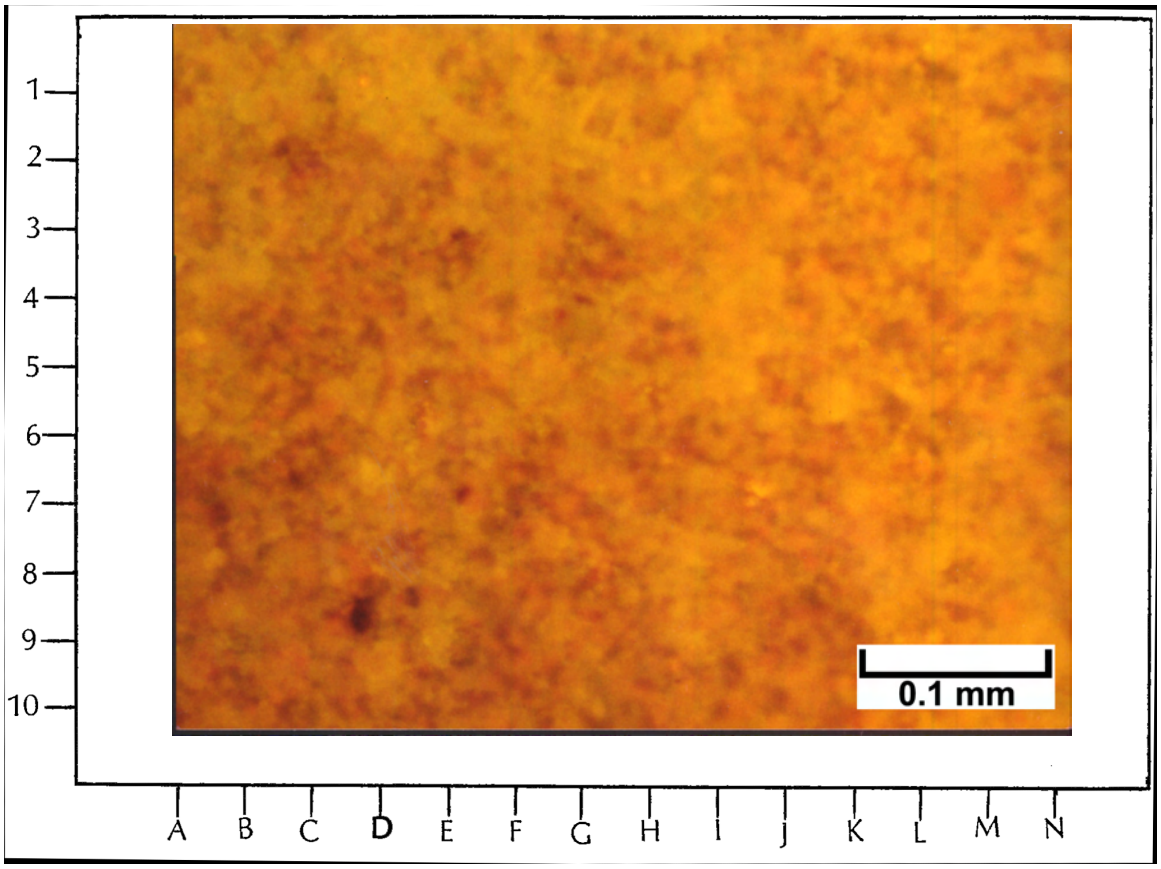
1
2
3
4
5
6
7
8
9
10
A B C D E F G H I J K L M N
0.1 mm

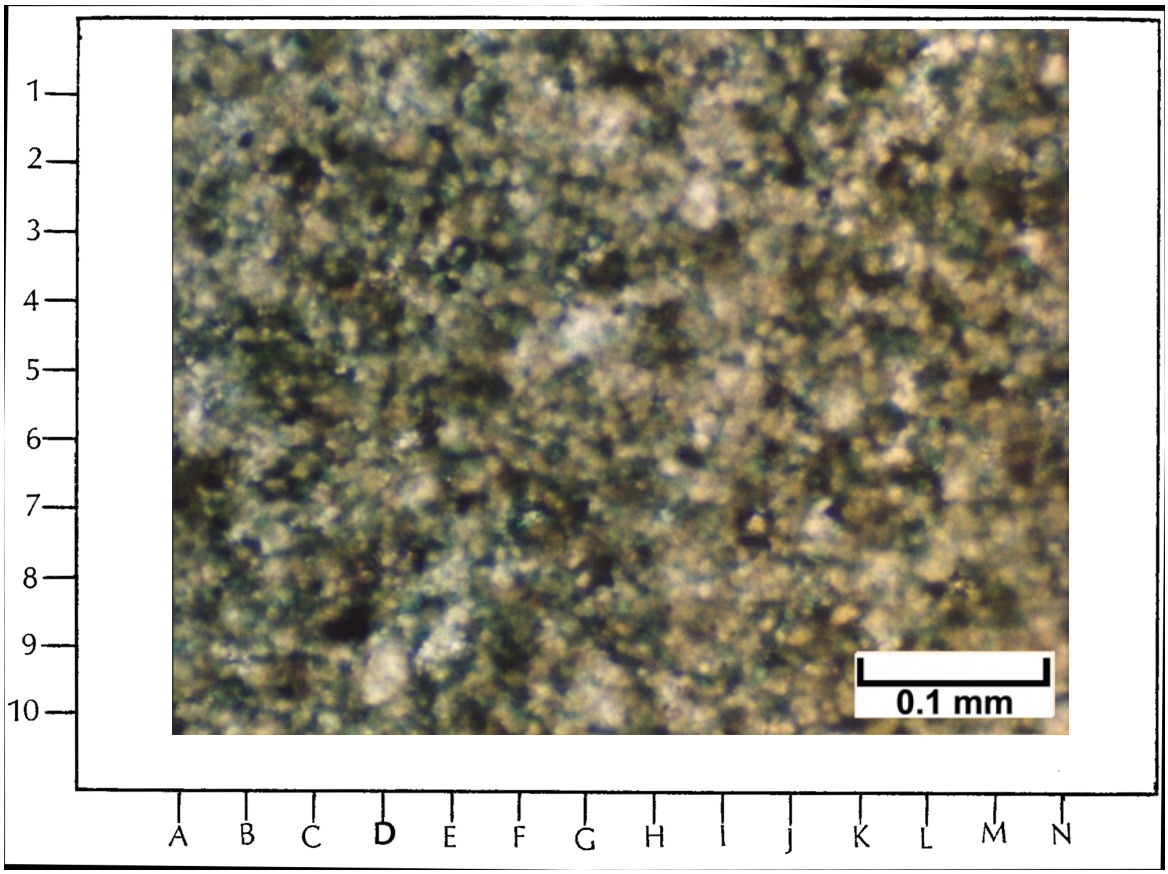
1
2
3
4
5
6
7
8
9
10
A B C D E F G H I J K L M N
0.1 mm

5778.1 feet

Top Photomicrograph

A representative EF photomicrograph under higher magnification than the previous photo pair nicely shows many of the grain outlines of the peloids and skeletal debris that make up this calcarenite (grainstone to packstone). The overprinting of dolomitization on this lithology can be seen as the abundant, small, rhombic crystal outlines (for example D-4, I-2, and J-7). The reddish and dark-colored areas of this photomicrograph are mostly pores, some of which contain bitumen linings. (The bright yellow spots in this view are surface contaminants.)

Bottom Photomicrograph

The same field of view as above is shown under Pl at the same magnification. The bluish color across this sample is due to blue-dyed epoxy filling some of the open microporosity. The black or opaque areas are indicative of abundant bitumen throughout the micropore system.

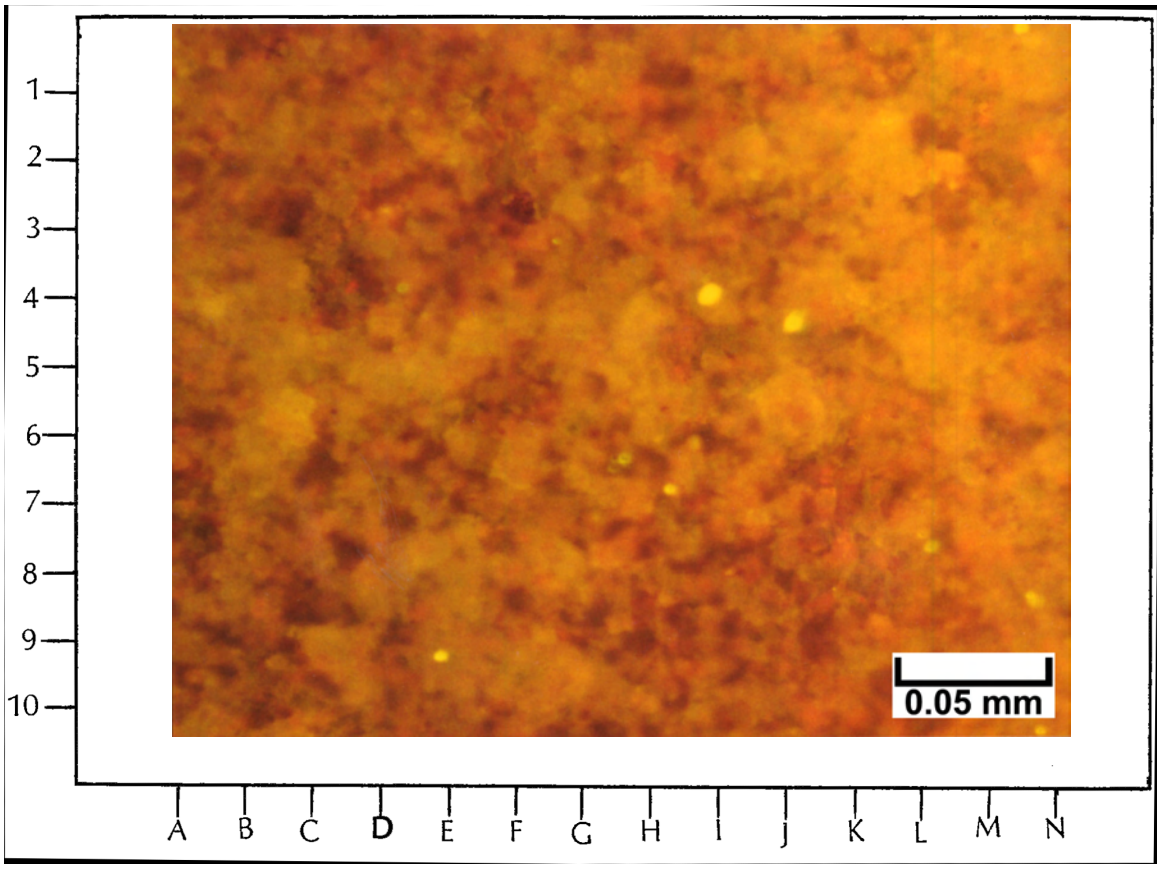
1
2
3
4
5
6
7
8
9
10
A B C D E F G H I J K L M N
0.05 mm

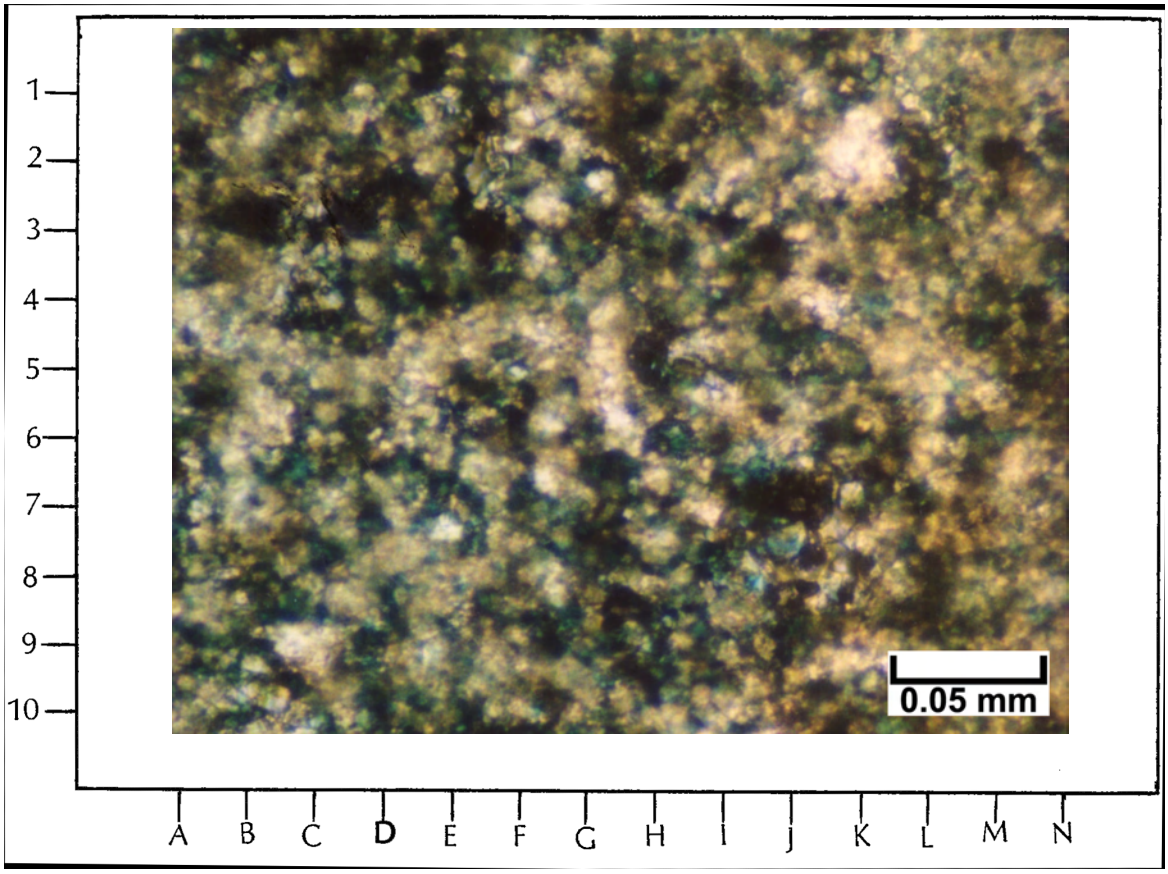
1
2
3
4
5
6
7
8
9
10
A B C D E F G H I J K L M N
0.05 mm

5783.5 feet

Top Photomicrograph

Epifluorescence in this field of view shows a very heterogeneous distribution of porosity. Here, the open-pores spaces are mostly in the red colors. Note the large, circular patch of red between B-9 and H-3. Here, pores are small, but appear to be well connected. Elsewhere, the reddish areas denoting porosity are much more patchy. Note also the areas with concentrated yellow colors. These are tighter dolomites which appear bright yellow due to the presence of trapped live oil. Within some of these tighter dolomites, it is possible to see "ghosts" of small rounded peloids (see, for instance, B-2, H-9, and H-2 to K-3).

Bottom Photomicrograph

The same field of view as above is shown under Pl at the same magnification. The presence of small amounts of black bitumen within the small pores of this sample makes it exceedingly difficult to identify pore boundaries. Only small amounts of the blue-colored epoxy that has been artificially impregnated into the pore spaces are visible in this view. The circular cross section of the concentrated area of microporosity between B-9 and H-3 may well have been a badly corroded large fossil such as a fusulinid. Note that the amount of porosity in cross section as well as the depositional texture of the tight dolomite "bridge" between I-1 and I-9 is much easier to determine in the fluorescent image above.

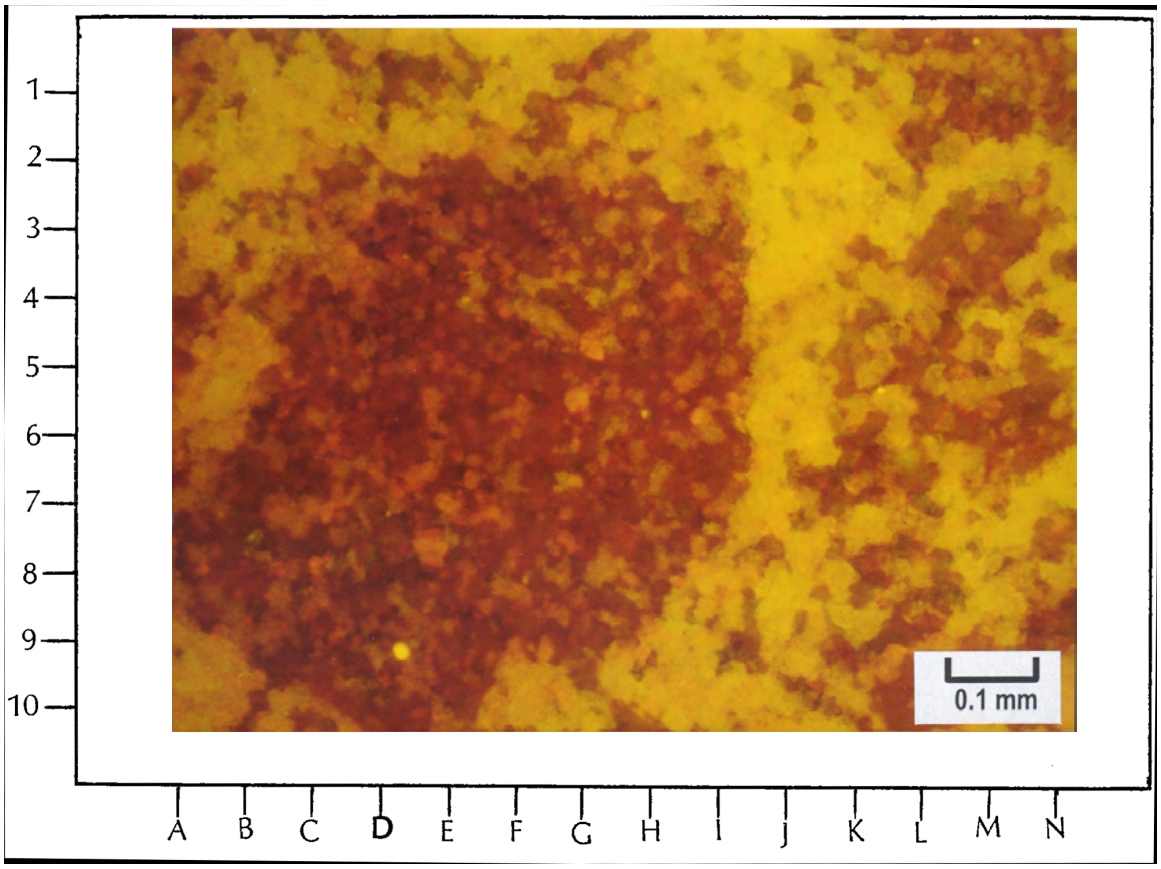
1
2
3
4
5
6
7
8
9
10
A B C D E F G H I J K L M N
0.1 mm

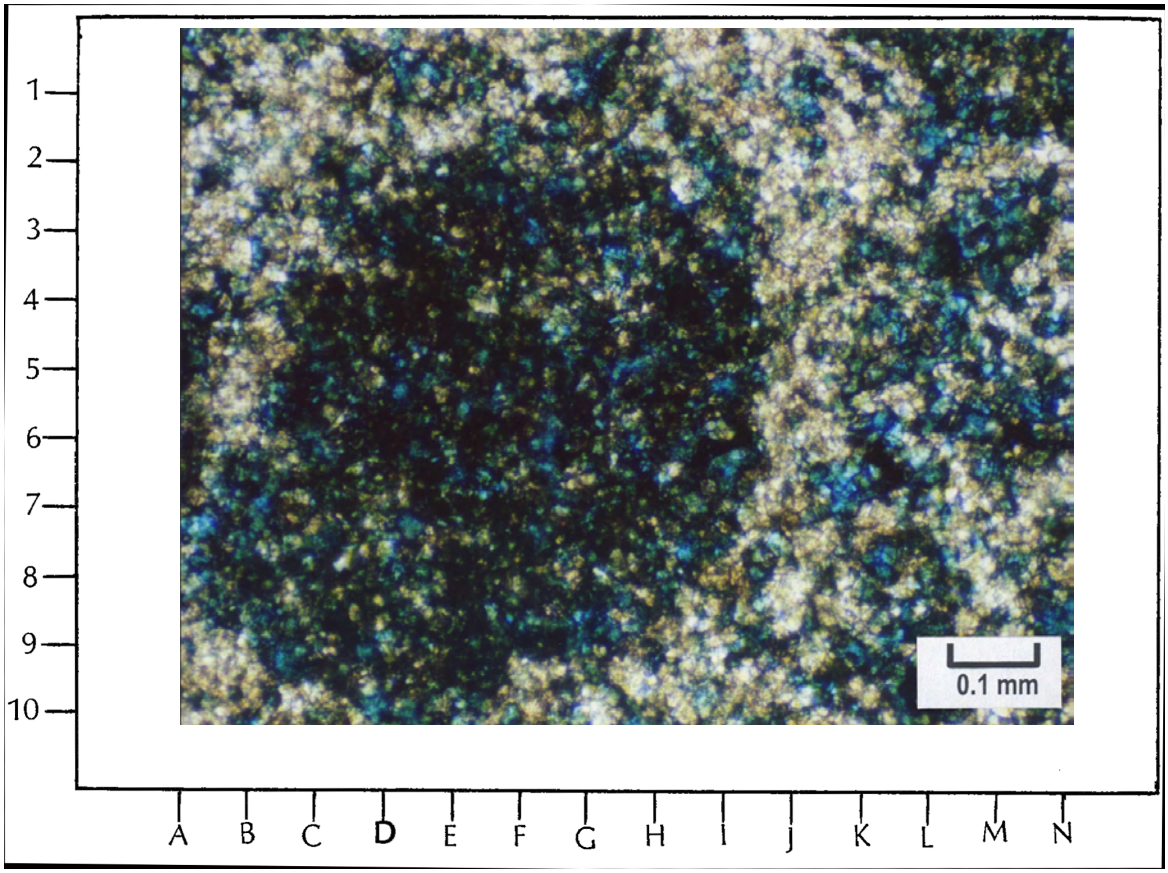
1
2
3
4
5
6
7
8
9
10
A B C D E F G H I J K L M N
0.1 mm

5783.5 feet

Top Photomicrograph

A wide range of information can be seen in this EF image. The amoeboid greenish-yellow feature in the center (from F-4 to M-7) is a small nodule of anhydrite surrounded by finely crystalline dolomite. The bright yellow rim around the anhydrite is due to live oil bleeding out of the dolomite and trapped against the impervious nodule. The dull yellow areas throughout the remainder of this image consist of dolomite containing small amount of fluorescing oils. The solid patch of dull fluorescence across the top of this photomicrograph (from E-2 to K-2) is a tight area with interlocking dolomite crystals. The black and dark red areas show where the open pore spaces occur, including pores with some bitumen coatings. Finally, the orangish areas are most likely weakly fluorescing portions of bitumen.

Bottom Photomicrograph

The same field of view as above is shown under Pl at the same magnification. Even though it is possible to identify the white nodule of anhydrite in the center of this field of view, the details of pore distribution as well as the fluorescence of live oils and bitumen distribution are not easy to see in this transmitted-light image.

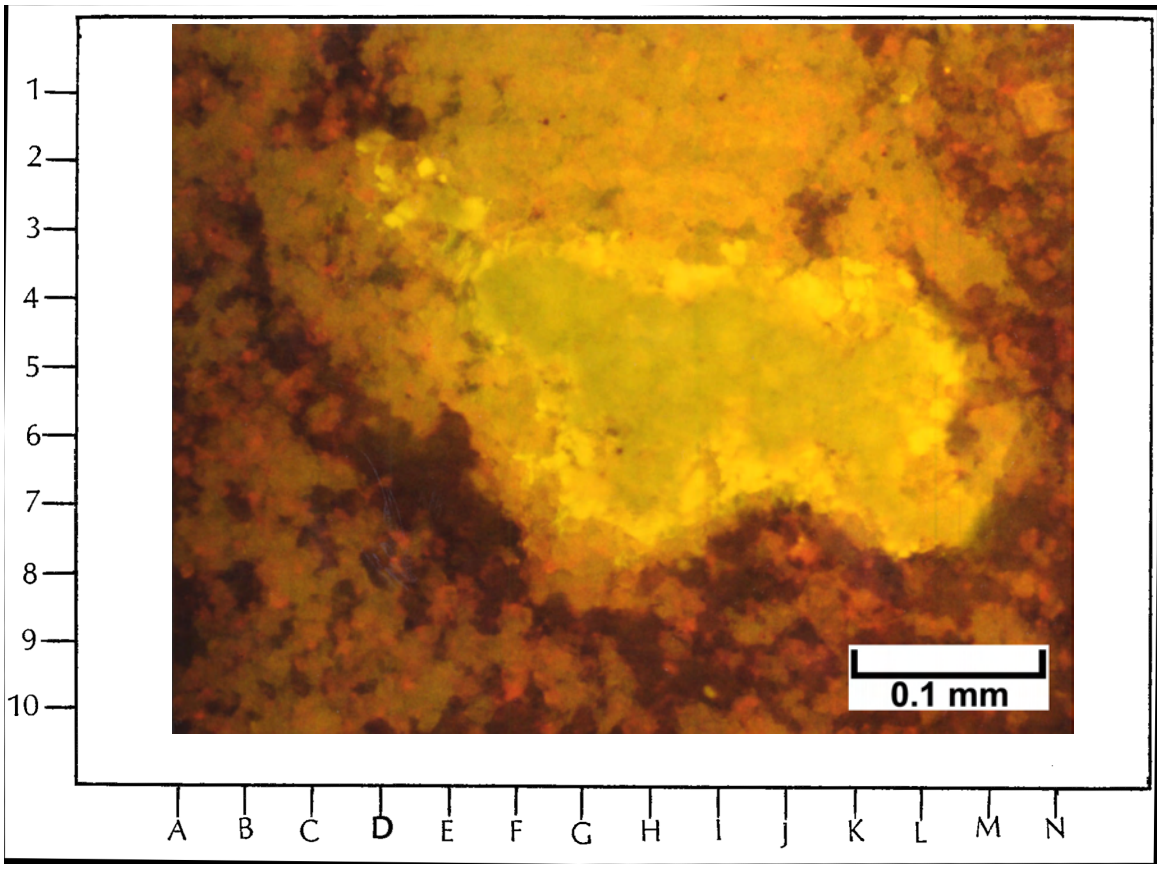
1
2
3
4
5
6
7
8
9
10
A B C D E F G H I J K L M N
0.1 mm

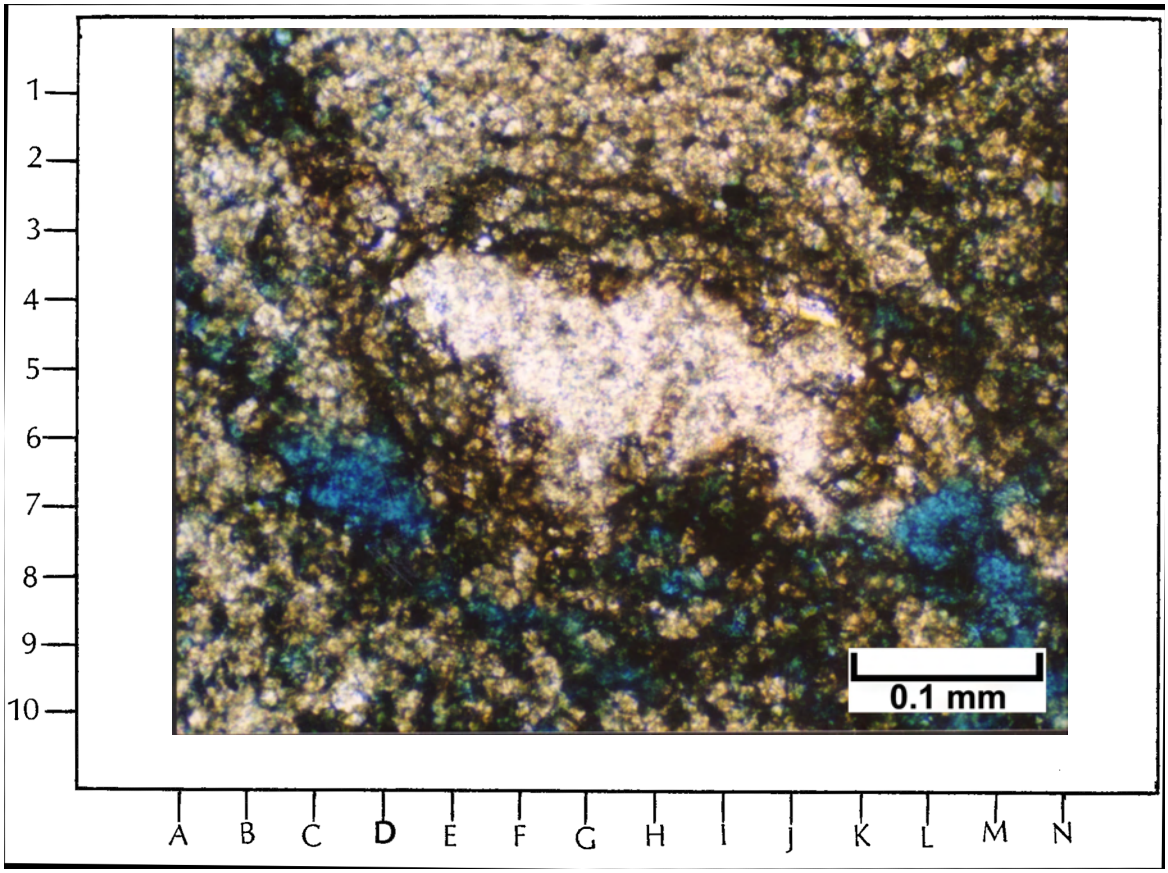
1
2
3
4
5
6
7
8
9
10
A B C D E F G H I J K L M N
0.1 mm

5783.5 feet

Top Photomicrograph

The patterns of fluorescence visible in this image provide a great deal of information when compared to the plane-polarized light view shown below. This image shows a concentration of microstylolites due to pressure solution between dolomites in dull yellow and patches of anhydritic dolomite in green. One of these stylolitic traces can be seen between C-6 and F-8. Note the large dolomite rhombs that can be seen at D-3 and F-2.5. Ghosts of former fossils and other carbonate grains of indeterminate origin can be seen at several places (for example D-7, L-8, and L-2). The small bright patches throughout this view are areas where oil is locally trapped in very tight places.

Bottom Photomicrograph

The same field of view as above is shown under Pl at the same magnification. Very little detail can be ascertained from this traditional transmitted light view due to the poor preservation within this area of tight dolomite with abundant black bitumen that masks rock details. The fluorescence view above significantly improves resolution of rock fabric from this type of rock.

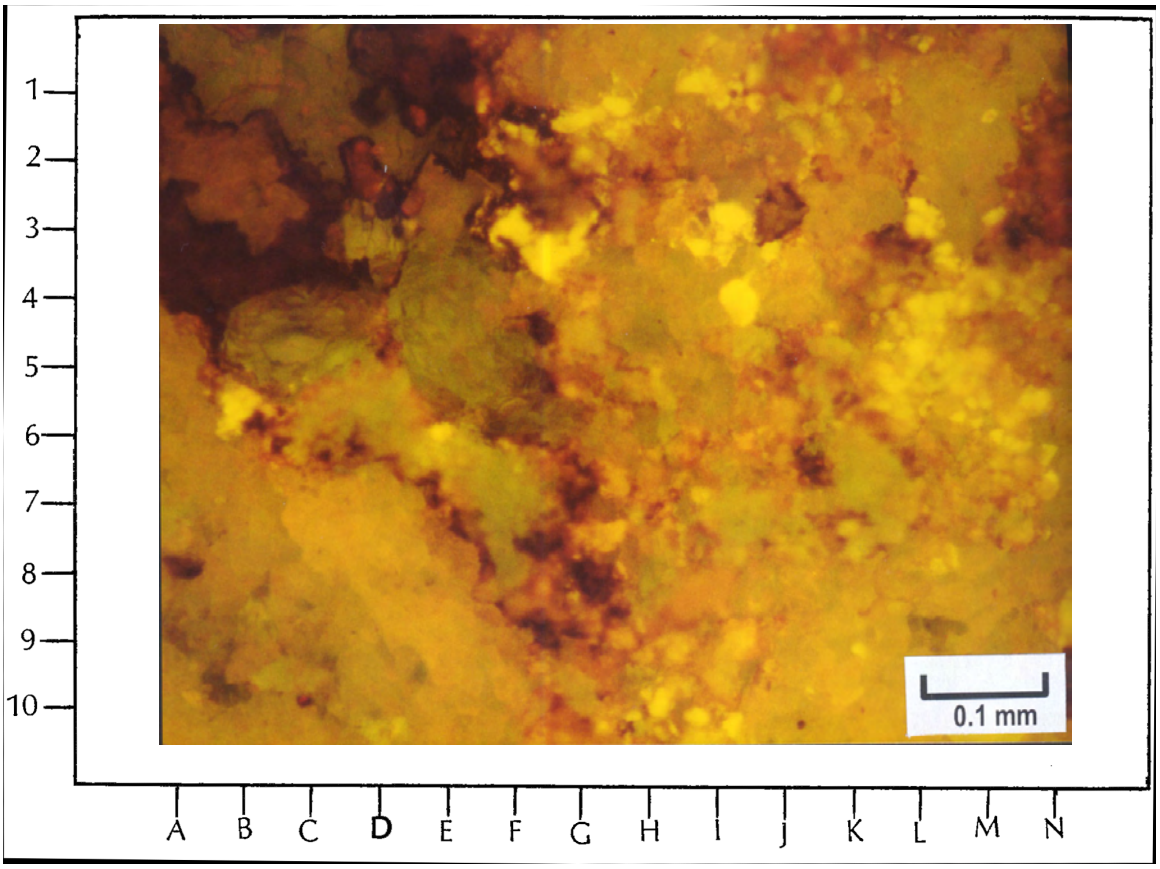
1
2
3
4
5
6
7
8
9
10
A B C D E F G H I J K L M N
0.1 mm

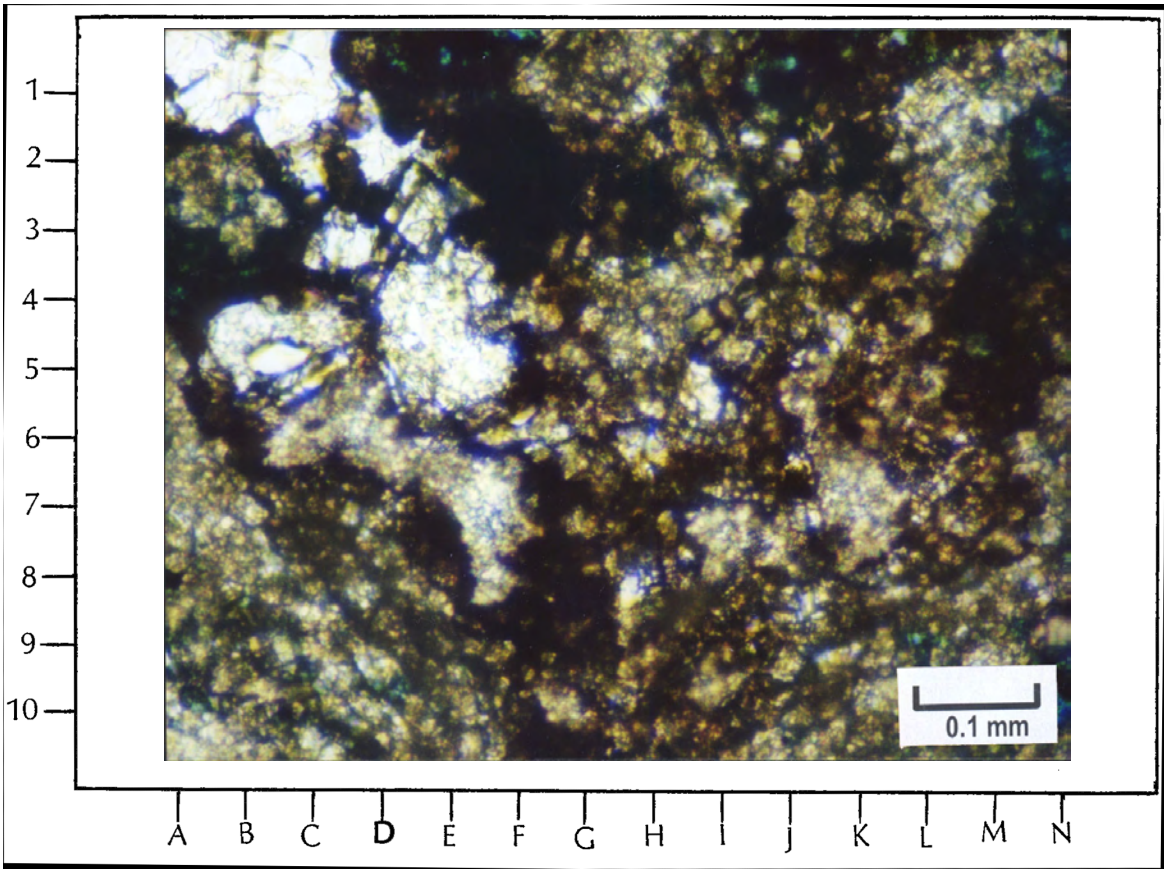
1
2
3
4
5
6
7
8
9
10
A B C D E F G H I J K L M N
0.1 mm

5783.5 feet

Top Photomicrograph

Large rhombs of dolomite replacement can be seen as the green crystals (for example E-3, G-7, K-4, and L-6) and the smaller yellow (oil-stained) crystals (for example G-2, H-7, and I-6). Open pores can be detected as the reddish areas throughout this field of view, indicating some small amounts of intercrystalline porosity.

Bottom Photomicrograph

The same field of view as above is shown under Pl at the same magnification. When comparing this photomicrograph to the one above, note that very little detail can be ascertained about the dolomite crystal size or pore distribution in this transmitted light image. One would not suspect that large dolomite rhombs with some attendant intercrystalline pore spaces were present in this lithology.

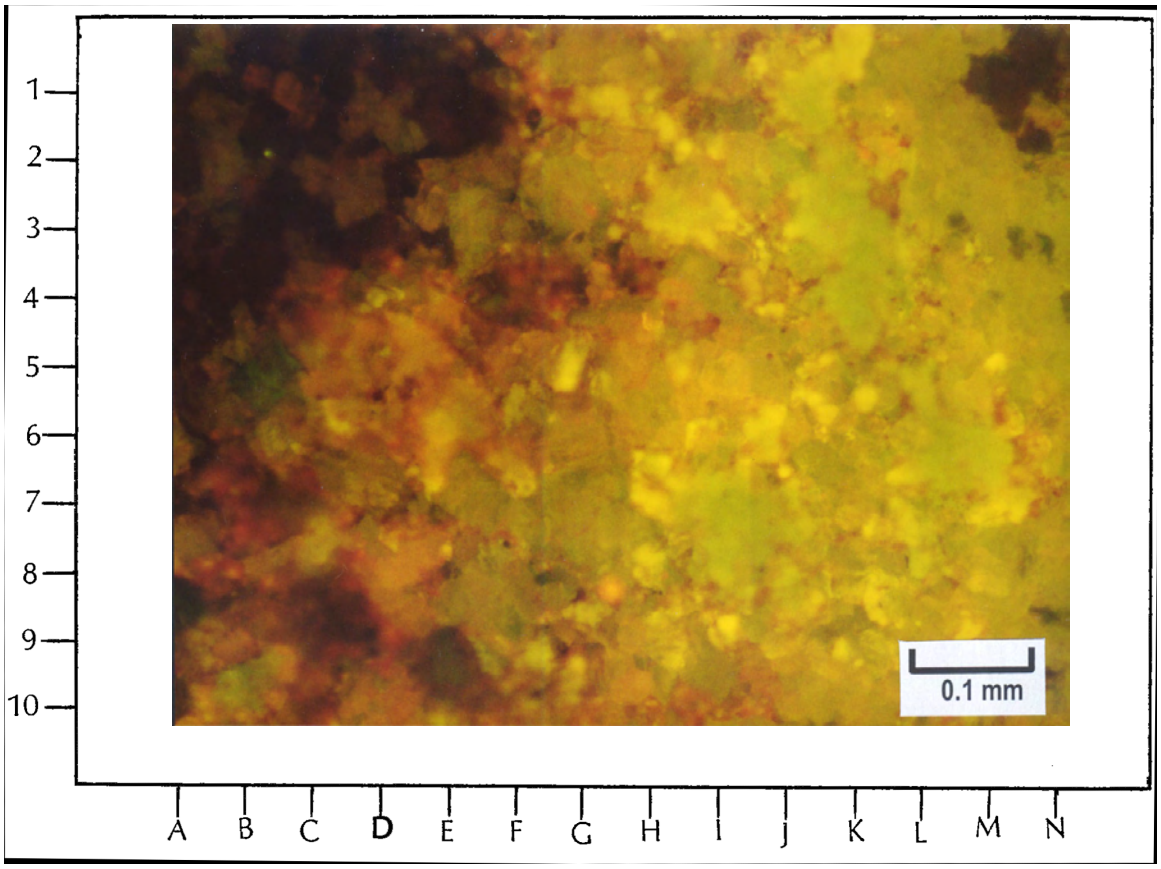
1
2
3
4
5
6
7
8
9
10
A B C D E F G H I J K L M N
0.1 mm

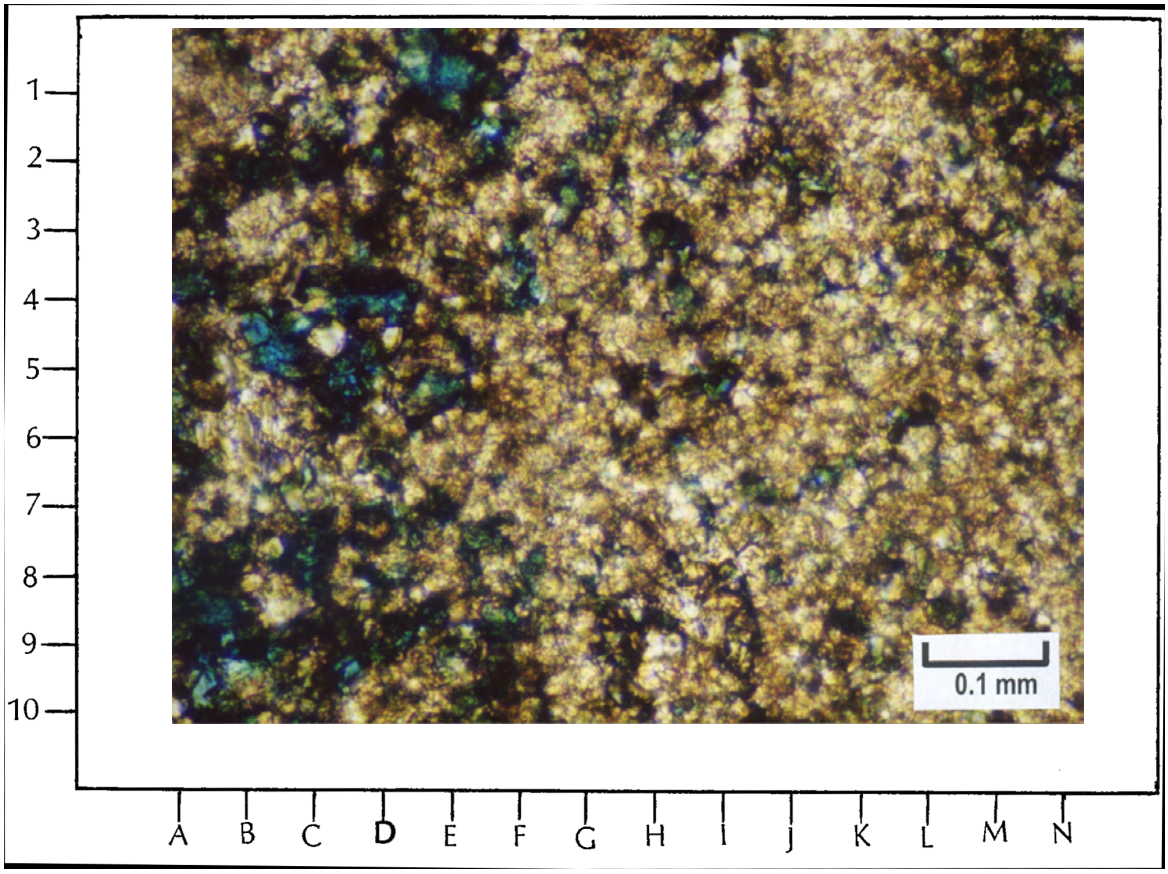
1
2
3
4
5
6
7
8
9
10
A B C D E F G H I J K L M N
0.1 mm

5783.5 feet

Top Photomicrograph

The colors shown here due to fluorescence provide some insight into the relative permeability of this dolomitic limestone as well as a visualization of the pore system. The central patch with bright yellow colors in this image represents an area of low permeability due to the concentration of live oil (in the brightest yellow colors) around the margins of the greenish yellow dolomite crystals. The reddish network in this image consists of better-connected and more permeable pores in which almost all of the live oil has been drained or evaporated from the pores. Note the intercrystalline, "microsucrosic" appearance of the dolomite crystals (in dull yellow) that are surrounded by the reddish pore network.

Bottom Photomicrograph

The same field of view as above is shown under Pl at the same magnification. This transmitted light image would be a difficult one with which to assess reservoir quality, that is permeability and pore distribution. Although there is an abundant amount of blue-dyed epoxy visible in this cross section, it is difficult to clearly resolve individual pore intersections. Only the brownish oil stain in the central region of this image would provide a hint of the low permeability region within this sample.

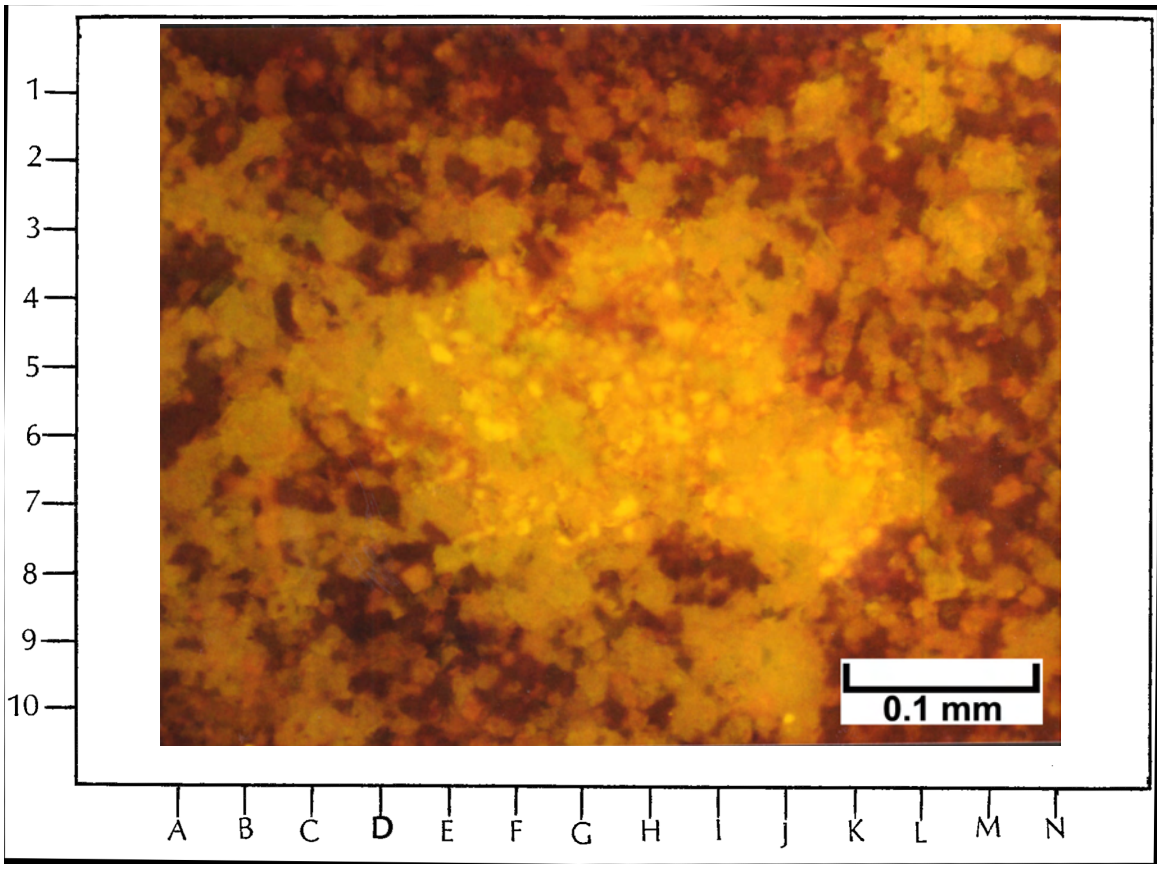
1
2
3
4
5
6
7
8
9
10
A B C D E F G H I J K L M N
0.1 mm

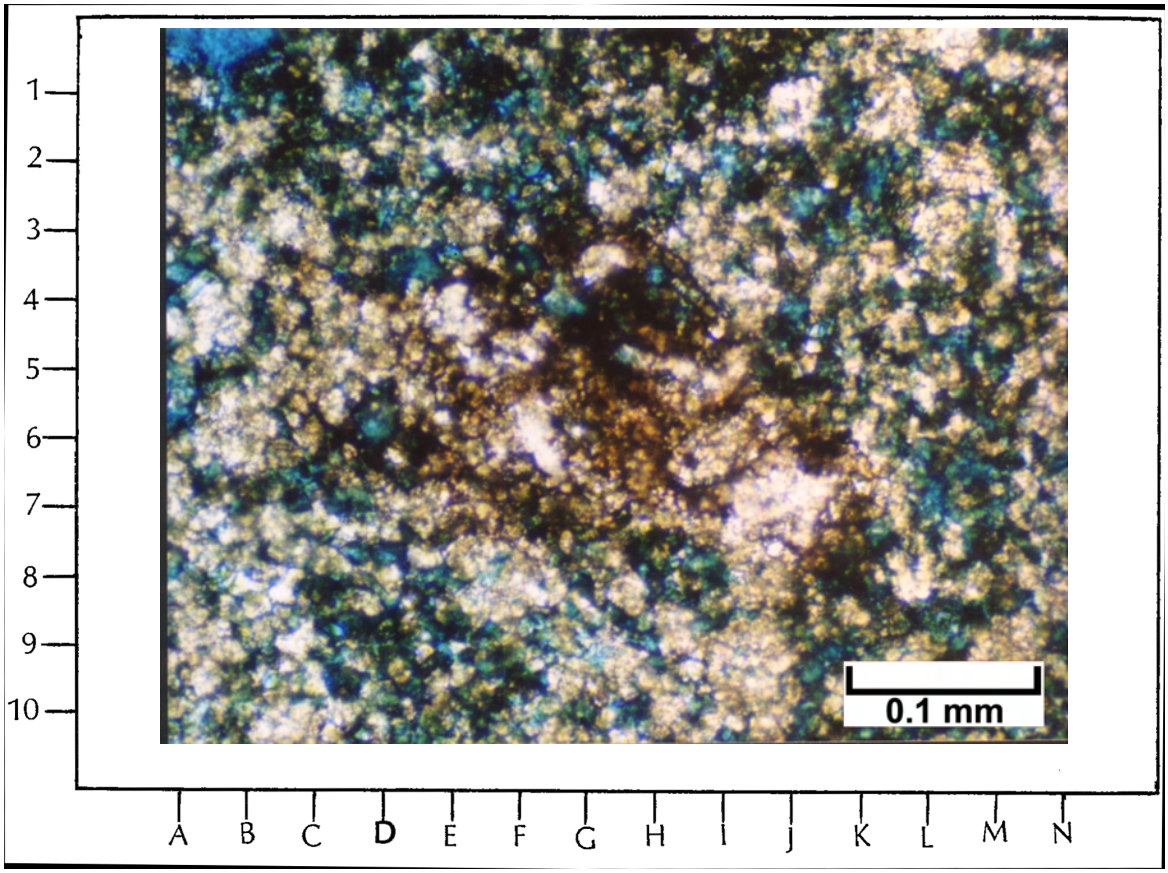
1
2
3
4
5
6
7
8
9
10
A B C D E F G H I J K L M N
0.1 mm

5801.3 feet

Top Photomicrograph

Abundant pore space can be seen in this fluorescence image, where the epoxy-impregnated pores appear red. Despite the heterogeneity of the distribution of pores, most of this microporosity seems to be moderately well connected. The greenish yellow and yellow colors in this image are from matrix areas composed of dolomite and limestone. The brightest yellow areas reflect staining of the matrix by live oil. Note the hints of earlier sand-sized carbonate grains (for example F-1.5, H-2, and L-5) and occasional isolated larger dolomite rhombs (for example B-1.5, G-7, and K-2).

Bottom Photomicrograph

The same field of view as above is shown under Pl at the same magnification. Note that the details of the pore sizes and shapes cannot be seen in this transmitted light photomicrograph. Abundant black bitumen throughout this microporous network makes it nearly impossible to see the amount of visible porosity. At best, the microporosity in this image shows up as an indistinct "blue haze." In addition, it is not possible to see any hints of original grains or the sizes of dolomite crystals.

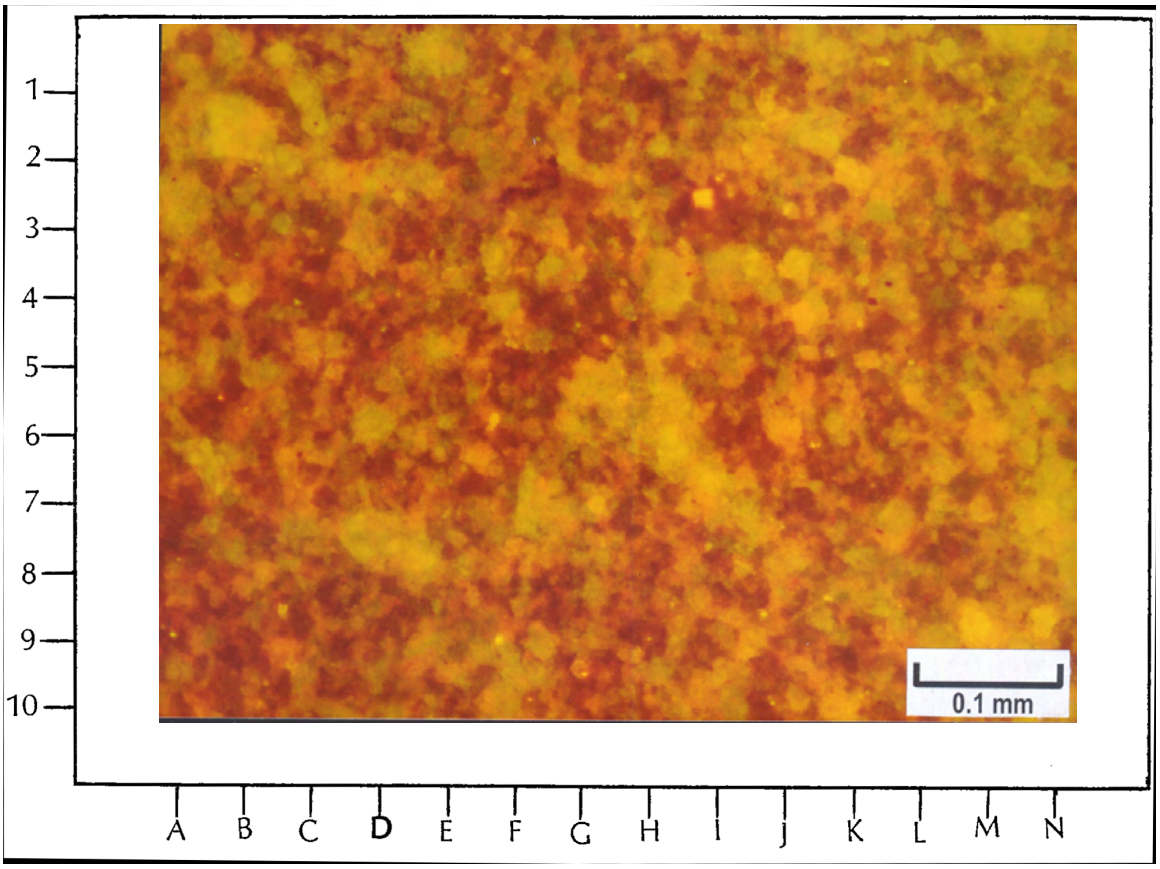
1
2
3
4
5
6
7
8
9
10
A B C D E F G H I J K L M N
0.1 mm

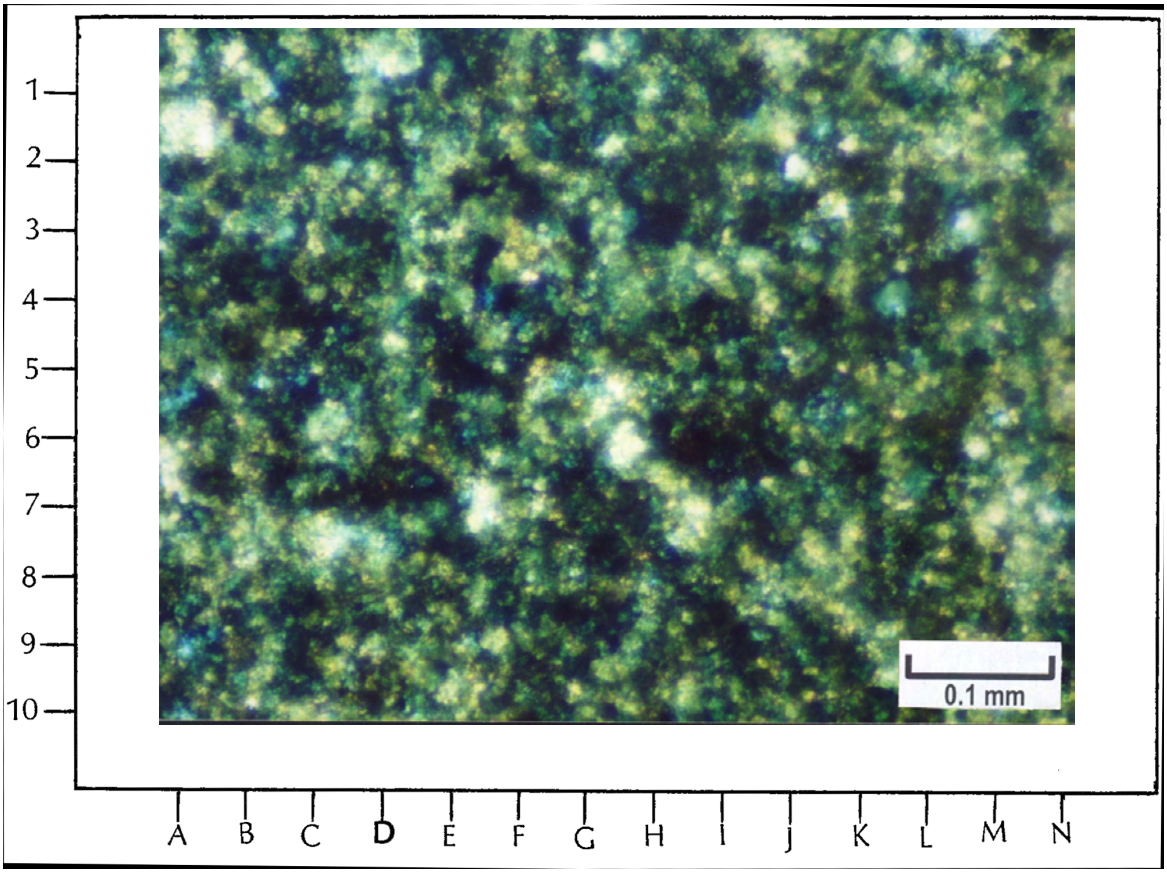
1
2
3
4
5
6
7
8
9
10
A B C D E F G H I J K L M N
0.1 mm

5801.3 feet

Top Photomicrograph

This high magnification fluorescence view nicely shows the individual mini-rhombs of dolomite making up the matrix of this sample. Note that some of the areas of dolomite fluoresce a brighter yellow due to live oil entrapment in areas of lower permeability. In general, most of the mini-rhombs of dolomite are dull yellow to light green due to the fairly uniform permeability throughout most of this sample. The reddish and dark-colored areas of this image show the open pores. Overall, this sample shows nice micro-intercrystalline porosity within a "microsucrosic" dolomite. The presence of black bitumen (see the photomicrograph below) does not seem to completely plug the pores as shown by the red fluorescing epoxy that has been impregnated into open-pore space.

Bottom Photomicrograph

The same field of view as above is shown under Pl at the same magnification. Very little detail can be discerned in this transmitted-light view compared to the fluorescent photomicrograph above. The black and opaque nature of bitumen linings within some pores overwhelms the image such that more pore boundaries are difficult to see.

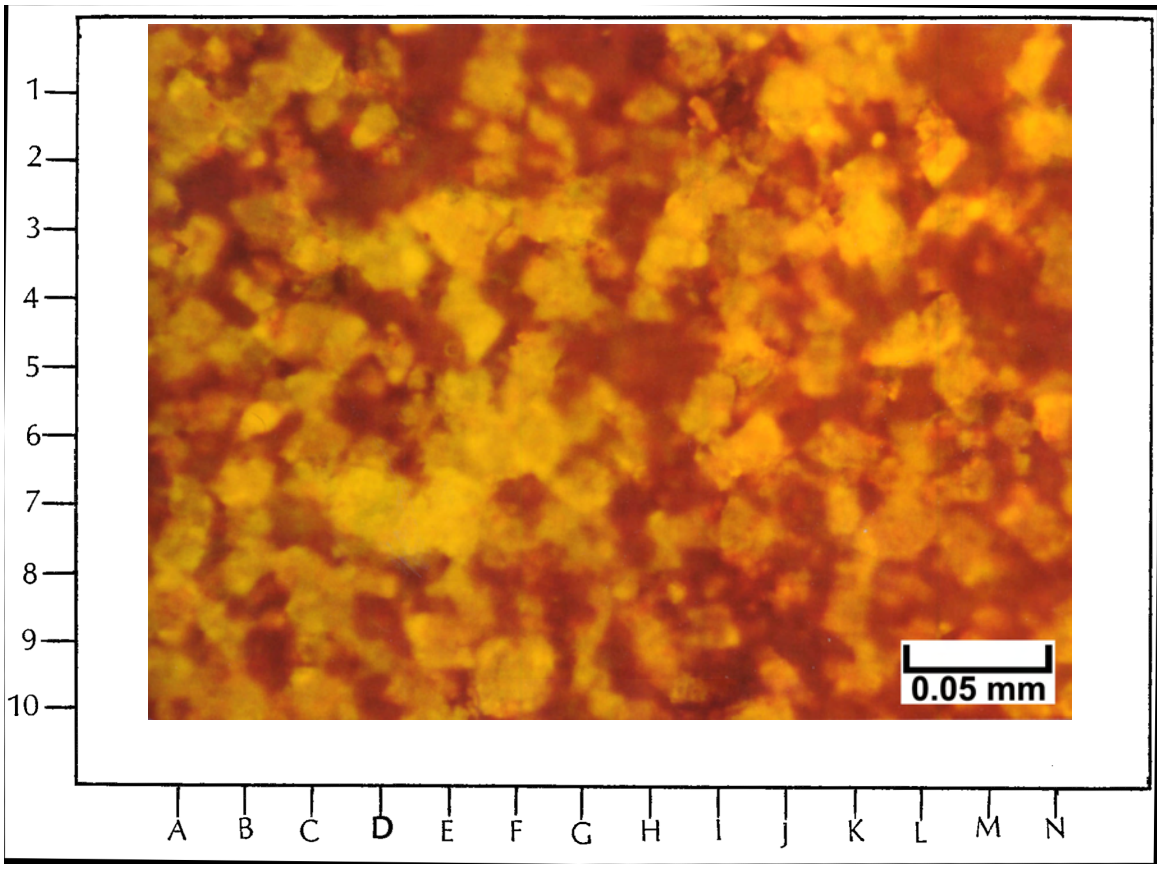
1
2
3
4
5
6
7
8
9
10
A B C D E F G H I J K L M N
0.05 mm

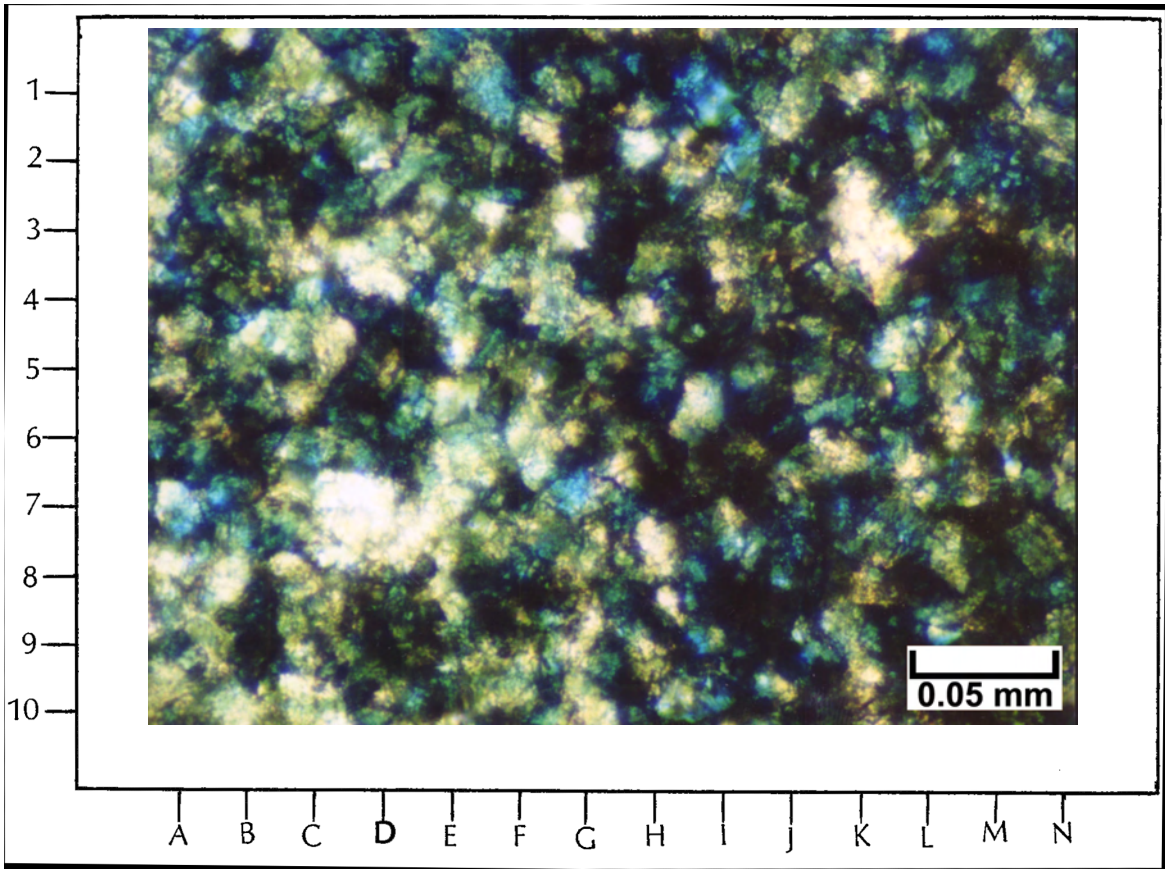
1
2
3
4
5
6
7
8
9
10
A B C D E F G H I J K L M N
0.05 mm

5801.3 feet

Top Photomicrograph

This image shows a permeability barrier along a pressure-solution or stylolitic seam with non-fluorescing insoluble residues. On either side of this stylolite, there is evidence of some matrix microporosity (in the reddish areas as well as relict carbonate grains within this limestone). A few dolomite crystals can also be seen as the occasional greenish areas in this image.

Bottom Photomicrograph

The same field of view as above is shown under Pl at the same magnification. The black material concentrated across the upper portion of this photomicrograph is the insoluble residue along the stylolitic seam. Hints of some of the matrix microporosity can be seen in the bluish color of the image along the bottom. Note that it is not possible to resolve any textural or compositional detail of this sample like the fluorescence photomicrograph at the top provides.

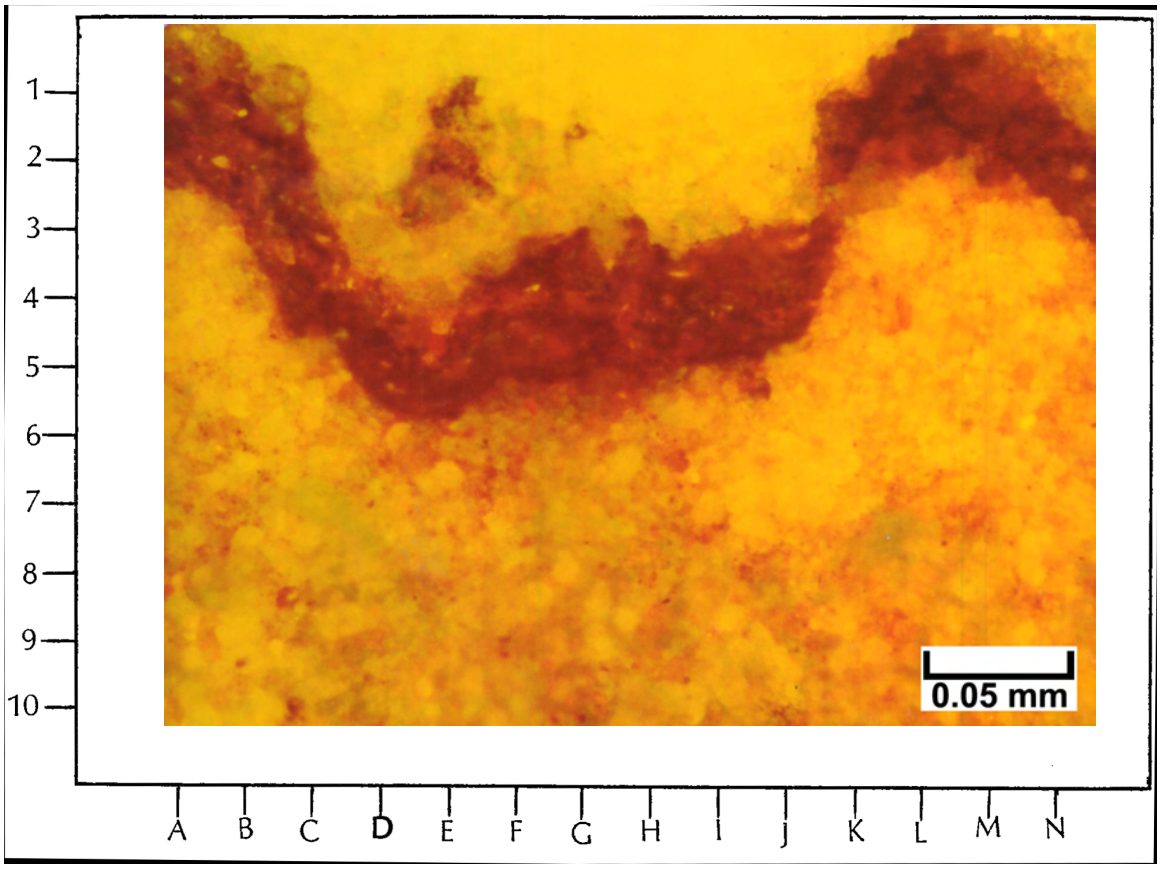
1
2
3
4
5
6
7
8
9
10
A B C D E F G H I J K L M N
0.05 mm

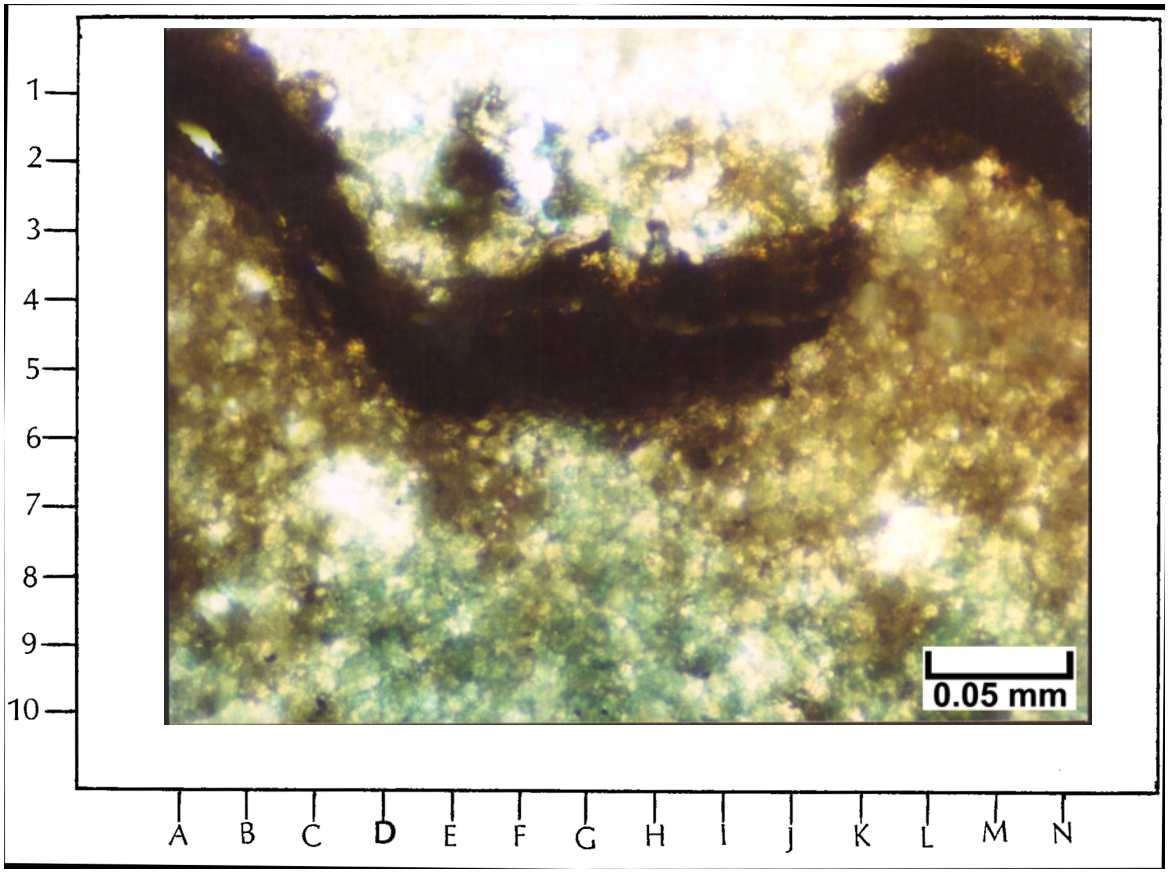
1
2
3
4
5
6
7
8
9
10
A B C D E F G H I J K L M N
0.05 mm

5813.8 feet

Top Photomicrograph

This sample shows a representative area with significant amounts of microporosity with bitumen linings which fluoresce red and orange in this image. The dolomitic limestone matrix in this specimen fluoresces yellow (where oil-stained) and green. There are a few small patches of tight matrix surrounded by pervasive microporosity throughout.

Bottom Photomicrograph

The same field of view as above is shown under Pl at the same magnification. This lighting does not image the extensive microporosity in this sample very well even though there are some hints of blue-dyed epoxy here and there. The porosity does not show up very well under transmitted light because the pores are much smaller than the thickness of the thin section. In addition, opaque bitumen linings block light from passing through some of the pores to the observer.

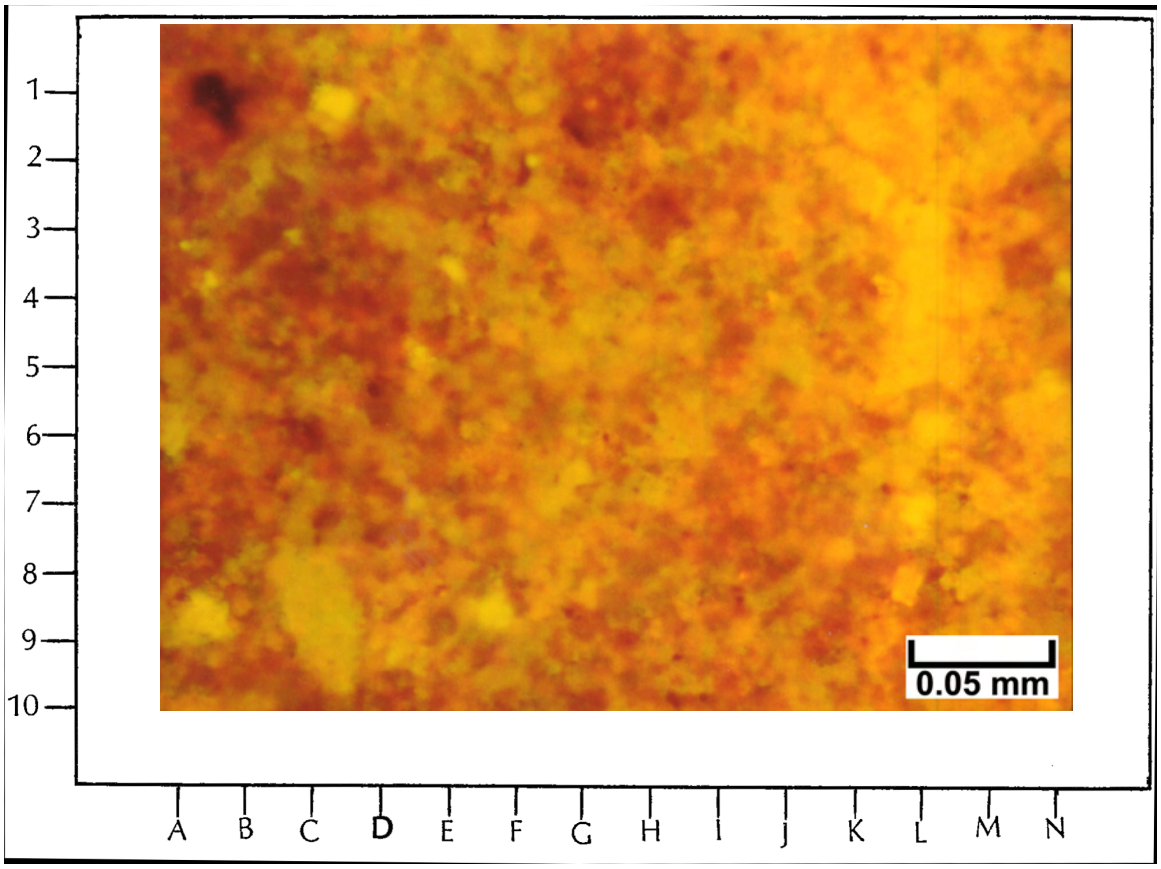
1
2
3
4
5
6
7
8
9
10
A B C D E F G H I J K L M N
0.05 mm

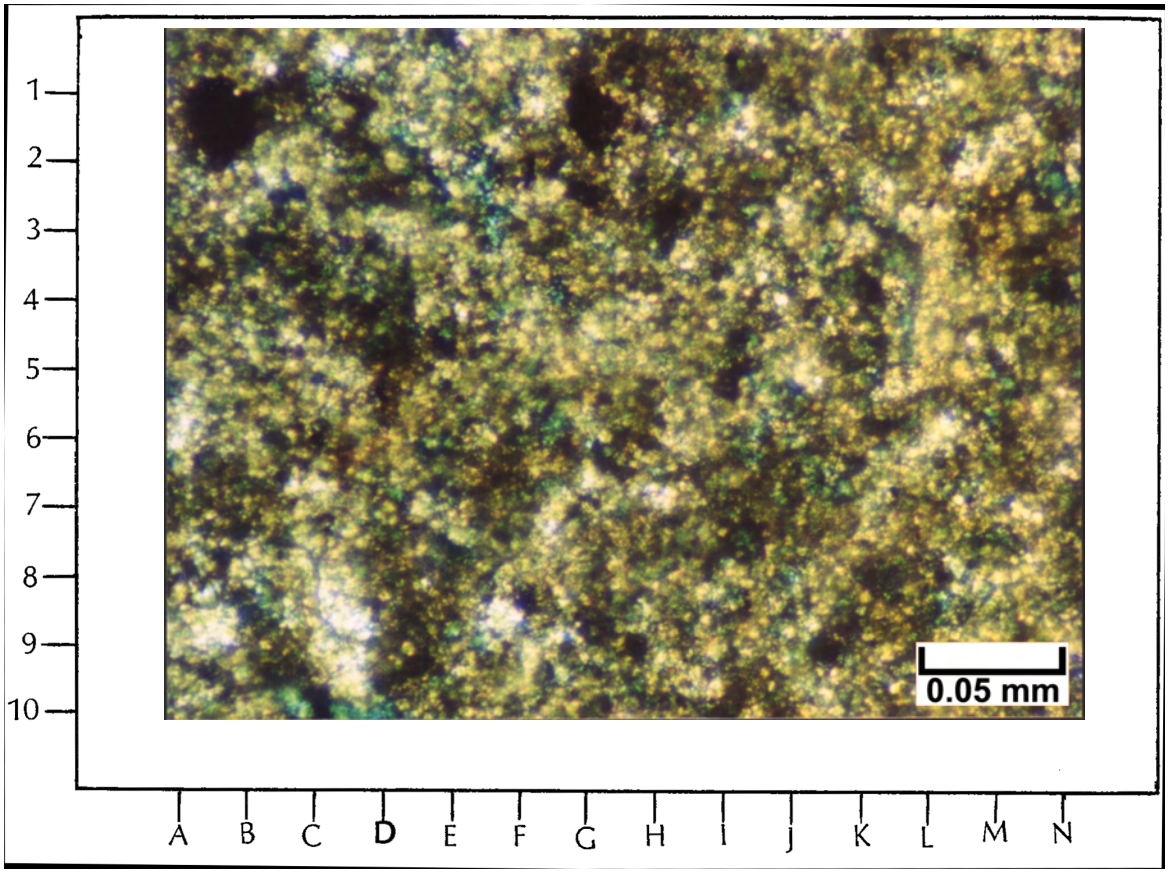
1
2
3
4
5
6
7
8
9
10
A B C D E F G H I J K L M N
0.05 mm

5831.8 feet

Top Photomicrograph

This sample comes from a limestone sample in an area that displays abundant pore space as indicated by the areas of red-fluorescing epoxy. Note that the left side displays well-connected areas of open pores while the right side shows a slightly dolomitic limestone with more isolated pores. The yellow-fluorescing areas are oil-stained carbonates surrounding the radiating pore networks in red. The presence of abundant bitumen in this sample (see below) does not seem to plug the pore space in any significant way.

Bottom Photomicrograph

The same field of view as above is shown under Pl at the same magnification. There is not much visible pore space under this lighting (a paucity of blue-dyed epoxy). Compare this photomicrograph with the fluorescence image above, where the red-colored areas show the open-pore spaces. The black (opaque) bitumen linings around most pores apparently block light from passing through some of the pores to the observer. (The red-brown areas in this bottom image are residues from artificial staining by Alizarin Red-S solution).

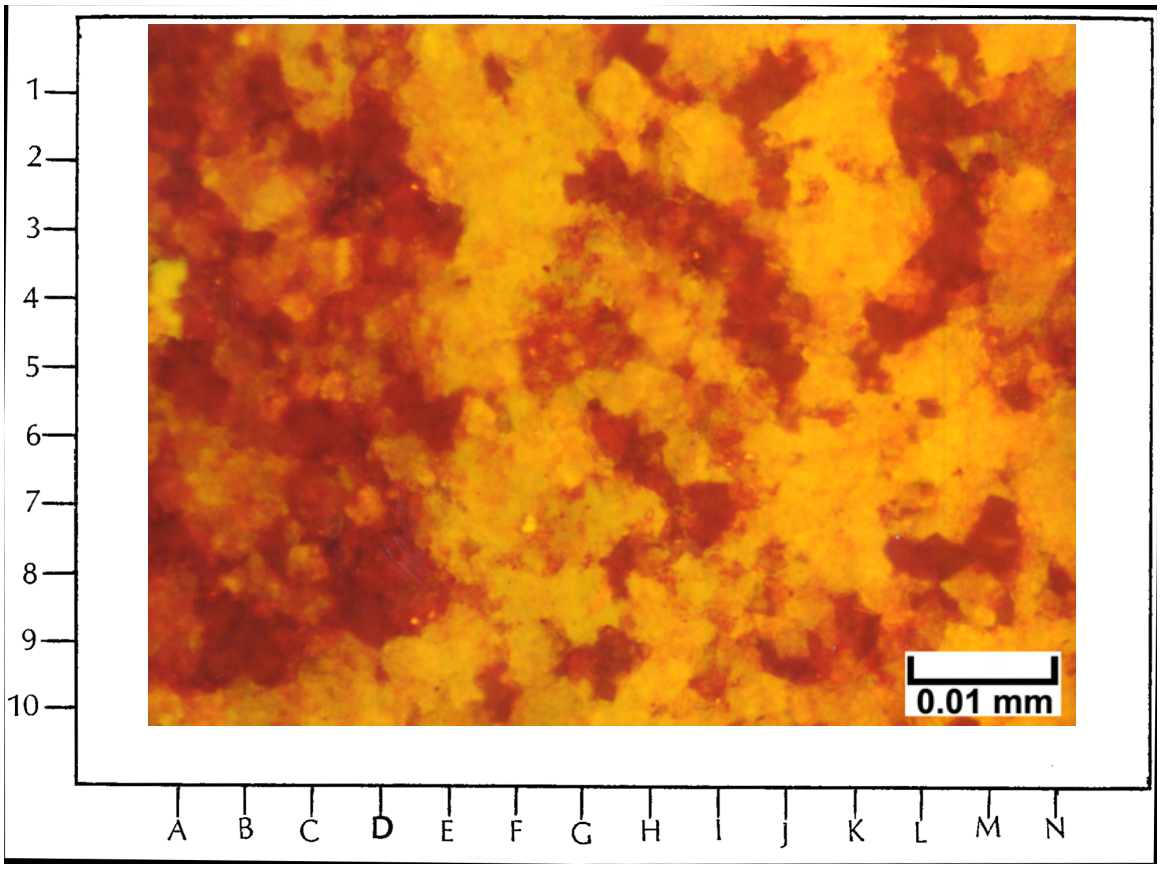
1
2
3
4
5
6
7
8
9
10
A B C D E F G H I J K L M N
0.01 mm

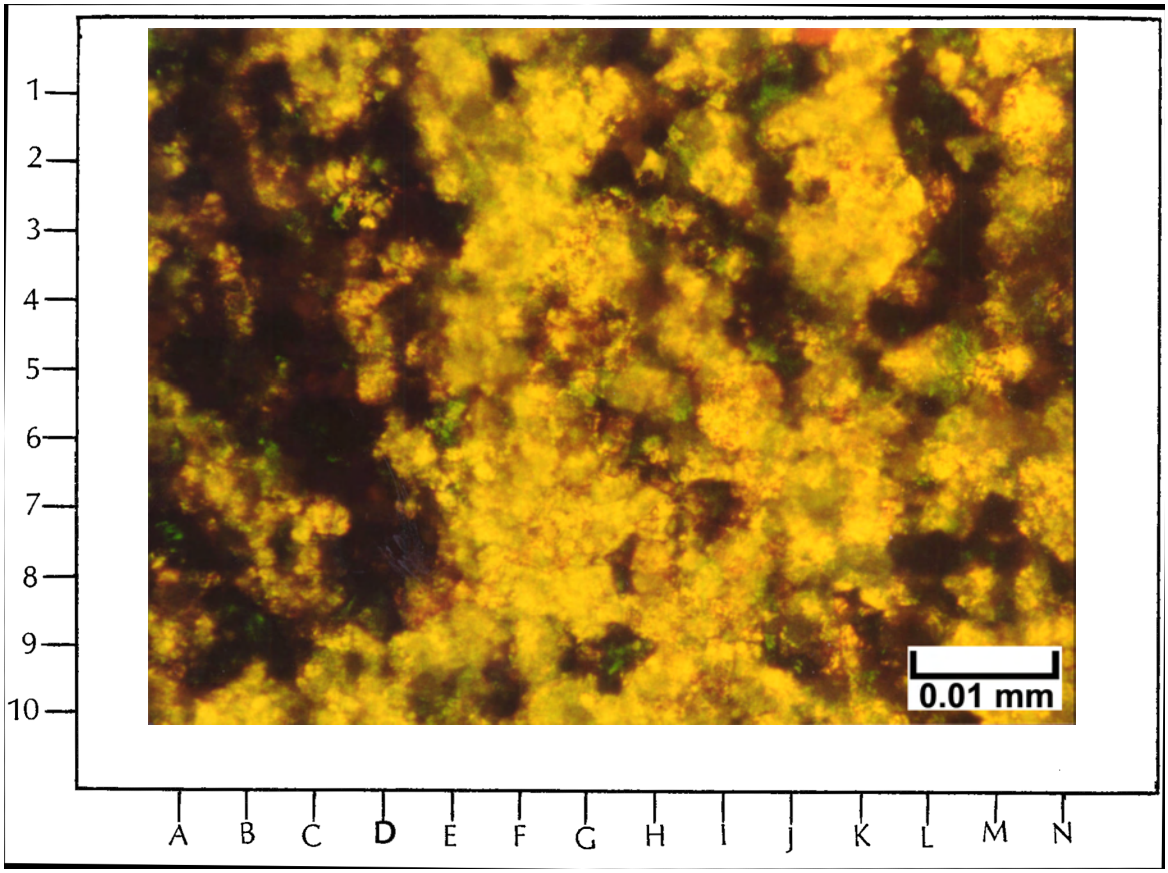
1
2
3
4
5
6
7
8
9
10
A B C D E F G H I J K L M N
0.01 mm

5864.1 feet

Top Photomicrograph

This sample comes from a rather tight limestone than has no visible matrix porosity under transmitted lighting (see photomicrograph below). However, under fluorescence microscopy, there is some red fluorescence from spiked epoxy that has been impregnated into matrix pore spaces. Therefore, the scattered red spots in this image show the presence of some porosity. The abundant bright yellow specks across the image are probably the result of live oil staining throughout this relatively low-porosity sample. Note the dull green areas which show some relict preservation of the peloids (for example E-3, F-4, and L-8) that were the principal constituent of this carbonate sediment.

Bottom Photomicrograph

The same field of view as above is shown under Pl at the same magnification. There is no visible matrix porosity in this image (that is no blue colors) despite the appearance of some areas of fluorescing epoxy-filled pores in the image above. In addition, the peloids that can be seen in the fluorescence view are very difficult to make out in this transmitted light view.

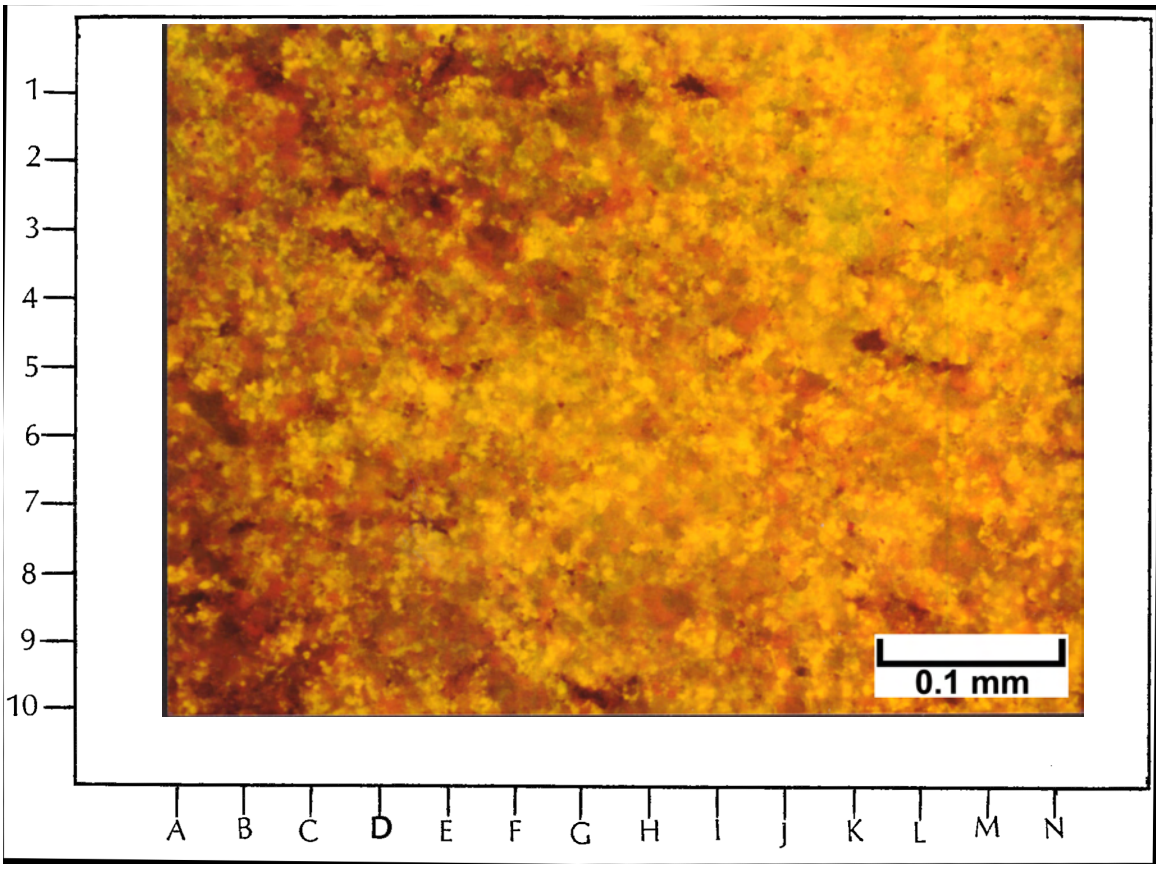
1
2
3
4
5
6
7
8
9
10
A B C D E F G H I J K L M N
0.1 mm

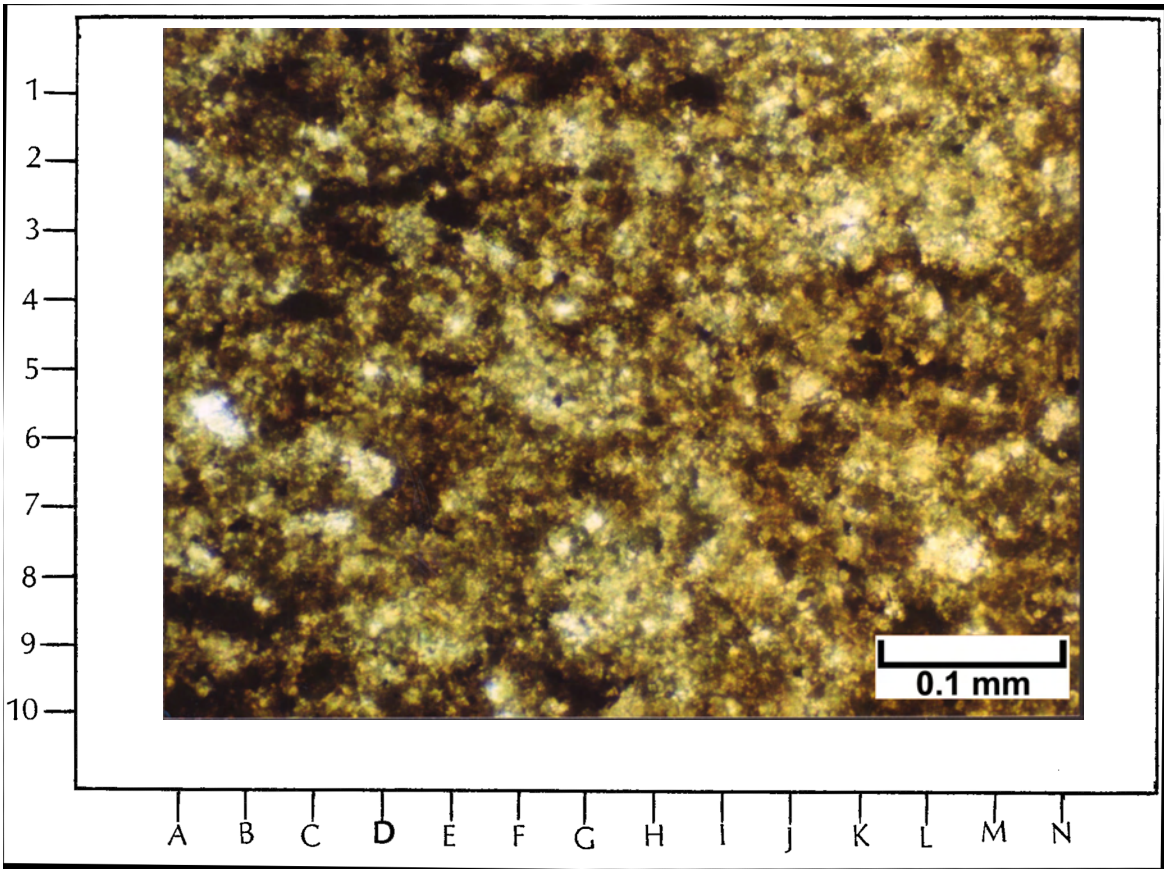
1
2
3
4
5
6
7
8
9
10
A B C D E F G H I J K L M N
0.1 mm

5864.1 feet

Top Photomicrograph

This sample shows significant heterogeneity in porosity distribution, especially in the vicinity of wispy stylolitic seams. The darkest areas (dark brown in color here) are mostly concentrations of insoluble residues along the stylolites. The red areas represent fluorescence of epoxy-impregnated microporosity. Note in particular the abundant pore spaces in the upper left corner of this photomicrograph, immediately above a relatively thick stylolitic seam. The bright yellow areas represent the fluorescence of mostly live oil surrounding tight rock matrix. Hence, the stylolitic seams in this field of view appear to segregate relatively porous versus very tight rock matrix. These stylolitic seams provide important permeability barriers to fluid flow between the relatively porous and the tight rock compartments.

Bottom Photomicrograph

The same field of view as above is shown under Pl at the same magnification. The stylolitic seams of pressure-solution origin shows up as the sinuous black patterns in this image. However, there is no visible matrix porosity under this lighting. The dense limestone matrix appears in this view to be equally tight between each stylolitic seam. However, the EF image above clearly shows significant variations in the open-pore space distribution.

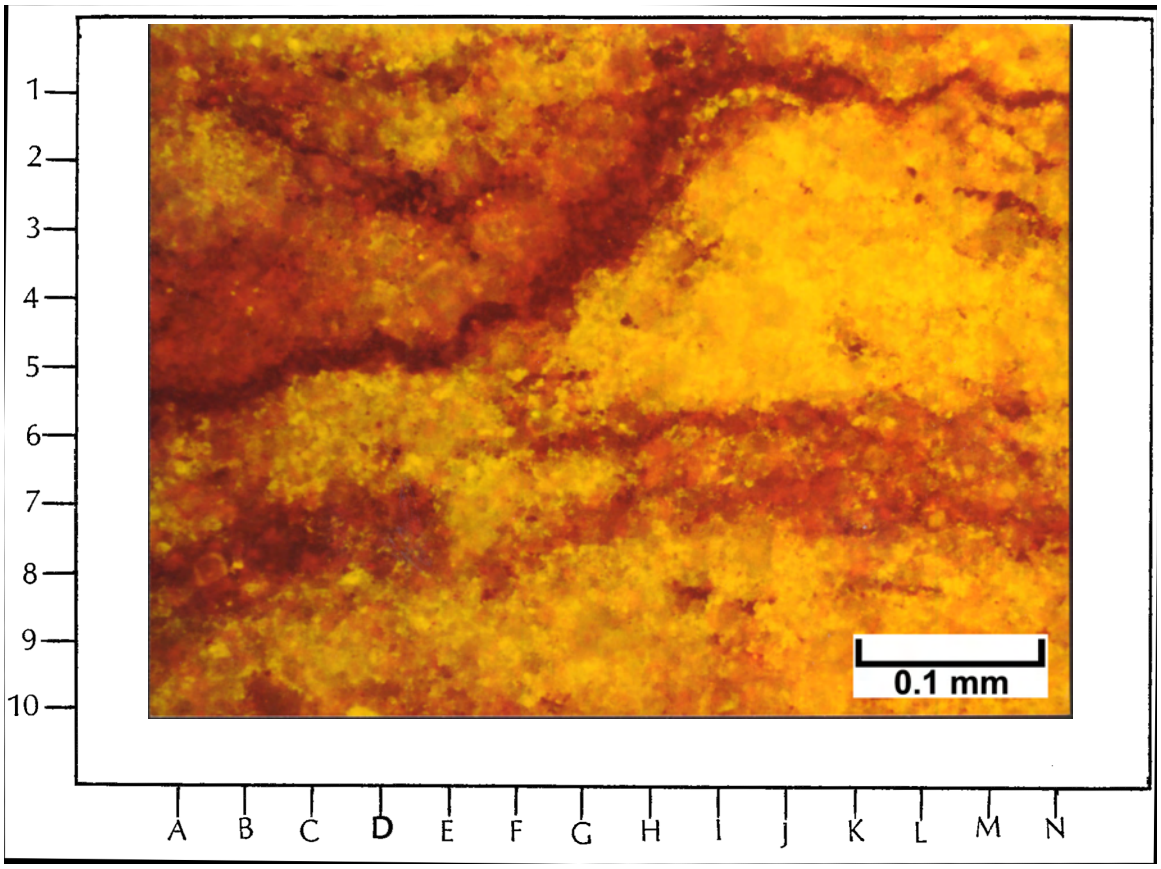
1
2
3
4
5
6
7
8
9
10
A B C D E F G H I J K L M N
0.1 mm

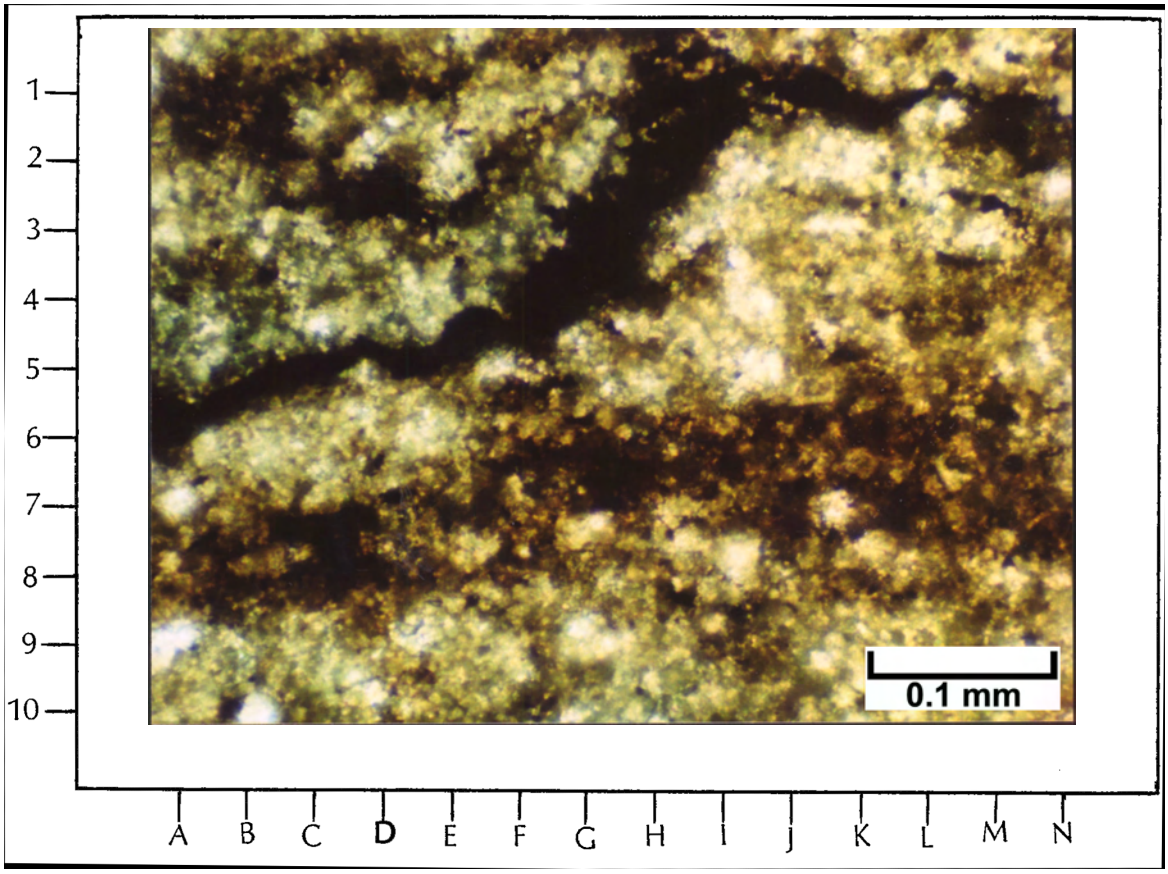
1
2
3
4
5
6
7
8
9
10
A B C D E F G H I J K L M N
0.1 mm

5864.1 feet

Top Photomicrograph

Epifluorescence of another representative portion of this stylolitic limestone sample shows significant matrix porosity in the lower left part of this image (in the reddish areas) and much tighter rock (in yellow) across the top and in the upper right part of the photomicrograph. The dark brown areas are wispy stylolitic seams with variable amounts of insoluble residues. The matrix porosity appears red here because of the fluorescence response of epoxy that has been impregnated into the pore spaces during sample preparation.

Bottom Photomicrograph

The same field of view as above is shown under Pl at the same magnification. None of the porosity imaged under fluorescence (see top photomicrograph) is visible under this lighting. The lower left portion of this field of view shows significant amounts of pore space under fluorescence, but is very dark colored due to opaque bitumen pore linings in this area. In other words, the black areas in the lower left are mostly located where pore space still exists and where epoxy was impregnated for this thin section work.

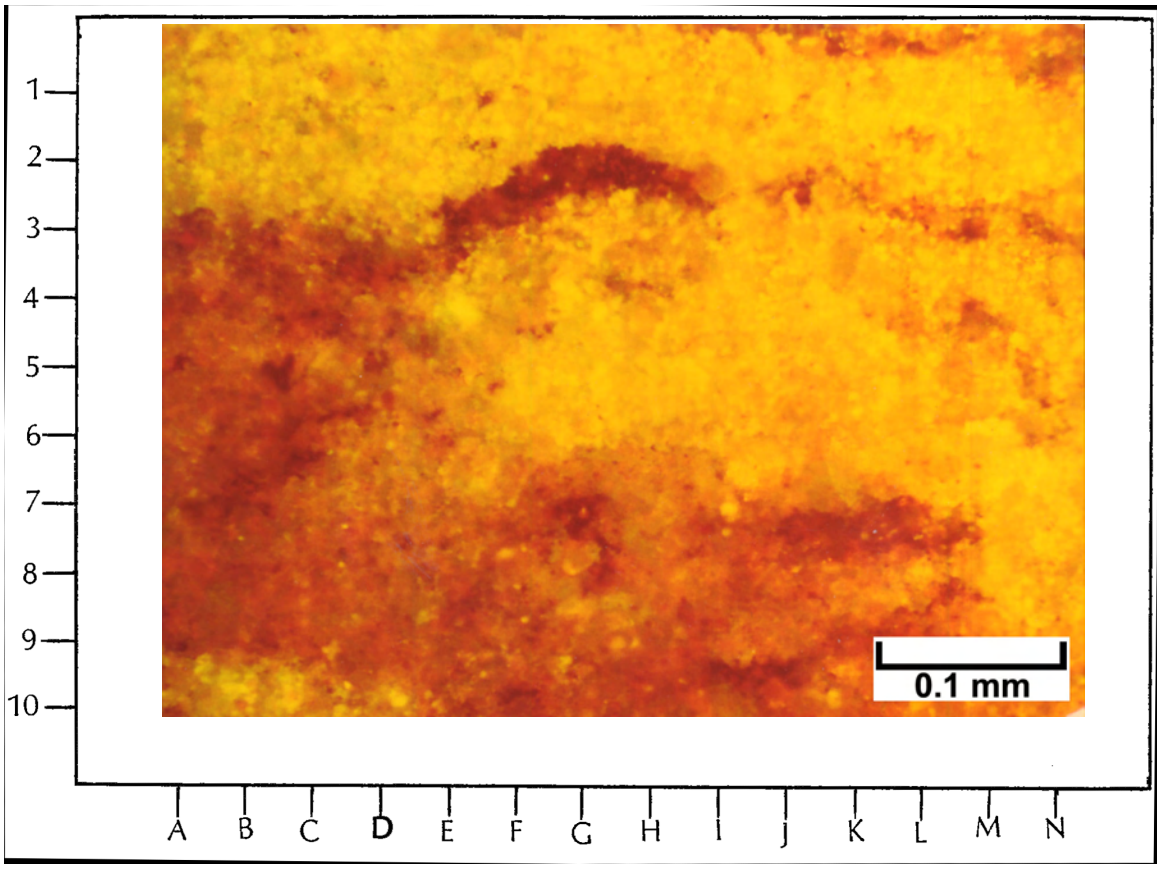
1
2
3
4
5
6
7
8
9
10
A B C D E F G H I J K L M N
0.1 mm

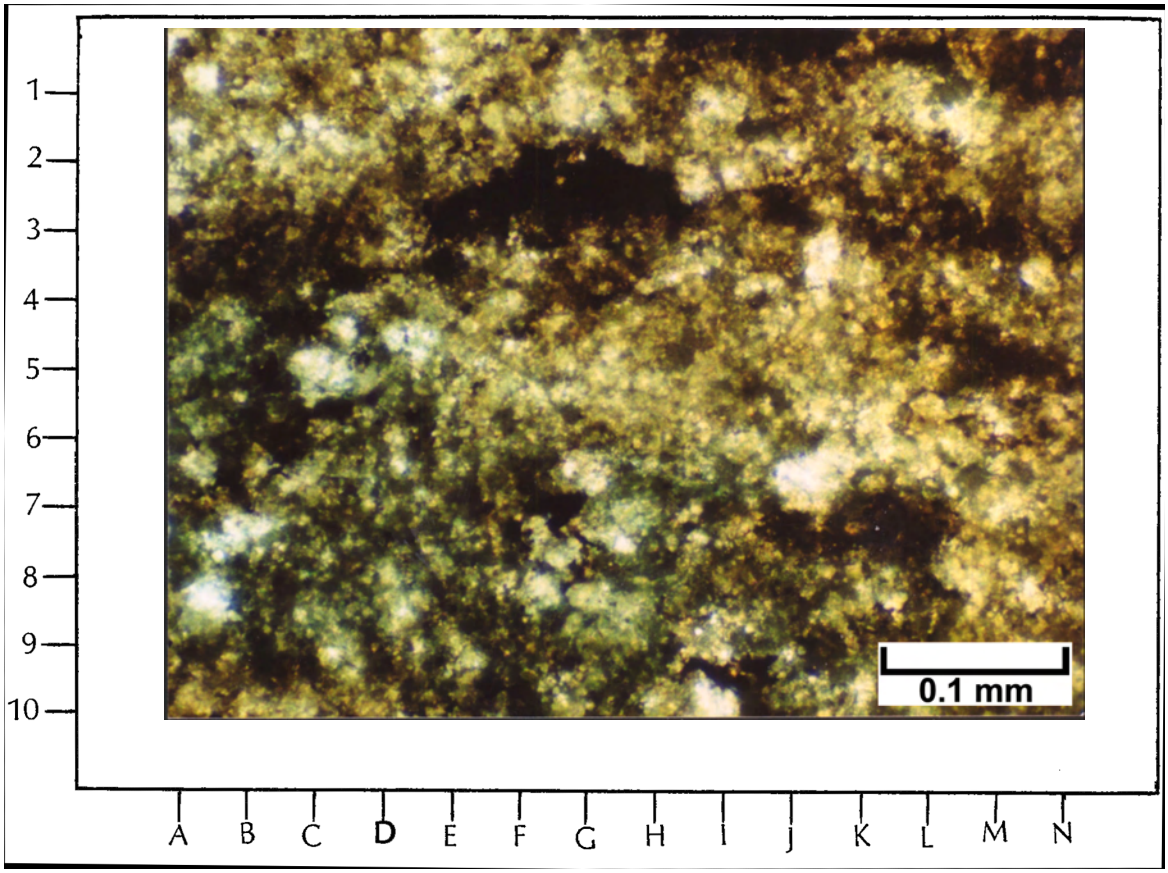
1
2
3
4
5
6
7
8
9
10
A B C D E F G H I J K L M N
0.1 mm

5773.9 feet

Top Photomicrograph

This representative EF photomicrograph nicely shows the distribution and shapes of open pores which appear here in the shades of red. Many of these pores are somewhat elongate and are moldic in origin. Most result from the dissolution of small phylloid-algal plates and possibly other fossil skeletons. Many of these dissolution pores appear to be well connected. The yellow areas are oil-stained carbonates which are mostly composed of limestone here. The light green areas (for example B-3.5 and M-7) are patches of anhydrite cementation.

Bottom Photomicrograph

The same field of view as above is shown under Pl at the same magnification. Note that the areas of visible blue-dye colored epoxy are not abundant or as distinct as the areas in red within the fluorescence photomicrograph above. Without the aid of the fluorescence view, the amount of visible open-pore space would be underestimated in the Pl image.

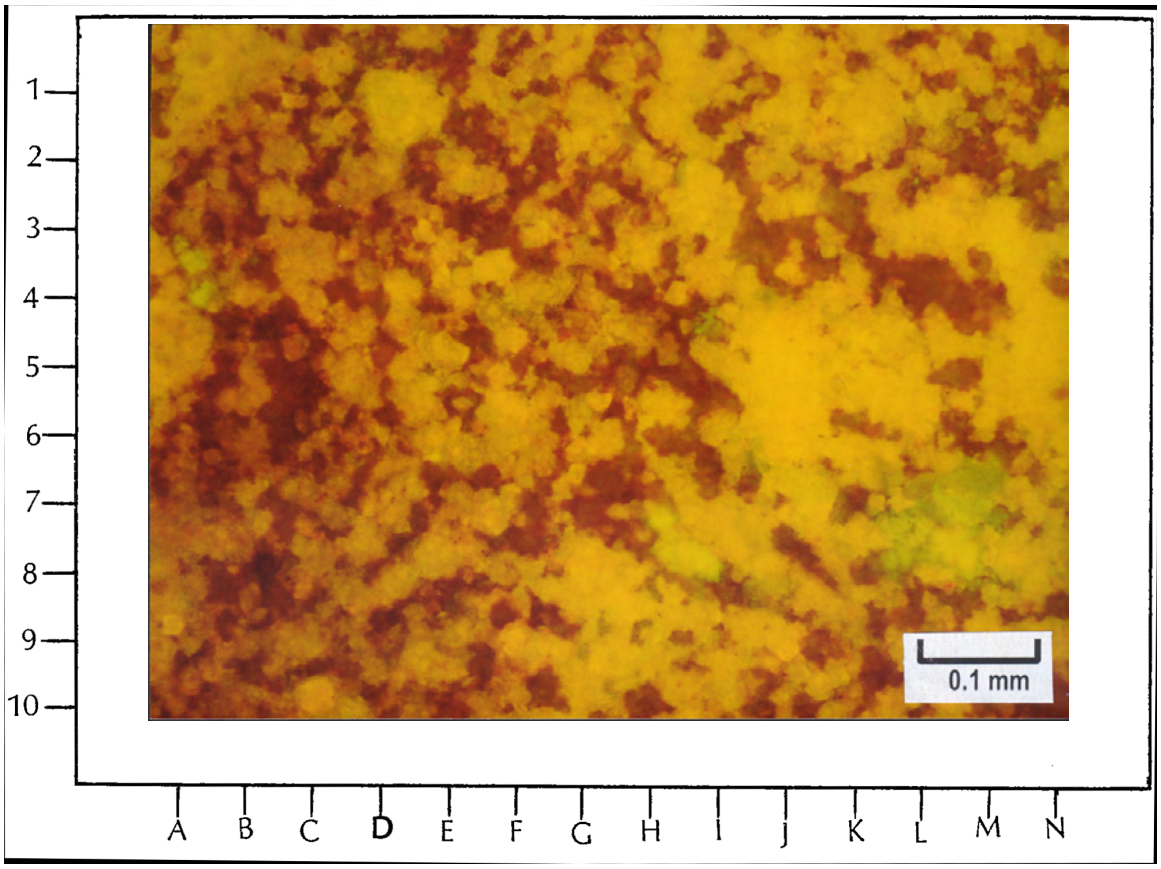
1
2
3
4
5
6
7
8
9
10
A B C D E F G H I J K L M N
0.1 mm

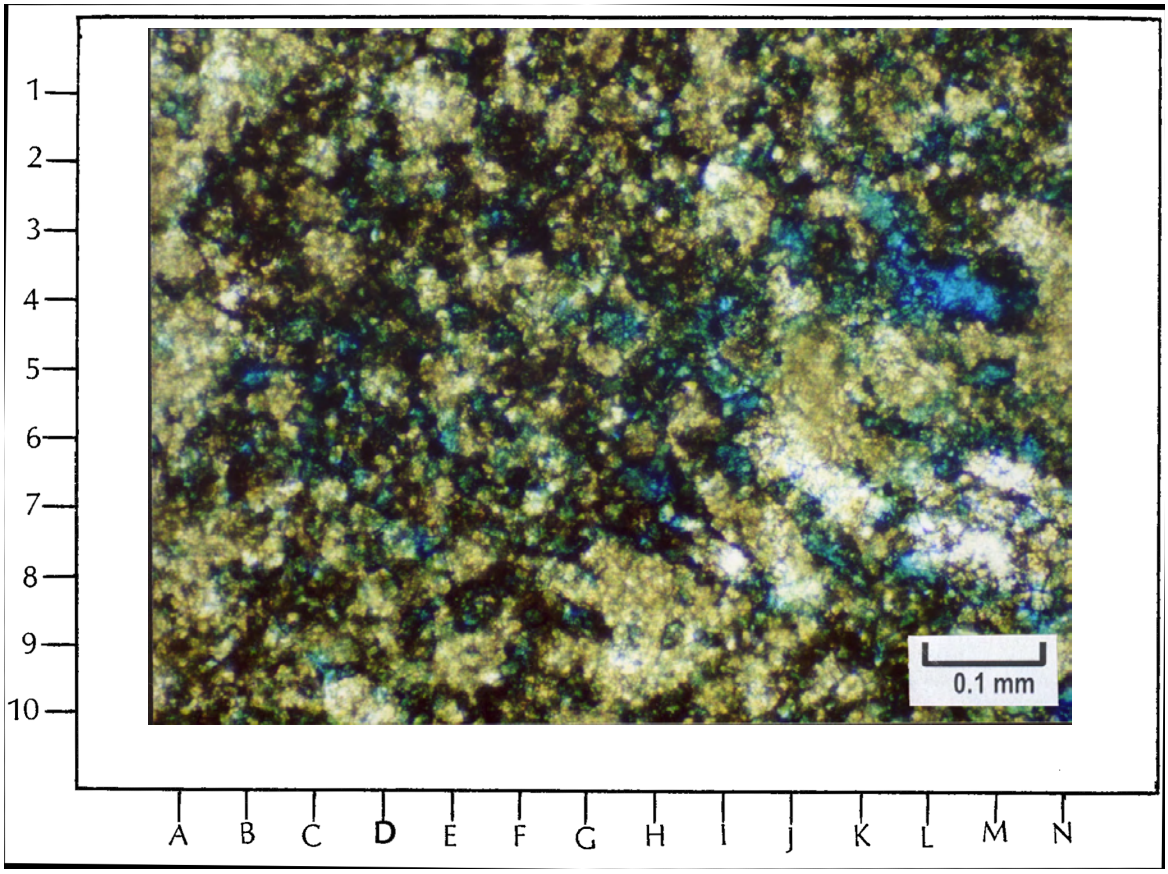
1
2
3
4
5
6
7
8
9
10
A B C D E F G H I J K L M N
0.1 mm

CHEROKEE FEDERAL NO. 33-14 WELL, CHEROKEE FIELD

5773.9 feet

Top Photomicrograph

This heterogeneous sample shows poorly sorted patches of tight carbonate matrix (in bright yellow and green fluorescence) separated by open-pore systems (in red fluorescence) under moderate magnification. Note that there are remnants of former grains that can be seen within the tighter (yellow) areas. For instance, observe the outlines of former fossil grains at F-1, I-3, M-3, and so forth) as well as probable peloids or ooids (for example J-9.5, L-8, and N-9). Most of the porosity in this view (in red) is probably from partial dissolution of earlier grains and cements.

Bottom Photomicrograph

The same field of view as above is shown under Pl at the same magnification. The blue areas (dyed-impregnated pores) show only part of the porosity imaged in the fluorescence view above. The black portions of this view mask some of the open pores by bitumen linings. In addition, the Pl view does not provide a sharp image of the pore boundaries or the relict grains within the carbonate sediment.

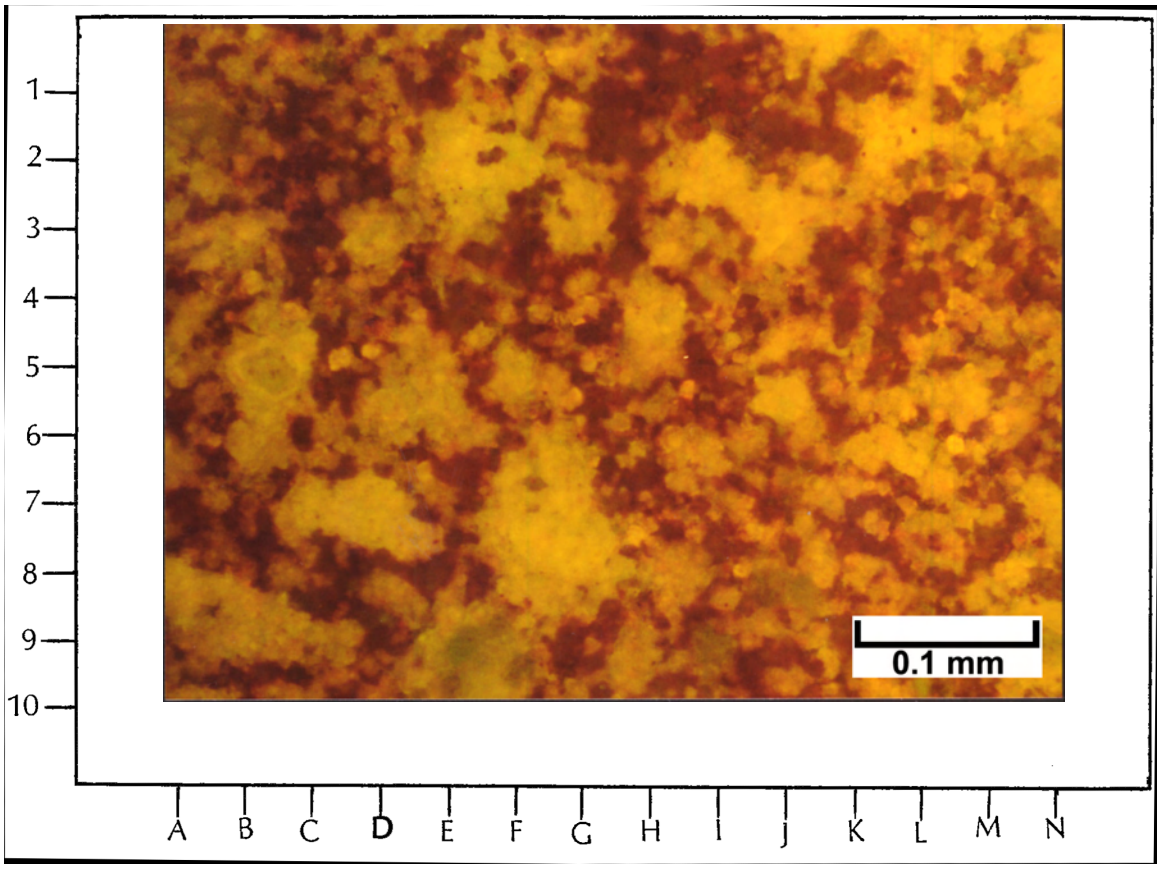
1
2
3
4
5
6
7
8
9
10
A B C D E F G H I J K L M N
0.1 mm

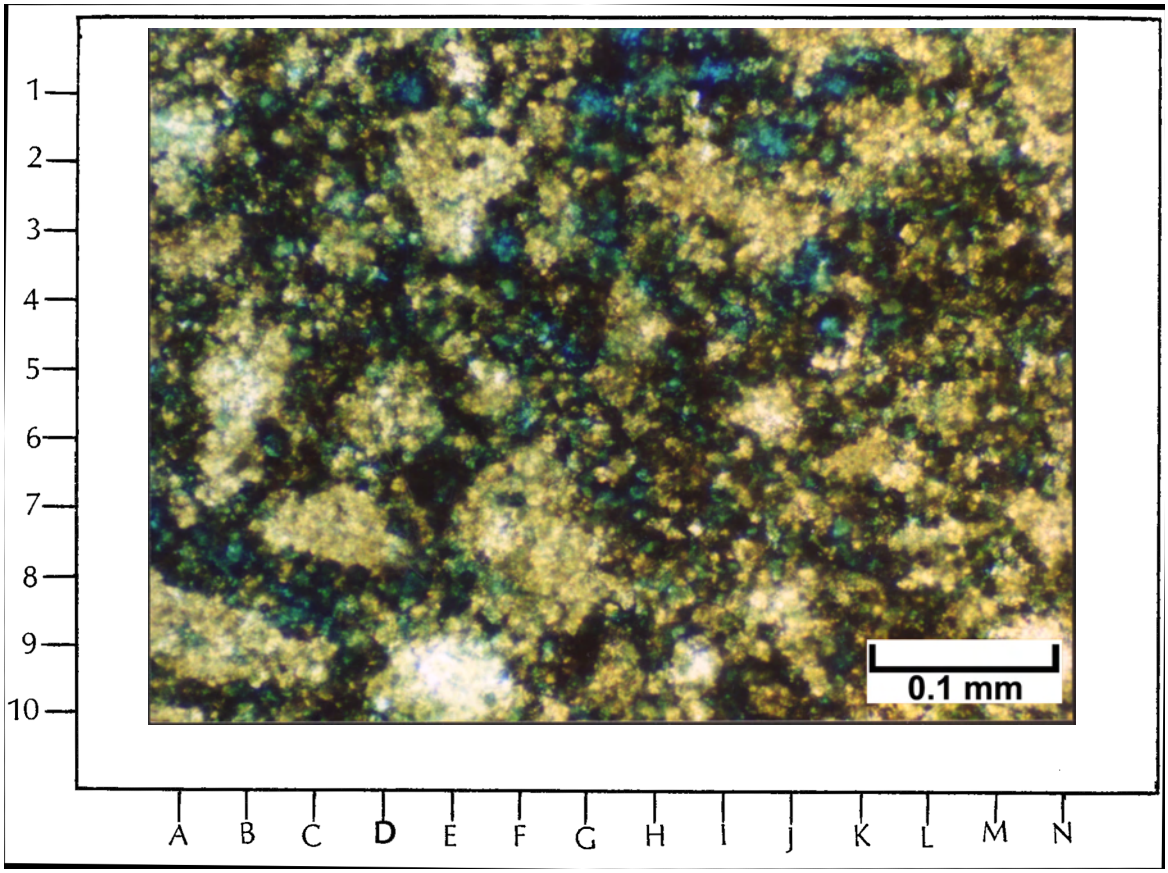
1
2
3
4
5
6
7
8
9
10
A B C D E F G H I J K L M N
0.1 mm

5773.9 feet

Top Photomicrograph

This fluorescence view is from a relative low porosity part of the sample. The bright yellow areas are tight portions of the carbonate matrix that show fluorescence due to live oil staining around the microcrystalline matrix and crystal faces. Isolated patches of pores occur as the red fluorescence of the impregnated epoxy. Note the nicely zoned dolomite crystal at I-6 that has replaced some of the carbonate matrix.

Bottom Photomicrograph

The same field of view as above is shown under Pl at the same magnification. The blue areas (dyed-impregnated pores) show only part of the porosity imaged in the fluorescence view above. The black portions of this view mask some of the open pores by bitumen linings. In addition, the Pl view does not provide a sharp image of the pore boundaries or the relict grains within the carbonate sediment.

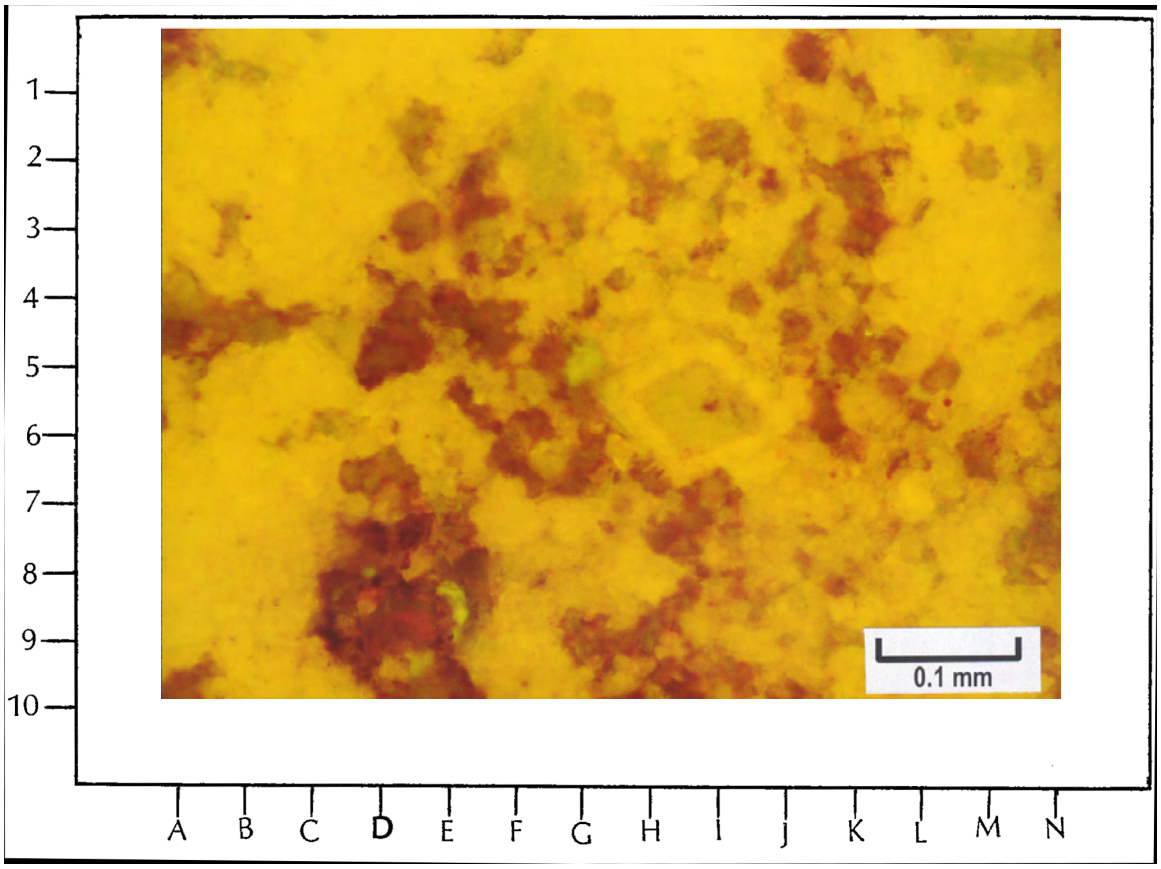
1
2
3
4
5
6
7
8
9
10
A B C D E F G H I J K L M N
0.1 mm

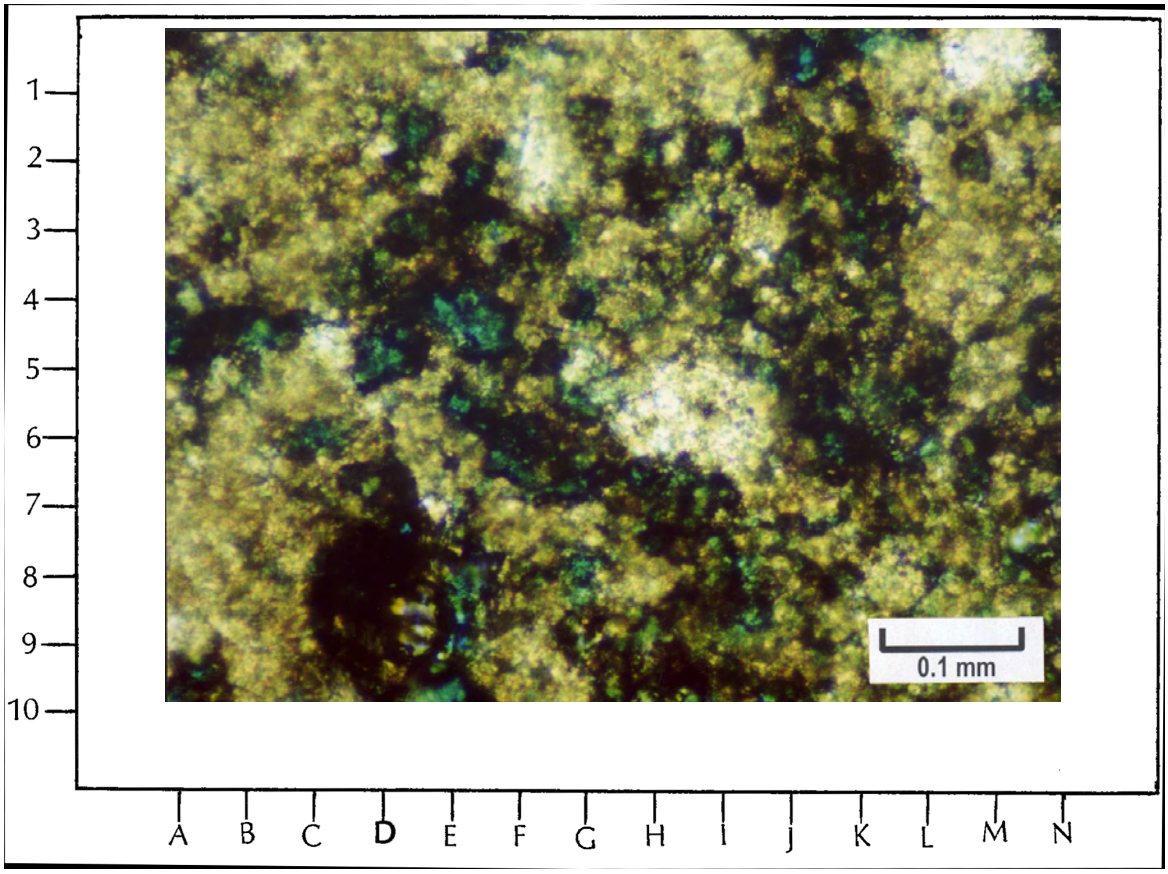
1
2
3
4
5
6
7
8
9
10
A B C D E F G H I J K L M N
0.1 mm

5773.9 feet

Top Photomicrograph

The red fluorescence in this view shows the open-pore spaces within this slightly dolomitic limestone. The darkest red colors (for example B-7, F-8, I-7, and M-8) are due to local concentrations of bitumen lining some of these pores. Remnants of possible fossil grains can be seen at C-2.5, K-2, and M-6. The bright yellow patch between H-9 and N-9 represents a very tight portion of the carbonate matrix that fluoresces because of trapped live oil within an area of very low permeability.

Bottom Photomicrograph

The same field of view as above is shown under Pl at the same magnification. Significant portions of this image show porosity (in blue), but much of the additional porosity is invisible due to opaque linings of bitumen which blocks the viewing of the other impregnated pores. Also, the pore outlines and shapes are much more difficult to see than in the fluorescence microscopy view above.

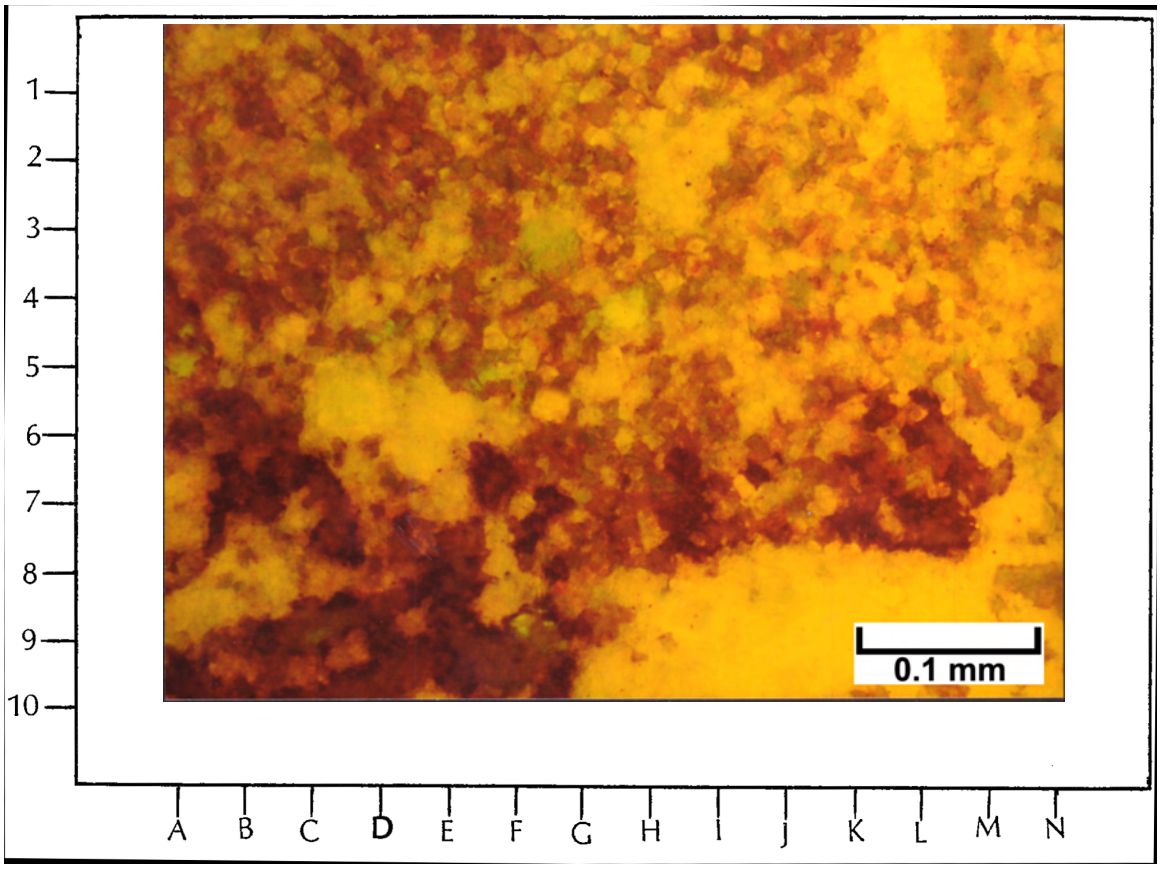
1
2
3
4
5
6
7
8
9
10
A B C D E F G H I J K L M N
0.1 mm

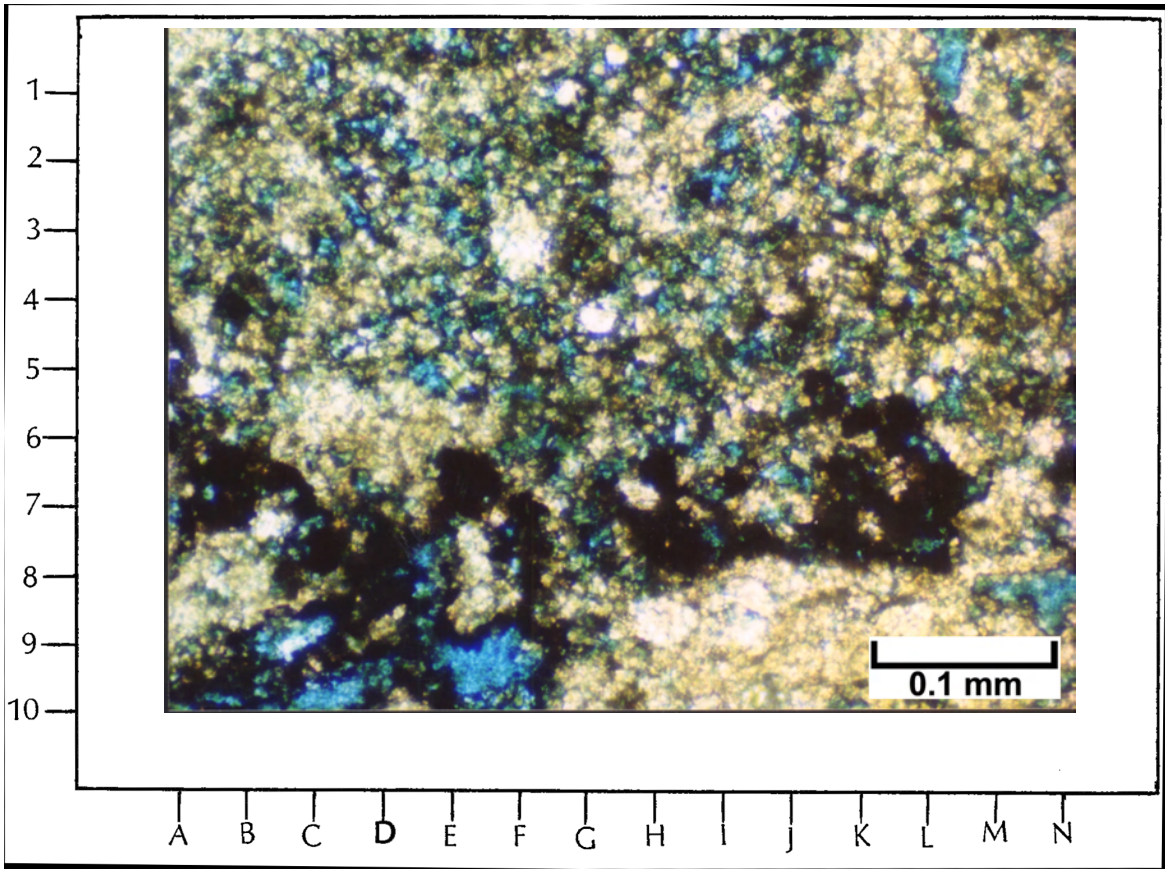
1
2
3
4
5
6
7
8
9
10
A B C D E F G H I J K L M N
0.1 mm

BUG NO. 7 WELL,
BUG FIELD

6359.3 feet

Top Photomicrograph

This dense dolomite matrix displays a number of features that are visible only under EF (compare with Pl below). A representative EF view of a very tight microcrystalline dolomite shows the absence of any significant megascopic matrix porosity. However, the matrix displays a yellowish orange color, indicating probable live oil saturation of this tight dolomite. Notably, there is an open microfracture, with an offset in the upper left center portion of the photomicrograph. It appears bright yellow here due to the fluorescence of "live" hydrocarbons. This microfracture crosses and post-dates a microstylolite marked by the black, jagged pattern across this view from lower left to right center. Most of the rest of the massive (mud-rich) matrix displays a mottled yellow and orange color due to oil saturation in this dolomite. Although there are no readily visible grains in the field of view, there are a few discrete dolomite crystals that appear as the dark green areas.

Bottom Photomicrograph

The same view as above is displayed here under Pl. Some of the medium to dark-brown color of this dolomite may be the result of oil staining as indicated by the yellowish orange color in the EF view above. Note the poorly preserved peloids and possible fossils in this aphanitic to anhedral dolomite. Some of the larger non-planar dolomite crystals appear white in this view. The open, en echelon (offset) fractures and the wispy microstylolites seen in the top image are very indistinct across the length of this photomicrograph.

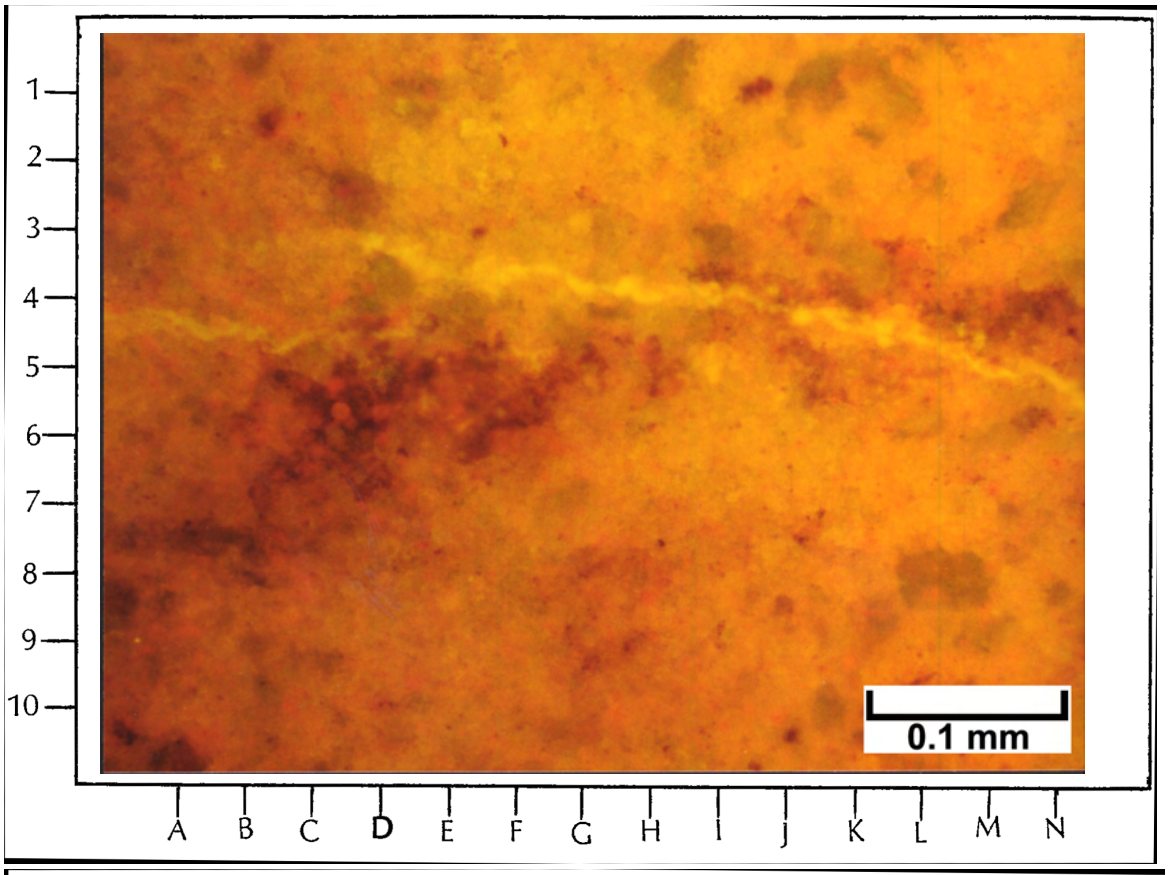
1
2
3
4
5
6
7
8
9
10
A B C D E F G H I J K L M N
0.1 mm

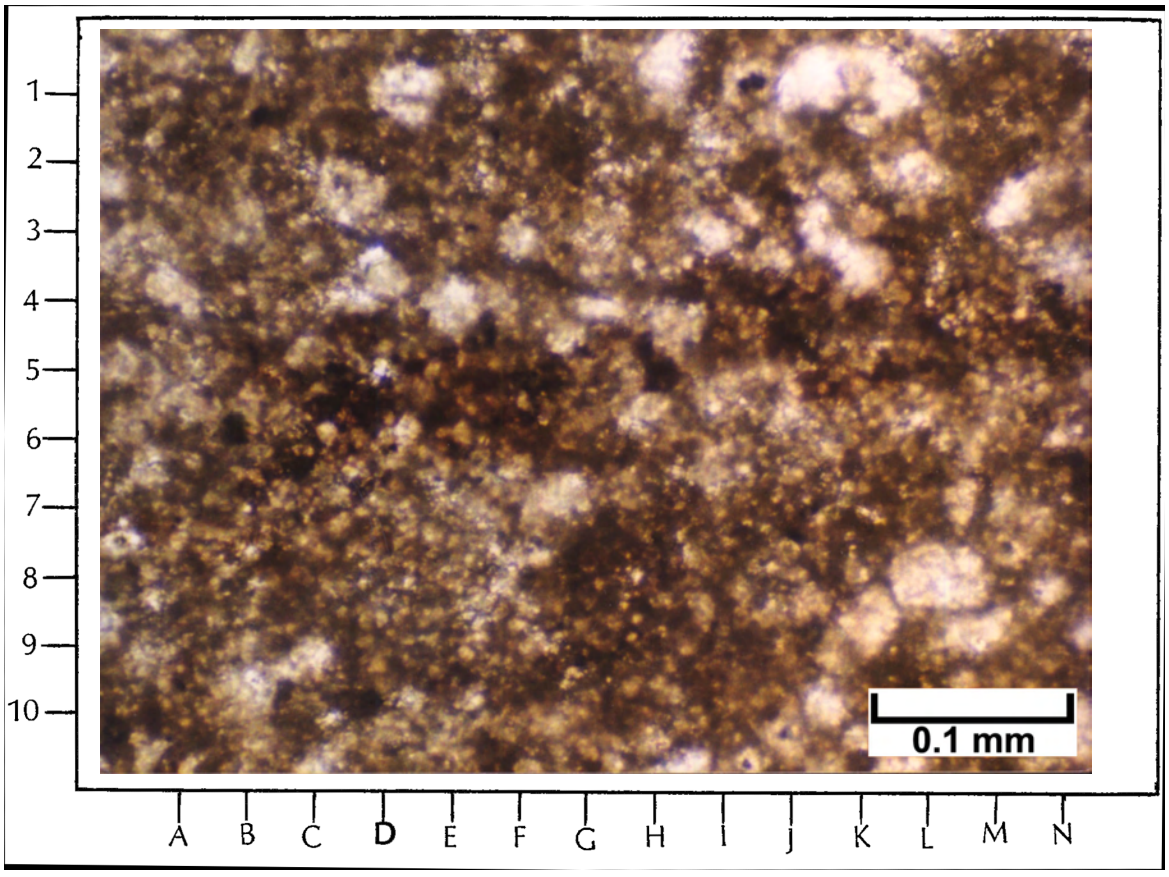
1
2
3
4
5
6
7
8
9
10
A B C D E F G H I J K L M N
0.1 mm

6359.3 feet

Top Photomicrograph

Epifluorescence of this tight dolomite matrix shows probable good oil saturation within the matrix (as shown in the yellowish orange hues). Relatively unsaturated areas are shown in the darker red and greenish colors. Note the partially healed fracture showing apparent oil staining (in bright yellow) across the length of this photomicrograph (from left center to right center).

Bottom Photomicrograph

The same view at the same magnification as above is shown here under Pl. Note the dark-colored matrix, which may partially be the result of oil staining (see the EF view above). Also observe that the length-wise fracture appears white in this image.

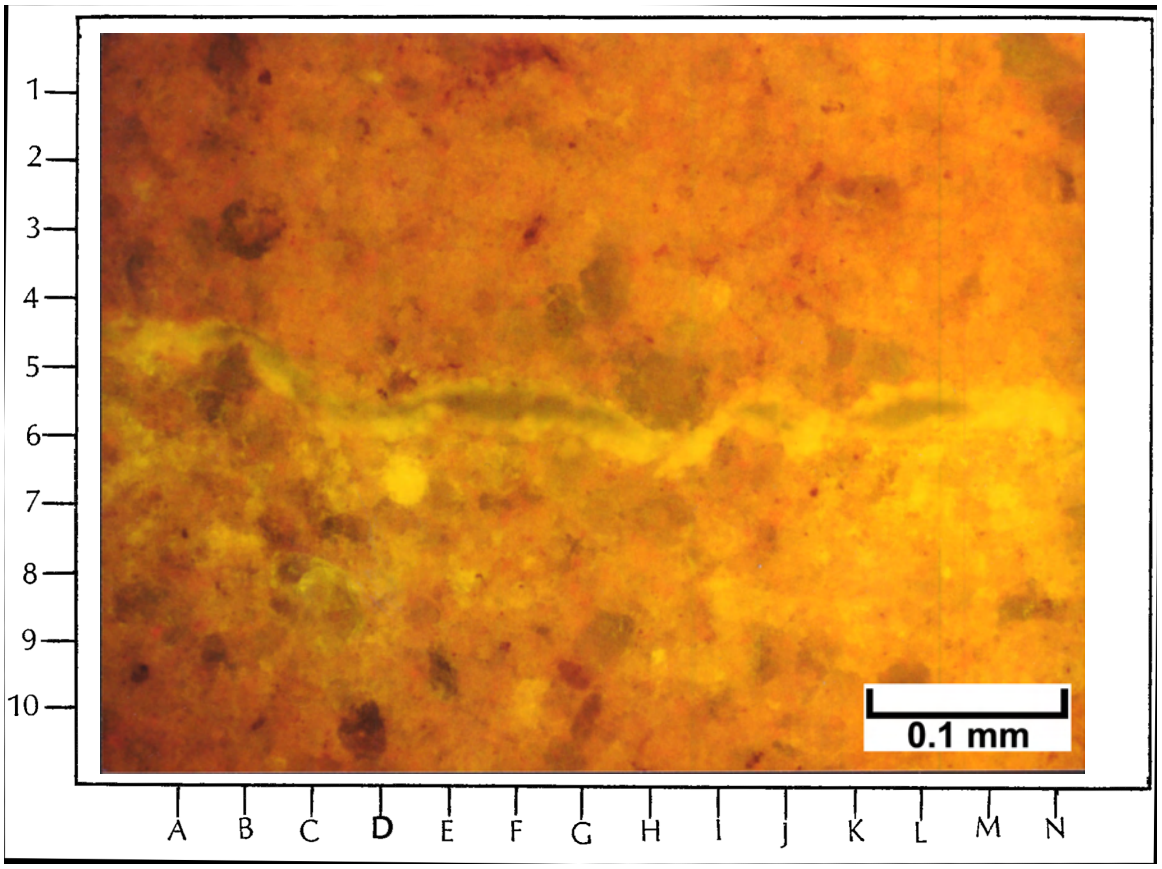
1
2
3
4
5
6
7
8
9
10
A B C D E F G H I J K L M N
0.1 mm

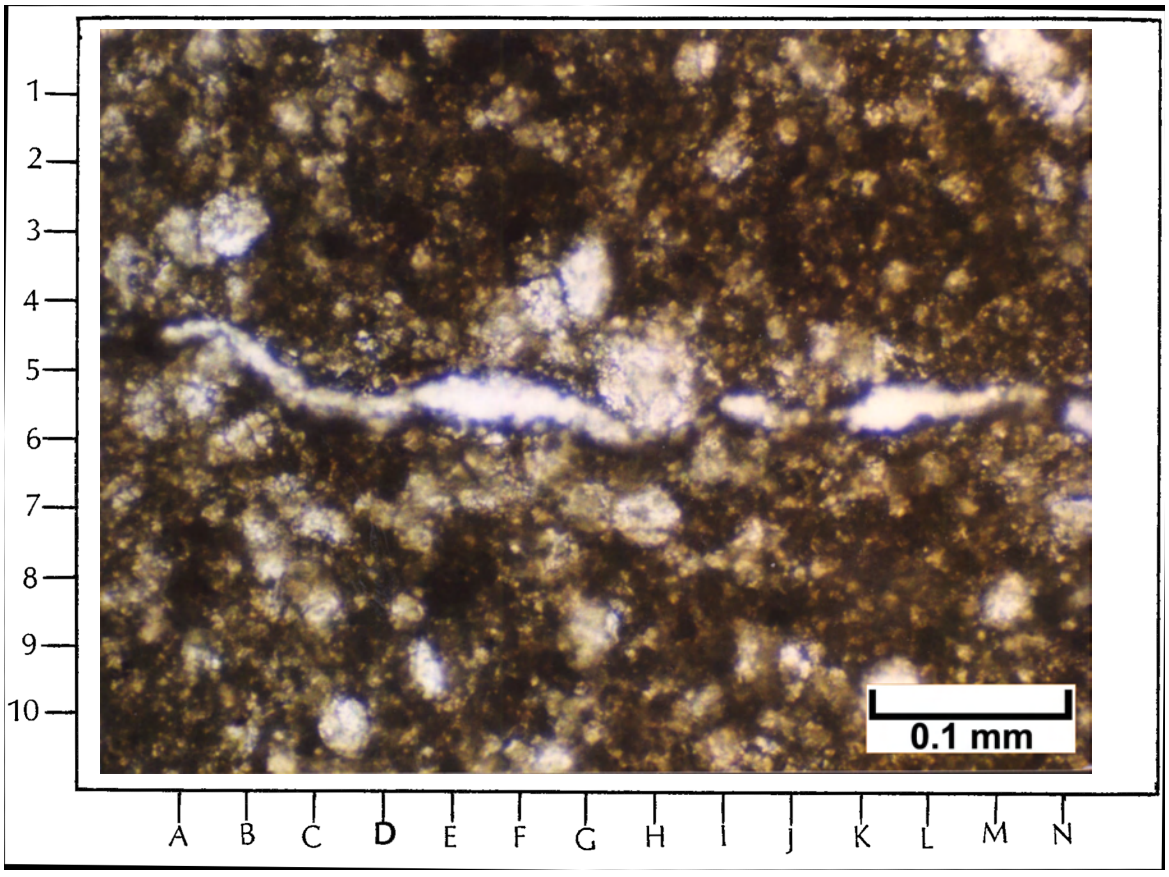
1
2
3
4
5
6
7
8
9
10
A B C D E F G H I J K L M N
0.1 mm

6359.3 feet

Top Photomicrograph

This is another EF view of a tight area of dolomite matrix that appears to have some oil saturation (as shown) in the yellowish orange hues. Larger individual dolomite crystals can be seen in the dark gray to greenish gray areas. Hints of carbonate grain outlines can also be seen. Note the low-amplitude stylolites and stylo-fractures with the live "oil" staining (in very bright yellow) across the bottom of this photomicrograph. Otherwise, the finely crystalline matrix of this dolomite is very tight.

Bottom Photomicrograph

The same view as above is shown under Pl. Note the mottled white and dark gray colors displayed by this very low-porosity dolomite. The low-amplitude stylolitic and stylo-fractured portions of this sample are very difficult to resolve under Pl.

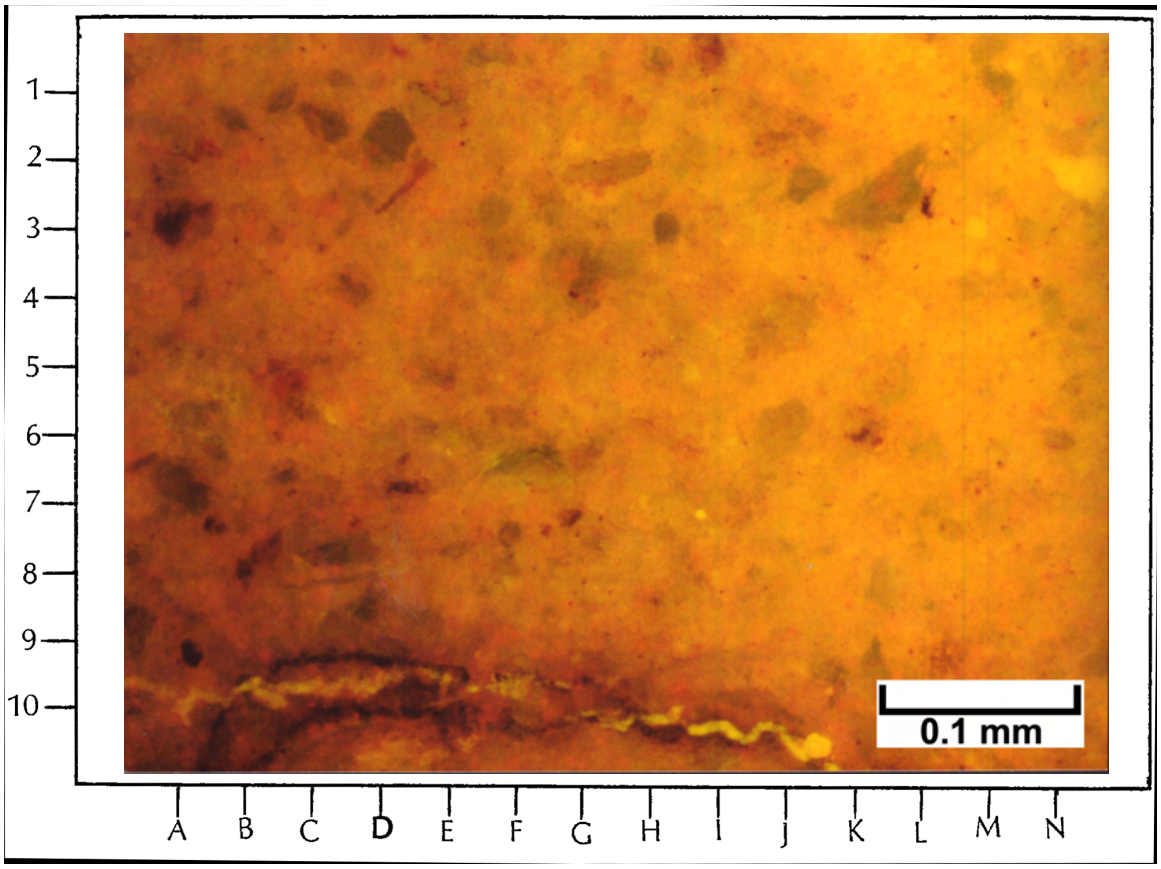
1
2
3
4
5
6
7
8
9
10
A B C D E F G H I J K L M N
0.1 mm

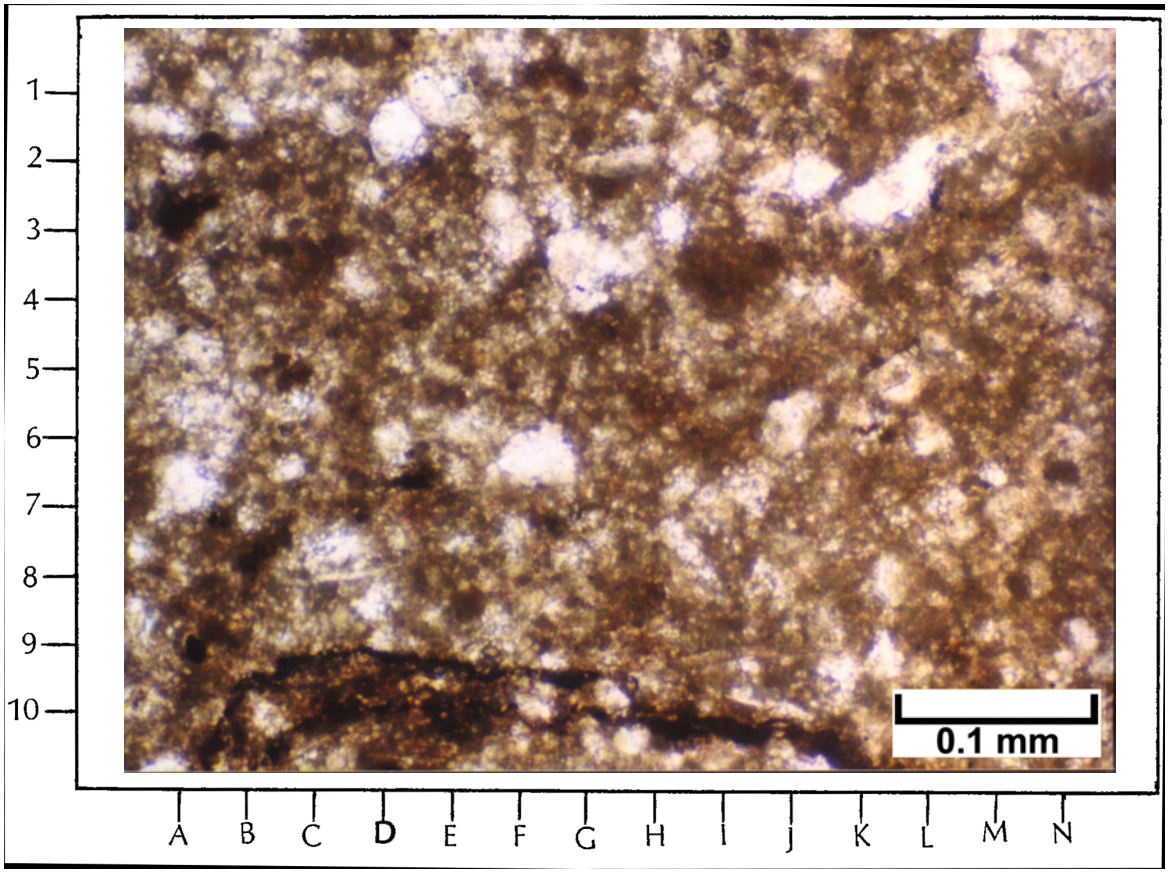
1
2
3
4
5
6
7
8
9
10
A B C D E F G H I J K L M N
0.1 mm

BUG NO. 10 WELL,
BUG FIELD

6327.9 feet

Top Photomicrograph

Isolated pore systems (in bright yellow) shown here are surrounded by dark, non-fluorescent dolomites. Note the open fracture (cutting across the length of this view) that is lined with dolomite crystals (the non-fluorescence crystal outlines). A small number of isolated pores (also in yellow) can be seen "floating" in the dense, tight dolomite matrix.

Bottom Photomicrograph

The same view as above under Pl does not show the clarity of the dolomite/pore relationships as the EF view. Although there is a linear bluish region across this photomicrograph (due to epoxy impregnation of the open fracture), the coarse dolomite crystals lining of the linear fracture cannot be seen here. In addition, it is impossible to see the isolated open pores such as those seen in the top EF photomicrograph.

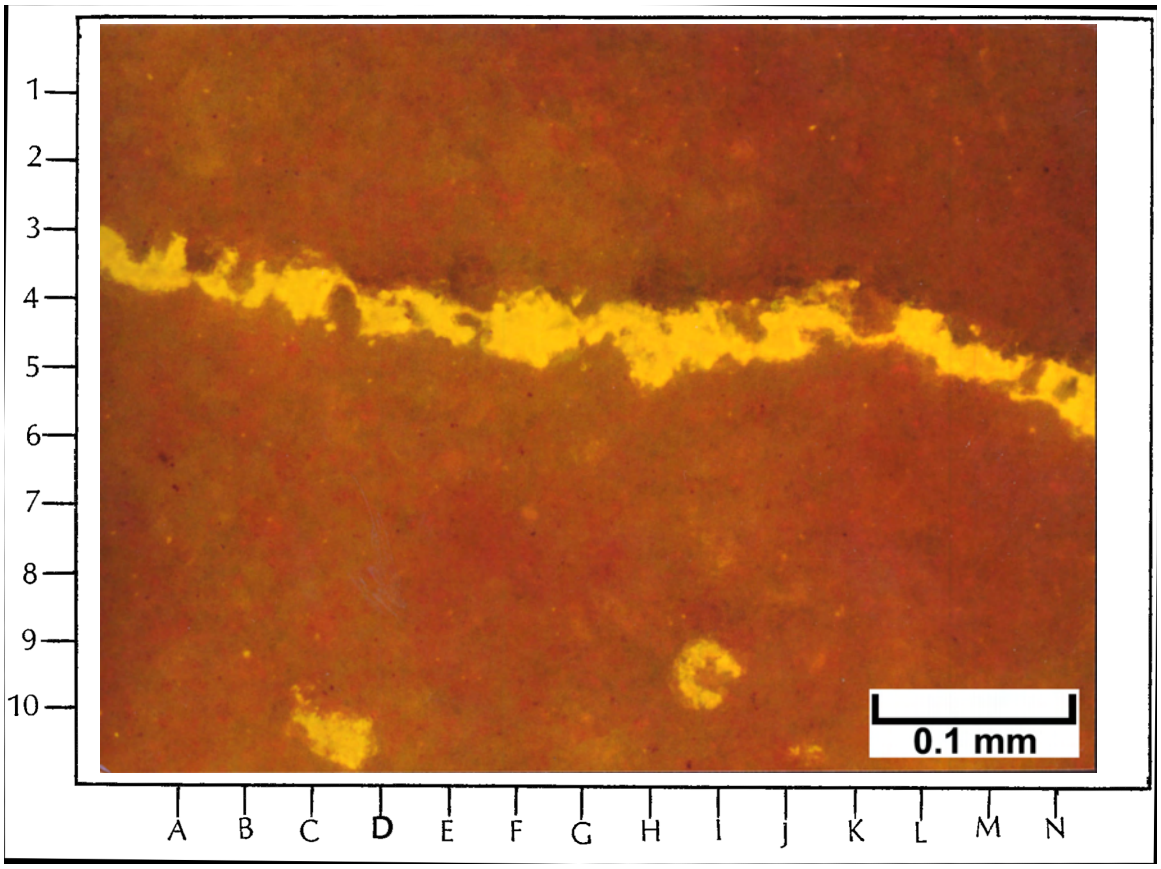
1
2
3
4
5
6
7
8
9
10
A B C D E F G H I J K L M N
0.1 mm

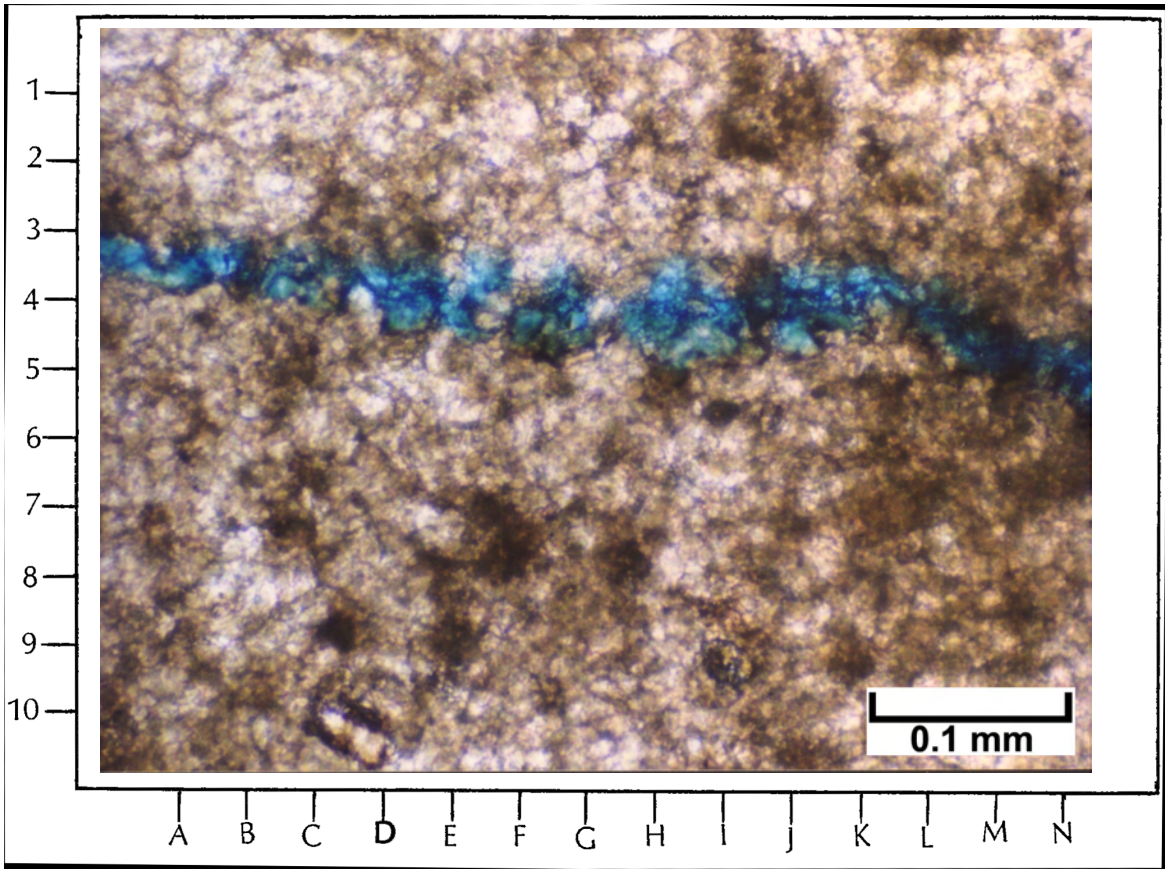
1
2
3
4
5
6
7
8
9
10
A B C D E F G H I J K L M N
0.1 mm

6327.9 feet

Top Photomicrograph

A heterogeneous micro-box-work of dolomite is displayed here, where the dolomite crystal aggregates appear dark gray and the open pores between the dolomite are bright yellow (due to spiked epoxy and "live oil" lining pores). Some of the pores appear to be well connected while others are isolated by interlocking dolomite crystals. Hence, some of these large pores may be "blind" or lack interconnections. Note that there is very little evidence of intercrystalline porosity within the dense dolomite areas.

Bottom Photomicrograph

The same field of view as above under Pl shows fuzzy relationships between the cross section of pores (impregnated with blue epoxy) and the poorly sorted dolomite crystal matrix. No grains or structures are visible within the dolomites in this image.

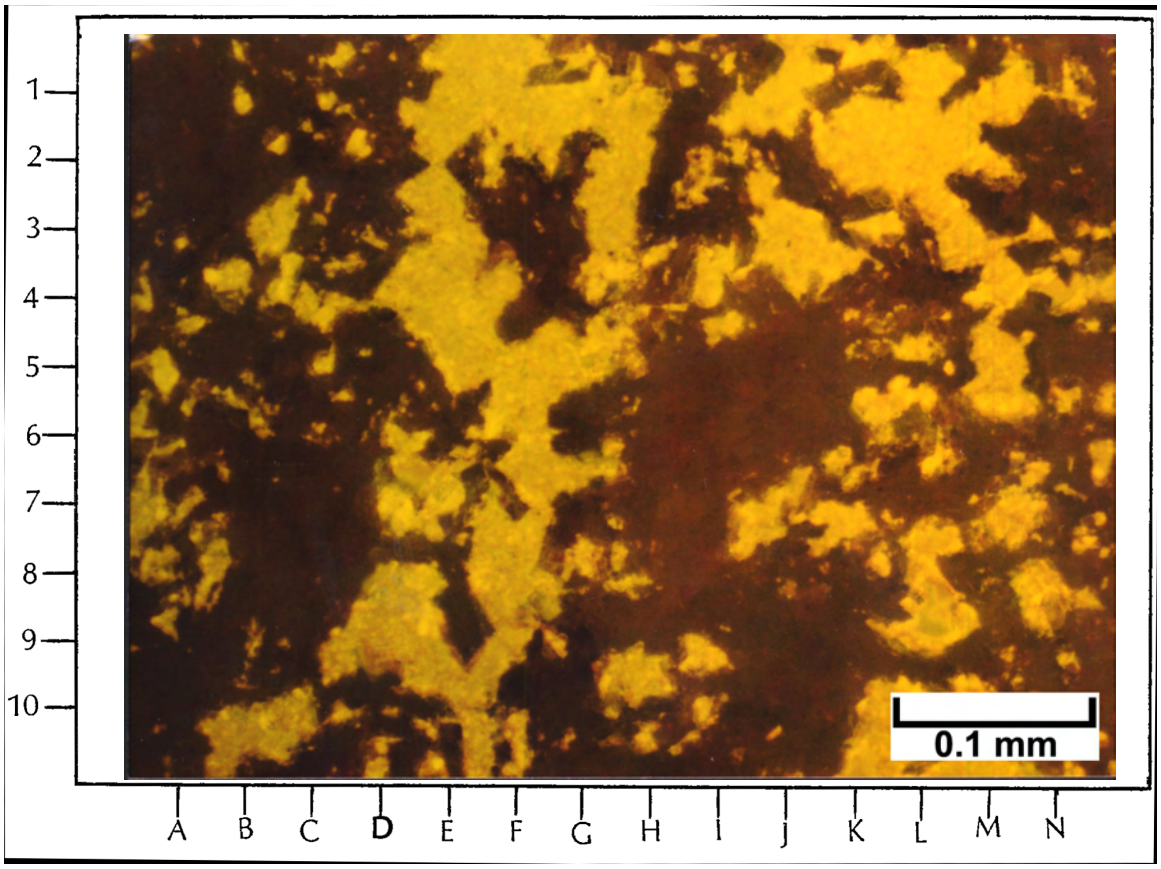
1
2
3
4
5
6
7
8
9
10
A B C D E F G H I J K L M N
0.1 mm

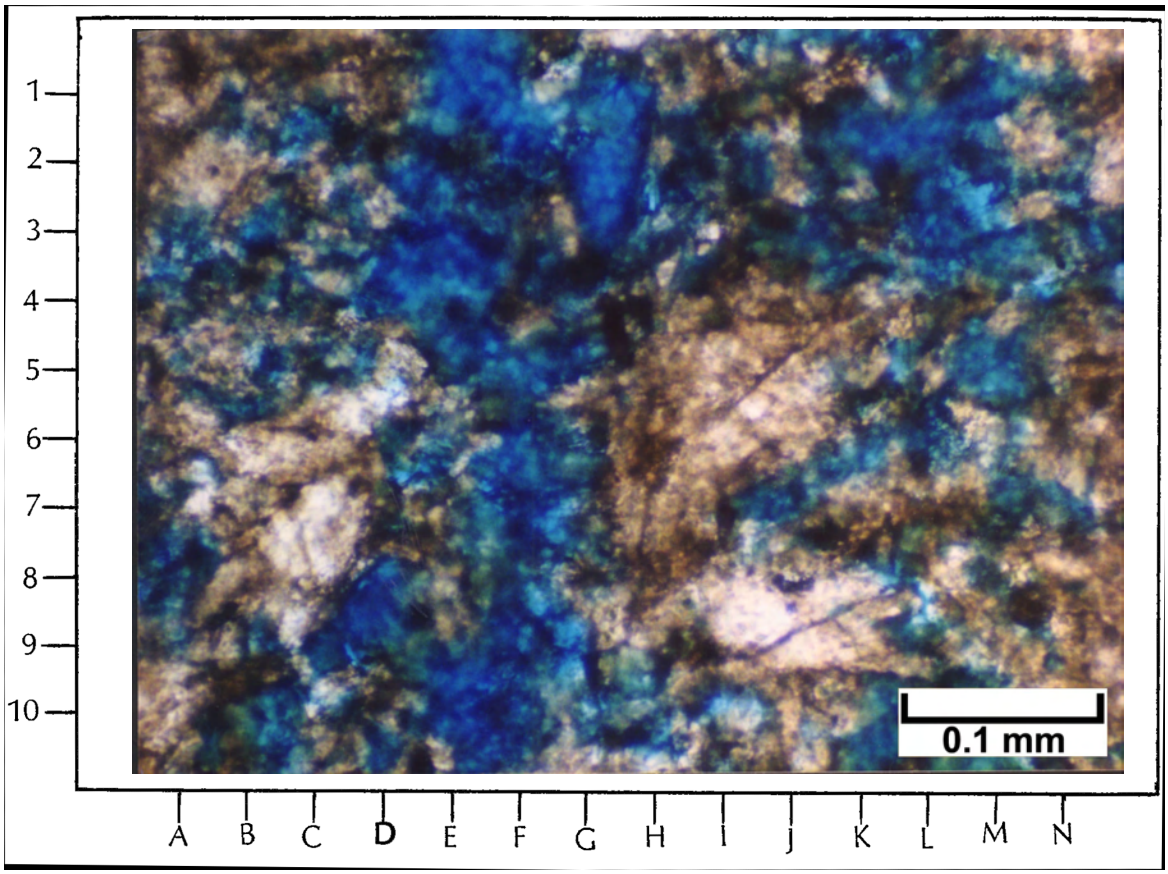
1
2
3
4
5
6
7
8
9
10
A B C D E F G H I J K L M N
0.1 mm

6327.9 feet

Top Photomicrograph

This EF view shows the distribution of open pore cross sections (in yellow). Some of the brightest yellow patches are probably due to "live oil" still "bleeding" from this reservoir rock. The dark areas that make up most of this photomicrograph are composed of a very tight dolomite matrix that tends to isolate the areas of porosity (in yellow). Note the very angular character of these crystal-pore boundaries. These dolomite crystals create a very delicate micro-box-work separating the pores. Note that some pore throats are wide and open while other pores are "blind" and dead end into dolomite partitions (the non-fluorescence elements between the bright yellow fluorescent areas).

Bottom Photomicrograph

The same view at the same magnification as above is shown in the Pl image. Note that the crystal/pore intersections are not as sharp or as "in-focus" as the EF view above. The blue-dyed epoxy that impregnates pore space is not as easy to view as the clearly defined yellow spaces in the top EF image.

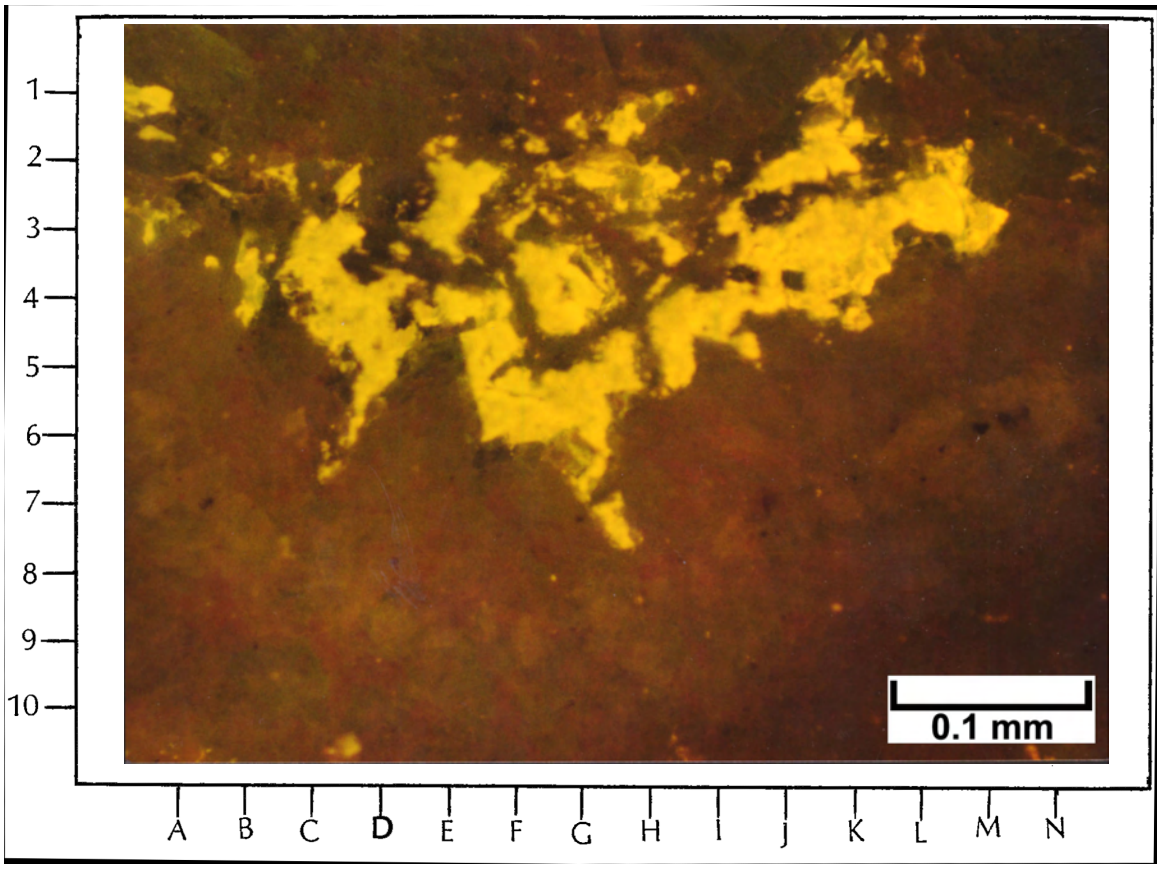
1
2
3
4
5
6
7
8
9
10
A B C D E F G H I J K L M N
0.1 mm

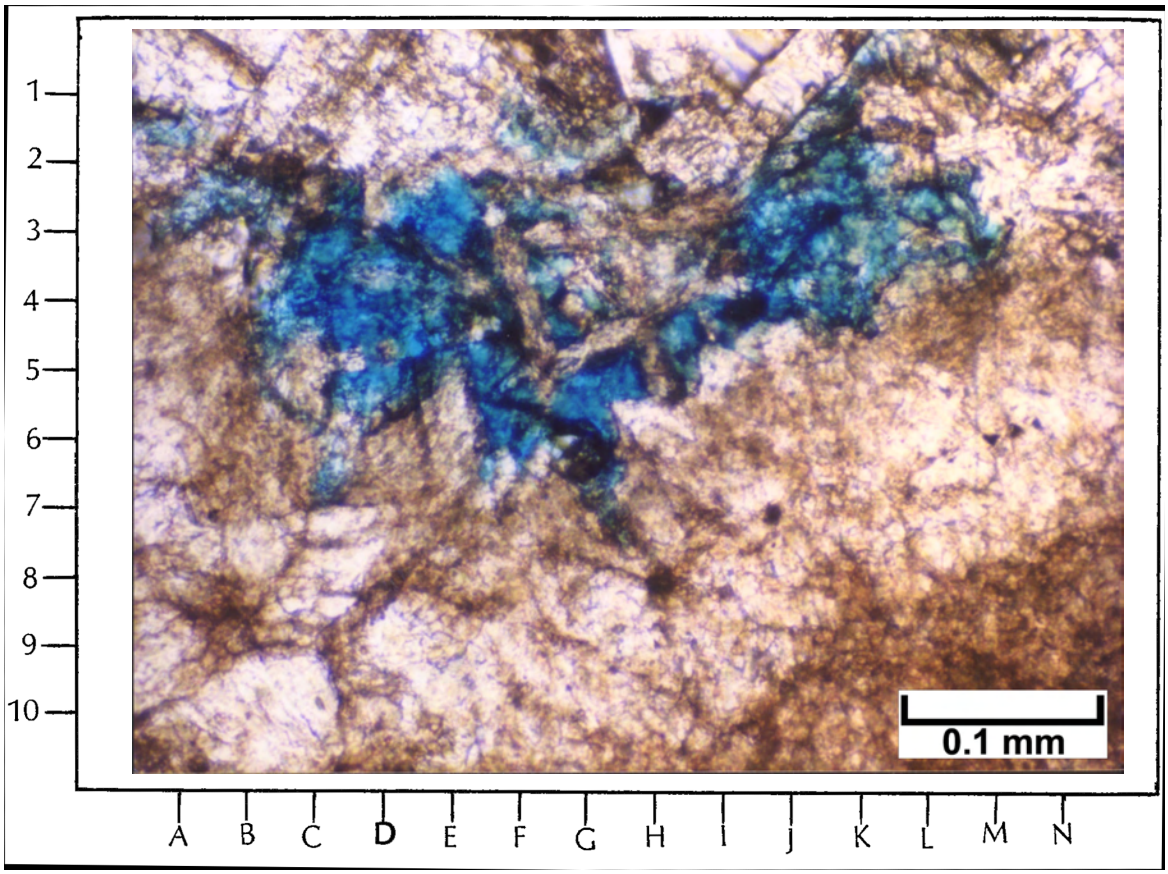
1
2
3
4
5
6
7
8
9
10
A B C D E F G H I J K L M N
0.1 mm

6327.9 feet

Top Photomicrograph

This overview EF photomicrograph shows a very complex network of micro-box-work structure throughout the entire field of view. The yellow areas show cross sections of open pores impregnated with epoxy and lined with some residual oil. The remaining dark areas in this field of view are non-porous dolomite crystal aggregates. In this view, most pores appear to be well connected, but some are isolated or "blind."

Bottom Photomicrograph

A Pl image of the same field of view as above shows pores in blue and dolomite crystals in white and brown. Note that the dolomite crystals appear to be uniformly dense or difficult to resolve, but the pore space/dolomite contacts are clearly defined under EF.

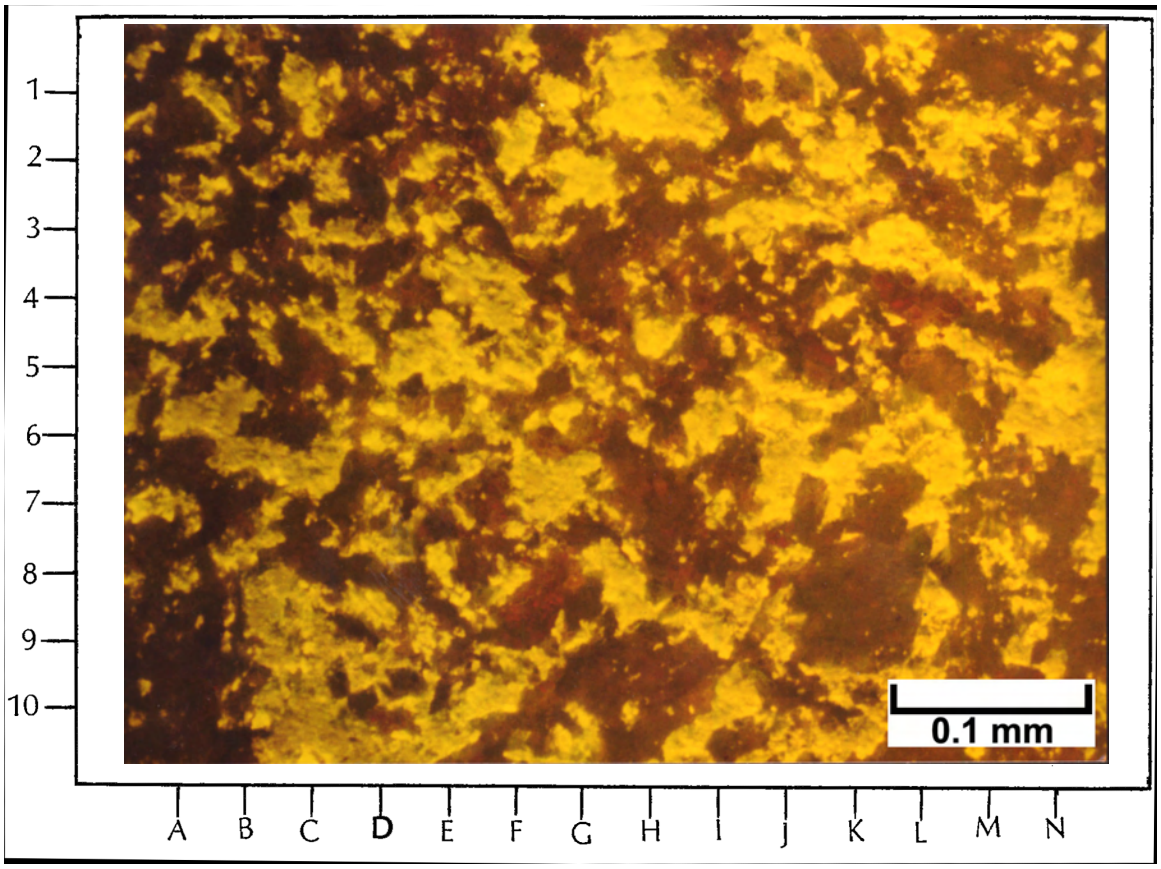
1
2
3
4
5
6
7
8
9
10
A B C D E F G H I J K L M N
0.1 mm

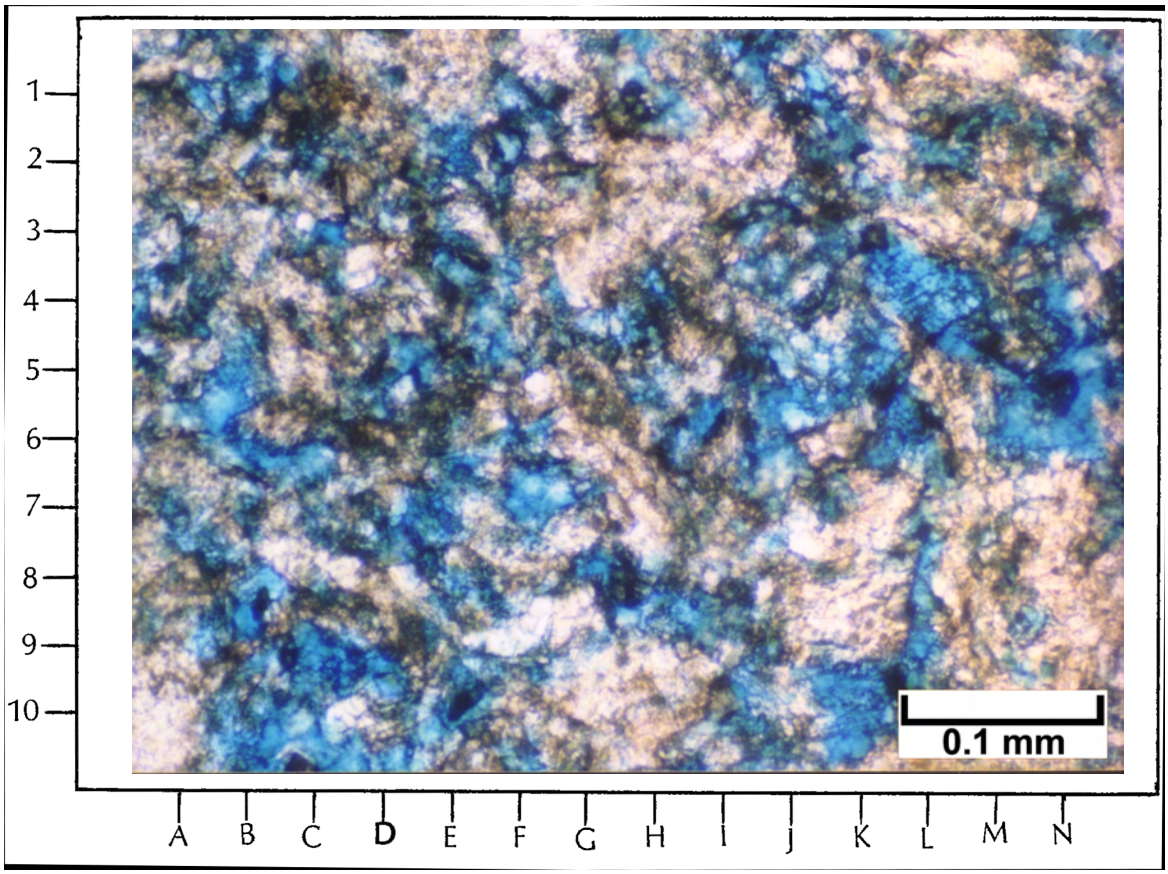
1
2
3
4
5
6
7
8
9
10
A B C D E F G H I J K L M N
0.1 mm

6327.9 feet

Top Photomicrograph

An extensive pore system (in bright yellow) shown here is surrounded by dark, non-fluorescent dolomite exhibiting a wide variety of shapes, including blunt-ended blades of dolomite as well as interlocking partitions. The open pores occur between a loose micro-box-work of hollow crystals and solid dolomite crystal aggregates, thus contributing considerable heterogeneity and some isolation to this pore system.

Bottom Photomicrograph

The same view as above under Pl does not show the clarity of the dolomite/pore relationships as does the EF view. Note that the boundaries between open pores and the dolomite partitions making up this micro-box-work are not very easy to see under Pl. The pores (in blue) clearly appear to be partly of a dissolution origin as shown by the corroded margins of many of the dolomite crystals and crystal aggregates.

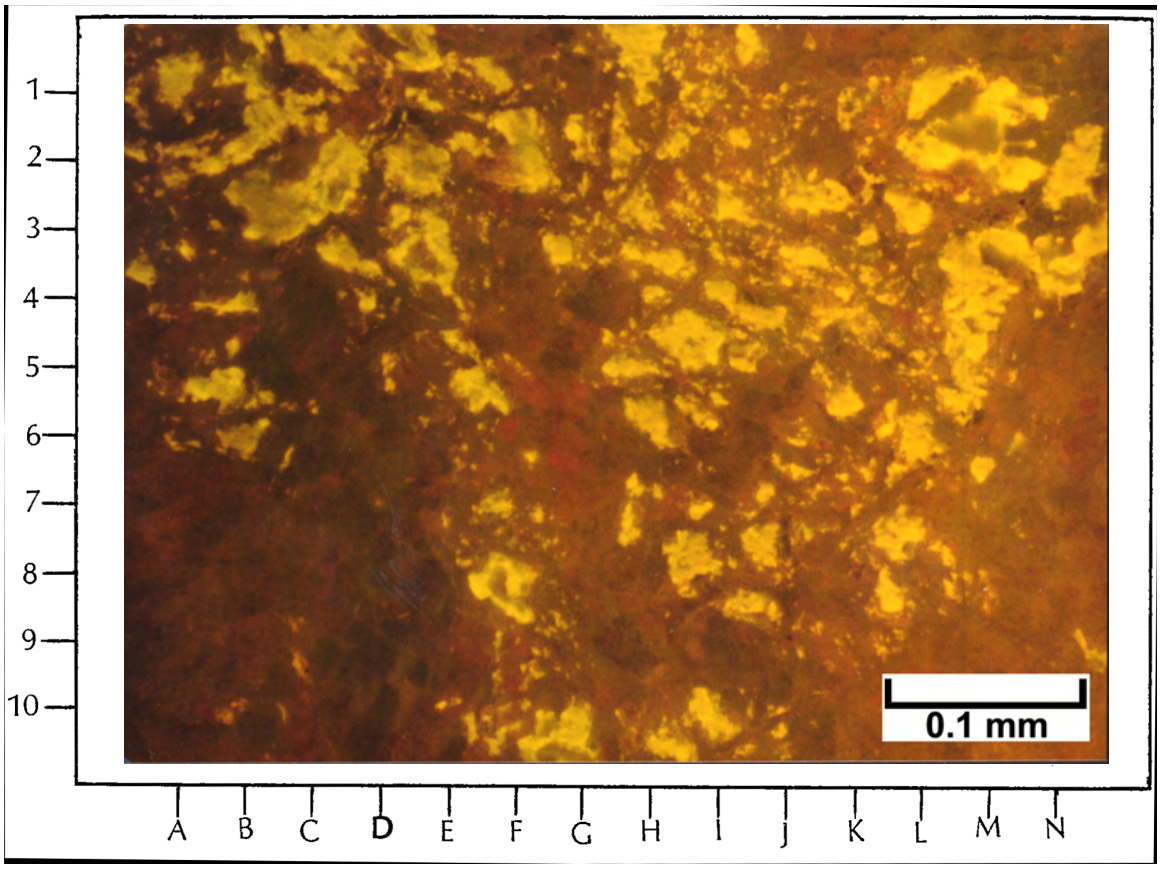
1
2
3
4
5
6
7
8
9
10
A B C D E F G H I J K L M N
0.1 mm

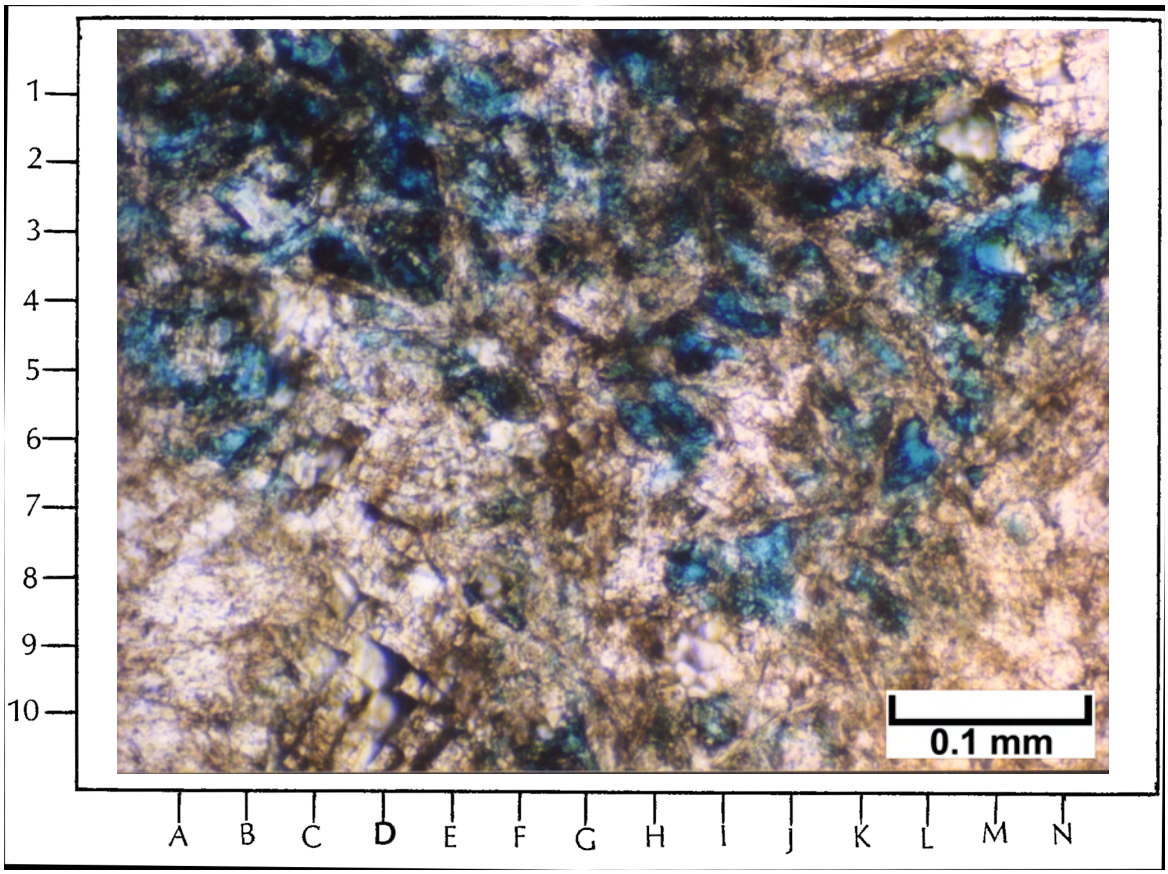
1
2
3
4
5
6
7
8
9
10
A B C D E F G H I J K L M N
0.1 mm

6327.9 feet

Top Photomicrograph

Epifluorescence shows an interconnected micro-box-work of interlocking dolomite crystal aggregates (in dark brown) that serves to isolate open pores (in bright yellow). Note the different apparent thicknesses of the elements of dolomite. This micro-box-work adds considerable heterogeneity to this oil-productive reservoir dolomite. Isolation of open pores is common within this micro-box-work dolomite.

Bottom Photomicrograph

The same view as above is shown here under Pl. Even though the blue areas show porosity here, the visible boundaries between interconnected dolomite crystals and pore outlines are less distinct than in the EF view above.

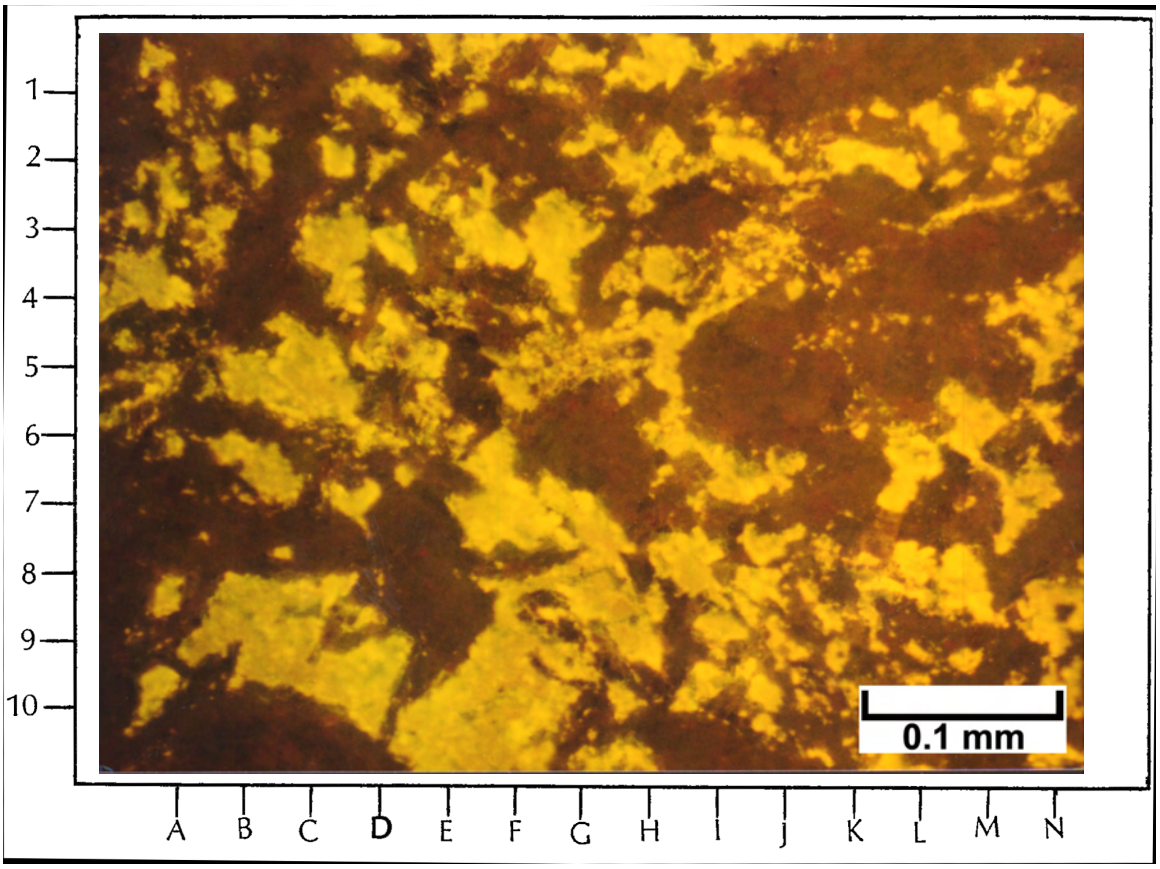
1
2
3
4
5
6
7
8
9
10
A B C D E F G H I J K L M N
0.1 mm

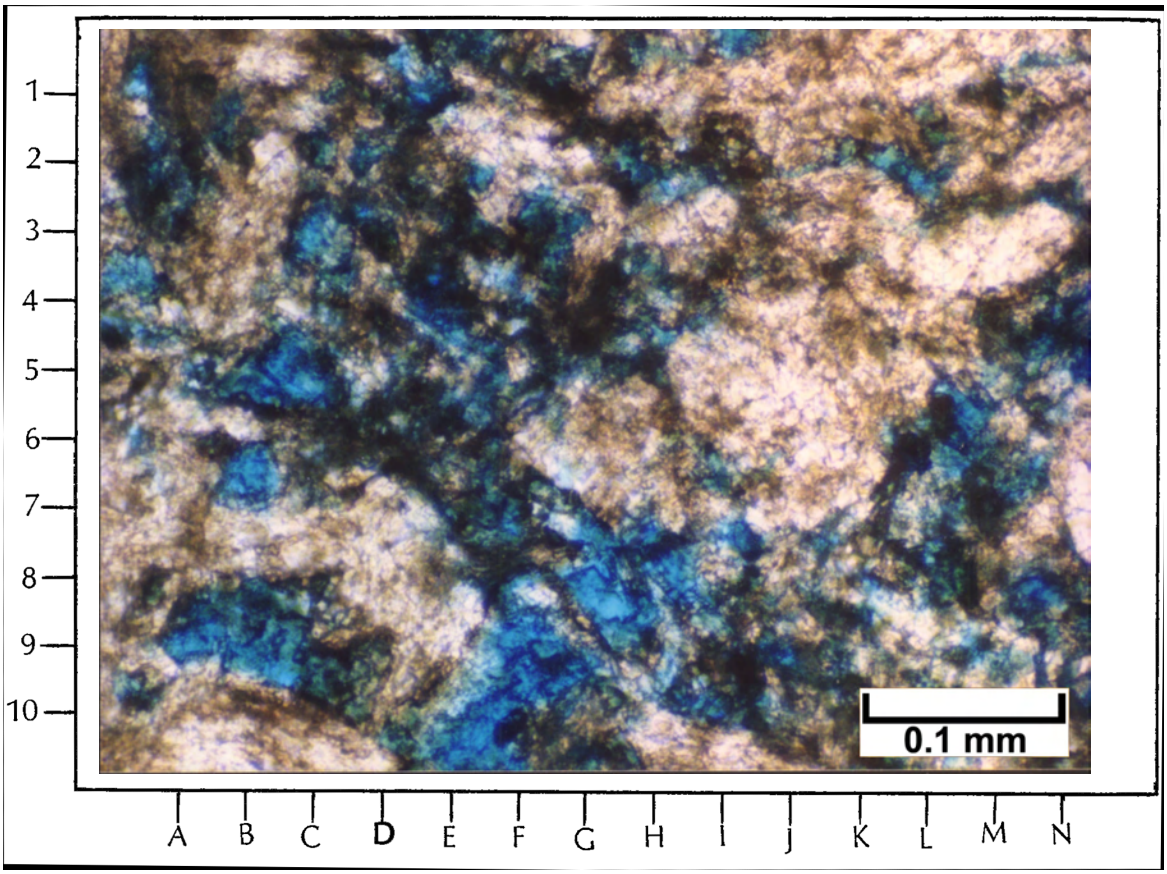
1
2
3
4
5
6
7
8
9
10
A B C D E F G H I J K L M N
0.1 mm

BUG NO. 16 WELL,
BUG FIELD

6299.3 feet

Top Photomicrograph

This portion of the sample displays very tight, moderately coarse, interlocking dolomite crystals with low visible porosity. Note the intense yellow to orangish yellow fluorescence that appears to surround the dolomite subcrystals and microfractures. This yellow fluorescence is probably due to the presence of "live" and/or relict hydrocarbons within the tight intercrystalline spaces. Some of the black and reddish colors in this view may be the result of bitumen lining some of the few isolated open pores.

Bottom Photomicrograph

The same photomicrograph as above is imaged here under Pl. The dark gray areas within the interlocking dolomite crystals are probably due to organic matter or oil staining. This staining makes it possible to see the subcrystal boundaries and probable microfractures within them. The small amount of open-pore space in this view is shown in blue, with black bitumen linings.

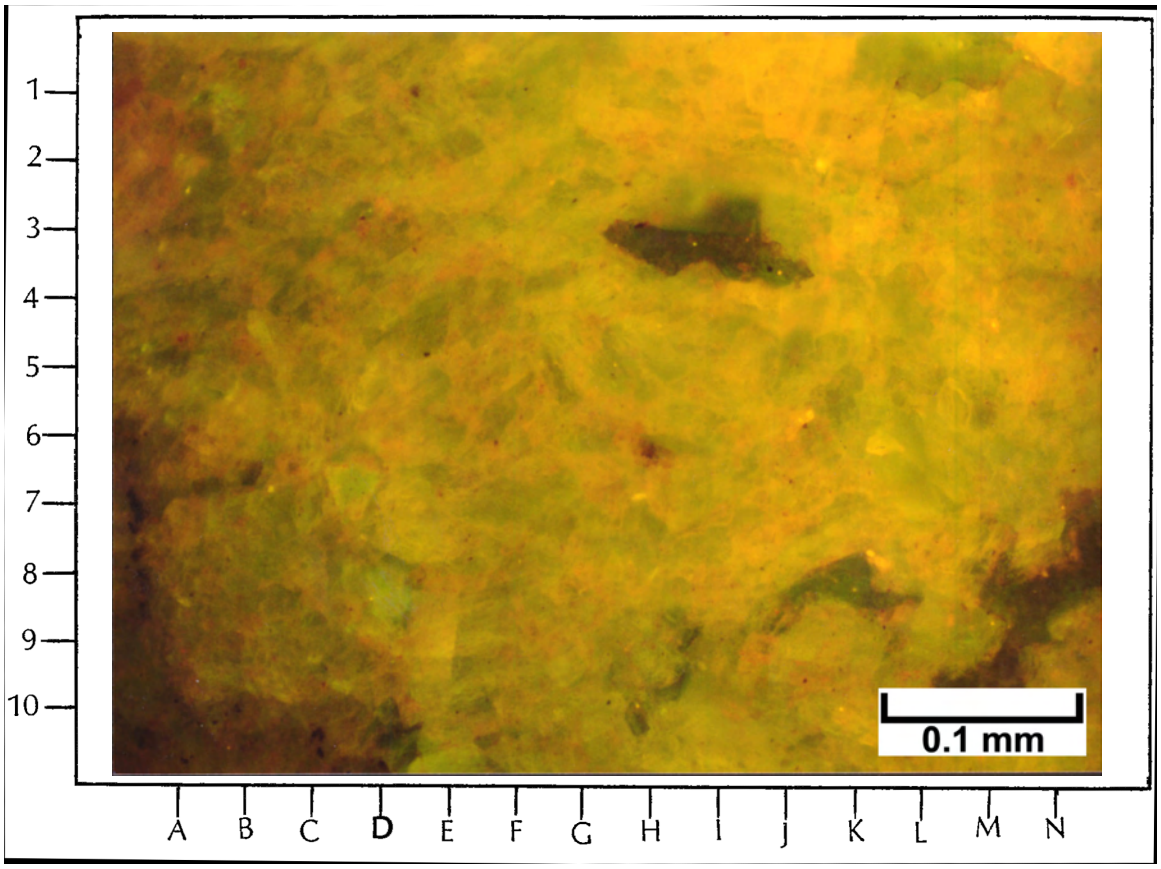
1
2
3
4
5
6
7
8
9
10
A B C D E F G H I J K L M N
0.1 mm

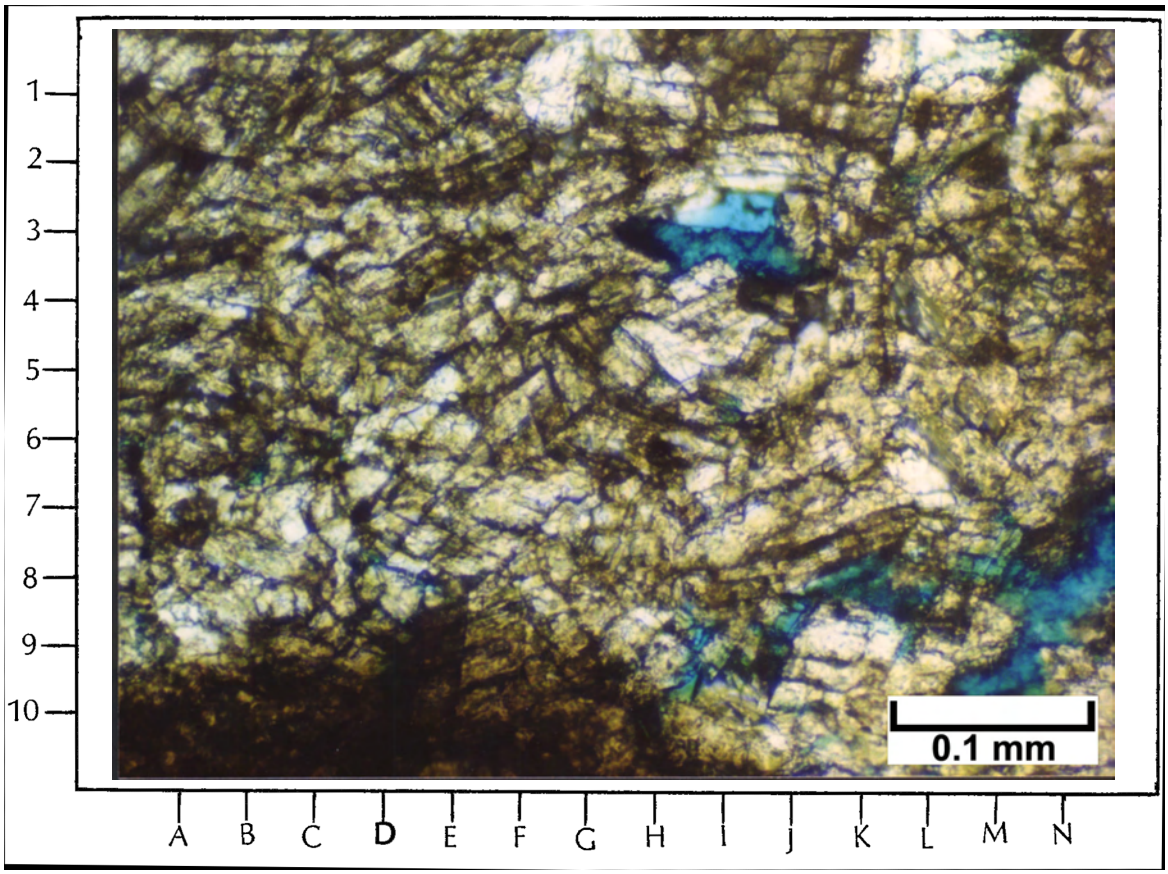
1
2
3
4
5
6
7
8
9
10
A B C D E F G H I J K L M N
0.1 mm

6299.3 feet

Top Photomicrograph

The EF view shows reddish fluorescence and non-fluorescence (black areas) where open pores and bitumen-lined pores have been impregnated with epoxy. The range of yellow fluorescence colors occurs within dolomites containing organic matter and live oils. Some of the dolomite crystals display very good crystal zonation as shown by the fluorescence patterns.

Bottom Photomicrograph

The Pl view shows epoxy-impregnated pores in blue, and dolomite crystals in the white to light brown areas. Note the outlines of crystals and pores are not as crisp as in the EF image above. In addition, the zonation of dolomite crystals and their organic content cannot be seen as well as in the EF view.

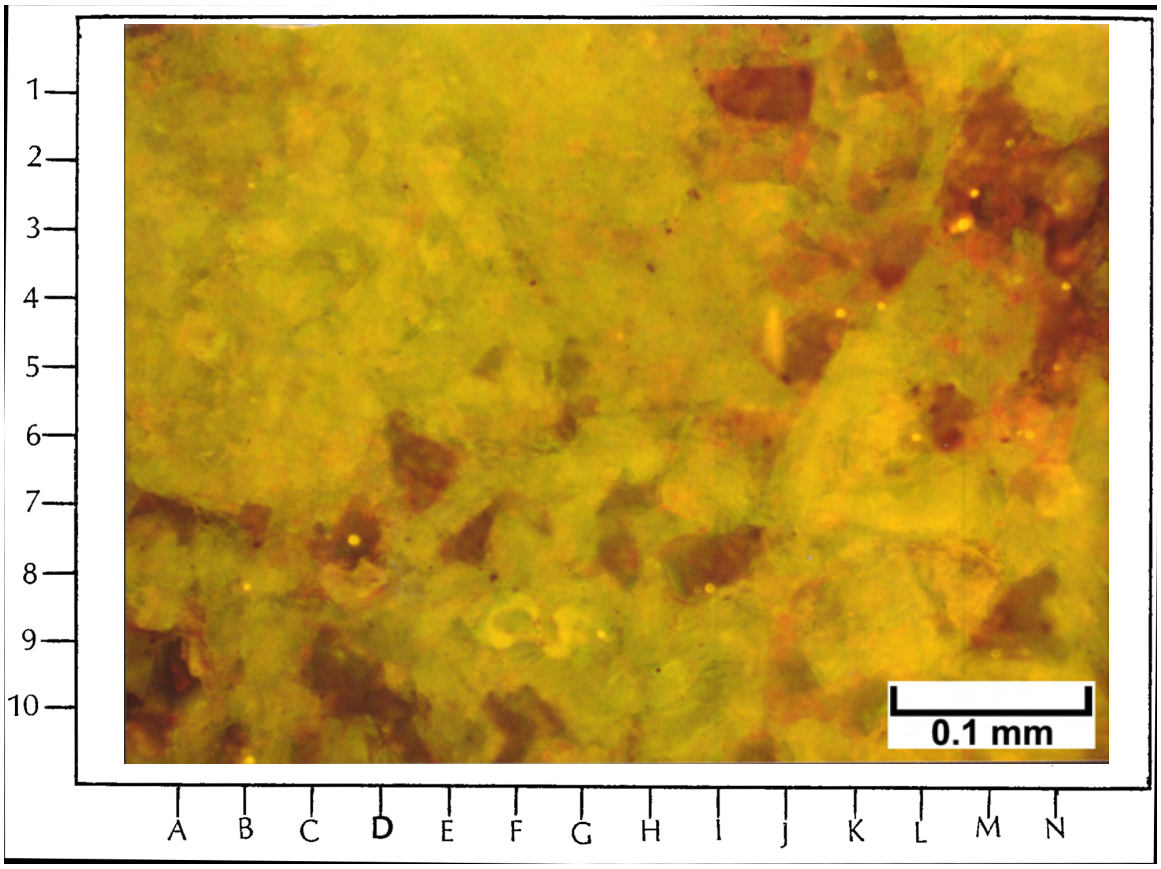
1
2
3
4
5
6
7
8
9
10
A B C D E F G H I J K L M N
0.1 mm

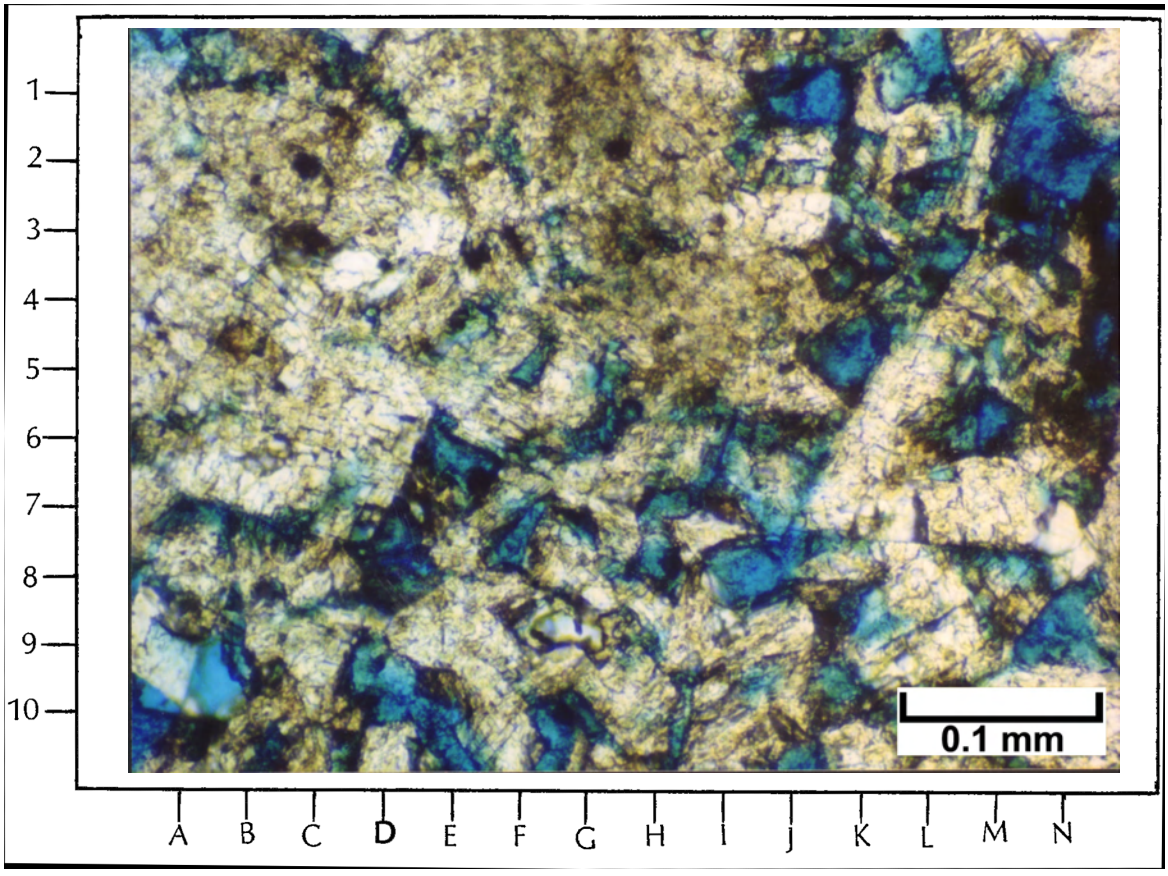
1
2
3
4
5
6
7
8
9
10
A B C D E F G H I J K L M N
0.1 mm

6299.3 feet

Top Photomicrograph

This EF view nicely shows another typical matrix view of fine- to medium-sized dolomite crystals that are very precisely imaged here. Many of these crystals appear to show good growth zones (the alternating green and yellow patterns within individual dolomite crystals). Possible "ghosts" or remnants of carbonate grain precursors to these dolomites can also be seen within some of the larger dolomite crystals. The reddish black areas are open pores.

Bottom Photomicrograph

This Pl view shows the same view as above at the same magnification. Note that this view does not provide much definition or show any internal zonation of the interlocking dolomite crystals within this sample. In addition, the outlines of pore boundaries are indistinct, despite the impregnation of these pores with blue-dyed epoxy.

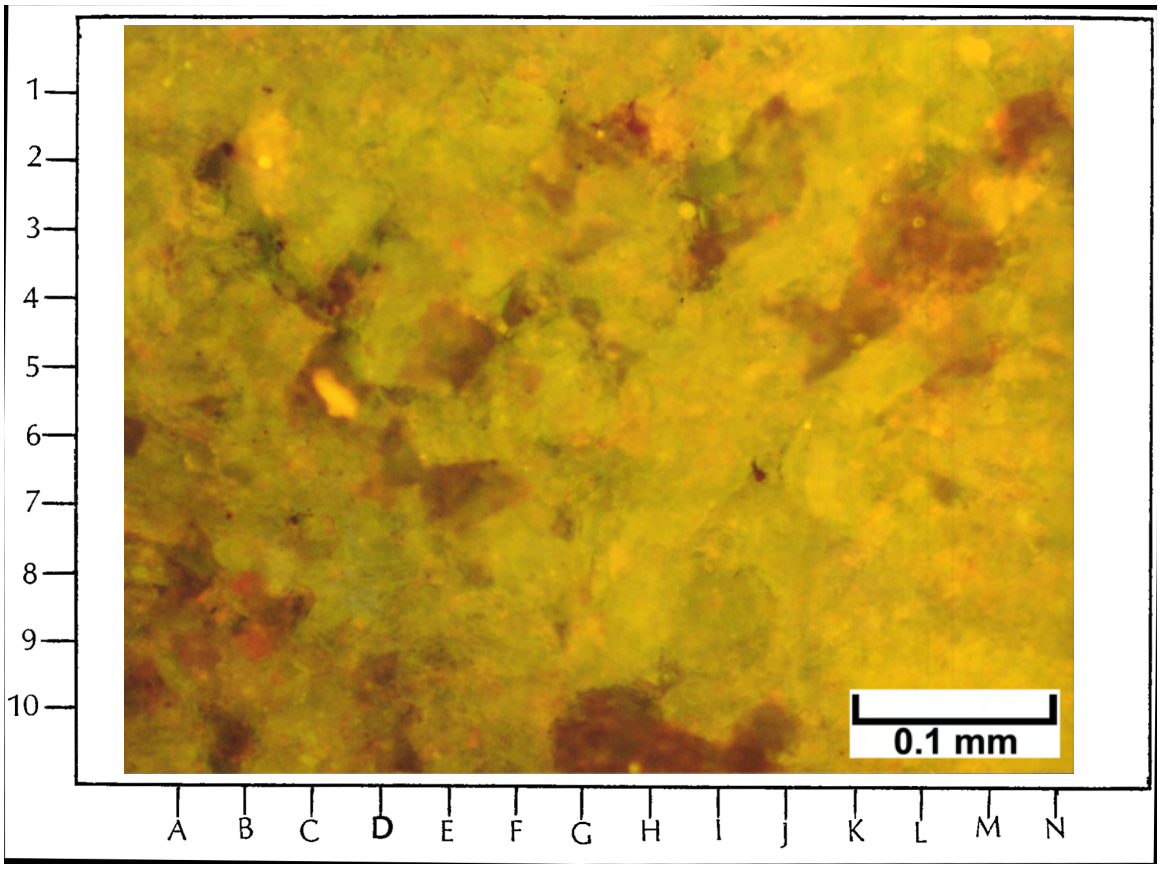
1
2
3
4
5
6
7
8
9
10
A B C D E F G H I J K L M N
0.1 mm

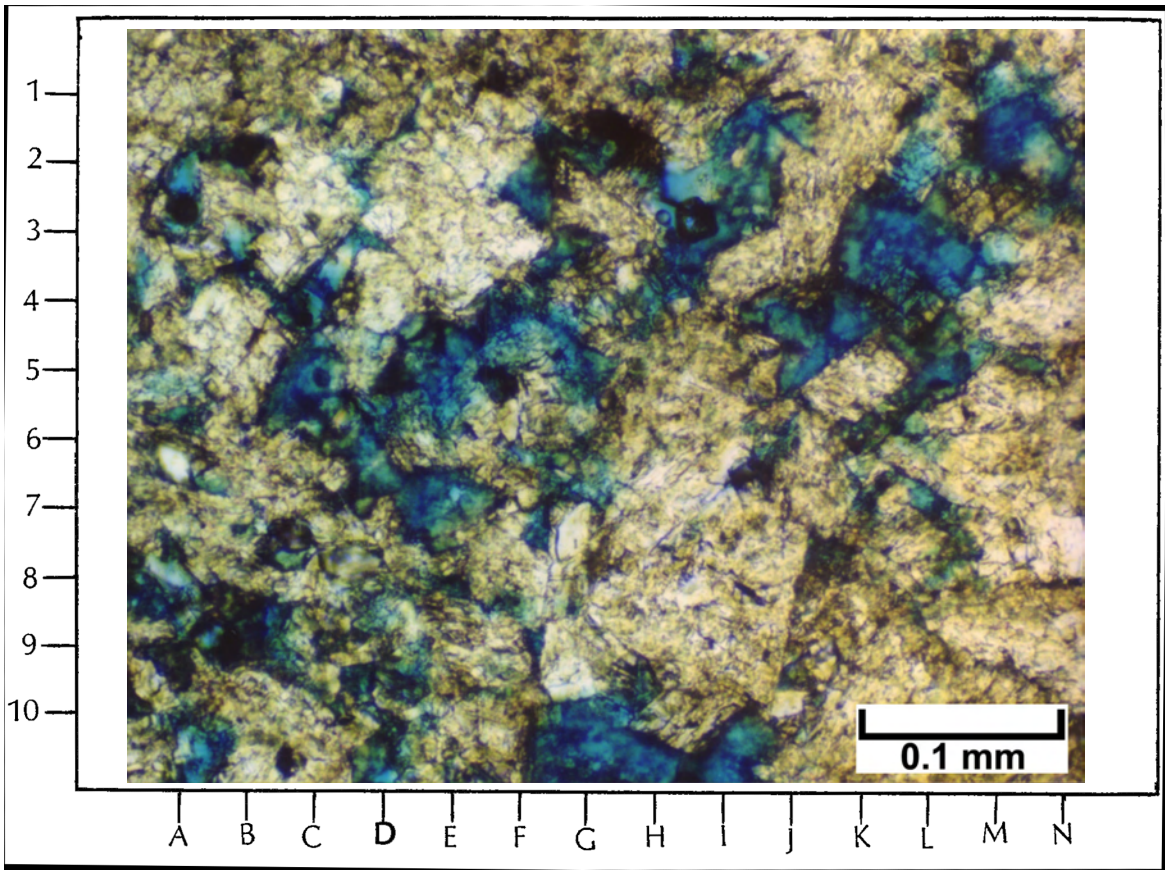
1
2
3
4
5
6
7
8
9
10
A B C D E F G H I J K L M N
0.1 mm

6300.5 feet

Top Photomicrograph

This EF view nicely displays rhombic and highly angular pores that fluoresce bright yellow. The rhombic dolomite crystals and crystal aggregates are dull gray and gray green in color. Note the sharp contacts between the dolomite crystals and the intercrystalline pores. This image is probably representative of a cross-sectional view of a typical sucrosic dolomite from the lower Desert Creek interval at Bug field.

Bottom Photomicrograph

This Pl view shows the same view as above at the same magnification. Although this view shows the sucrosic dolomite crystals well (in the white to light brown areas), the definition of pore/dolomite contacts is indistinct, in part because of bitumen linings. Pore outlines are much easier to see in the EF image.

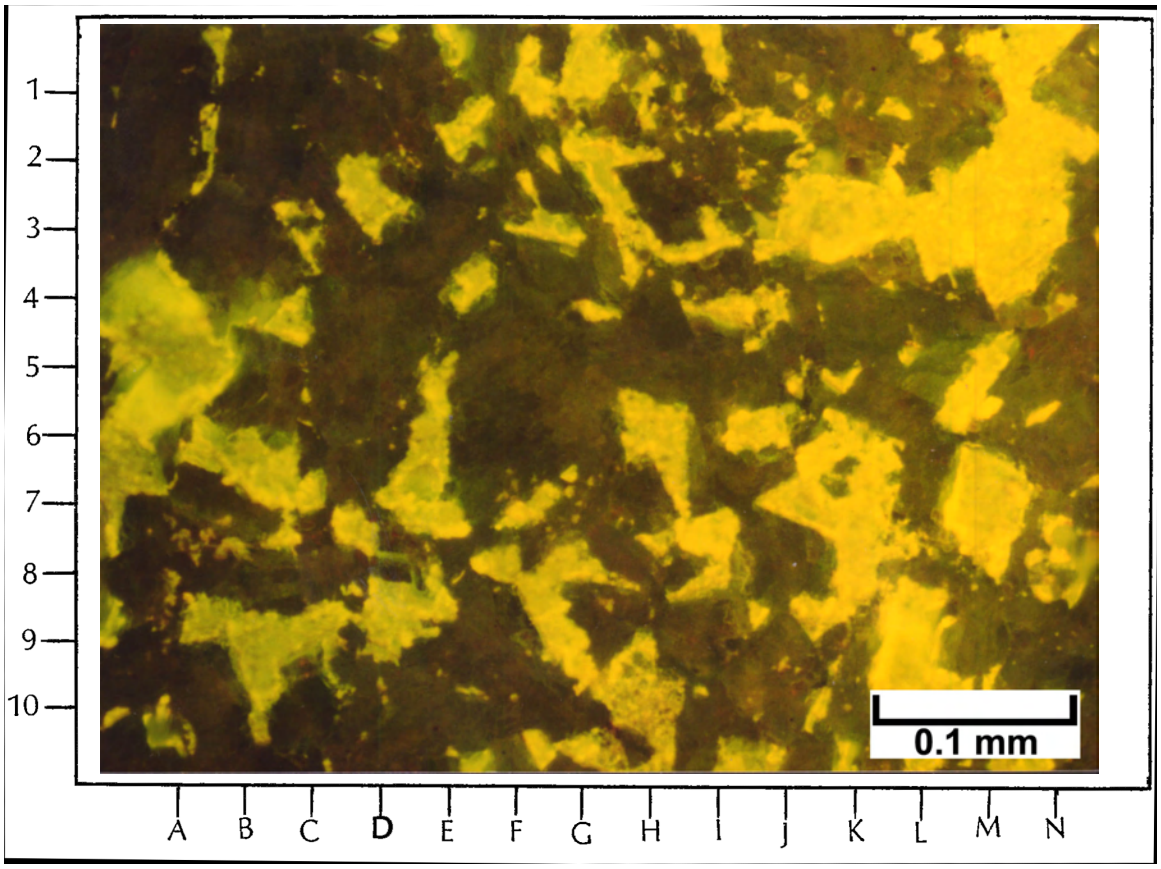
1
2
3
4
5
6
7
8
9
10
A B C D E F G H I J K L M N
0.1 mm

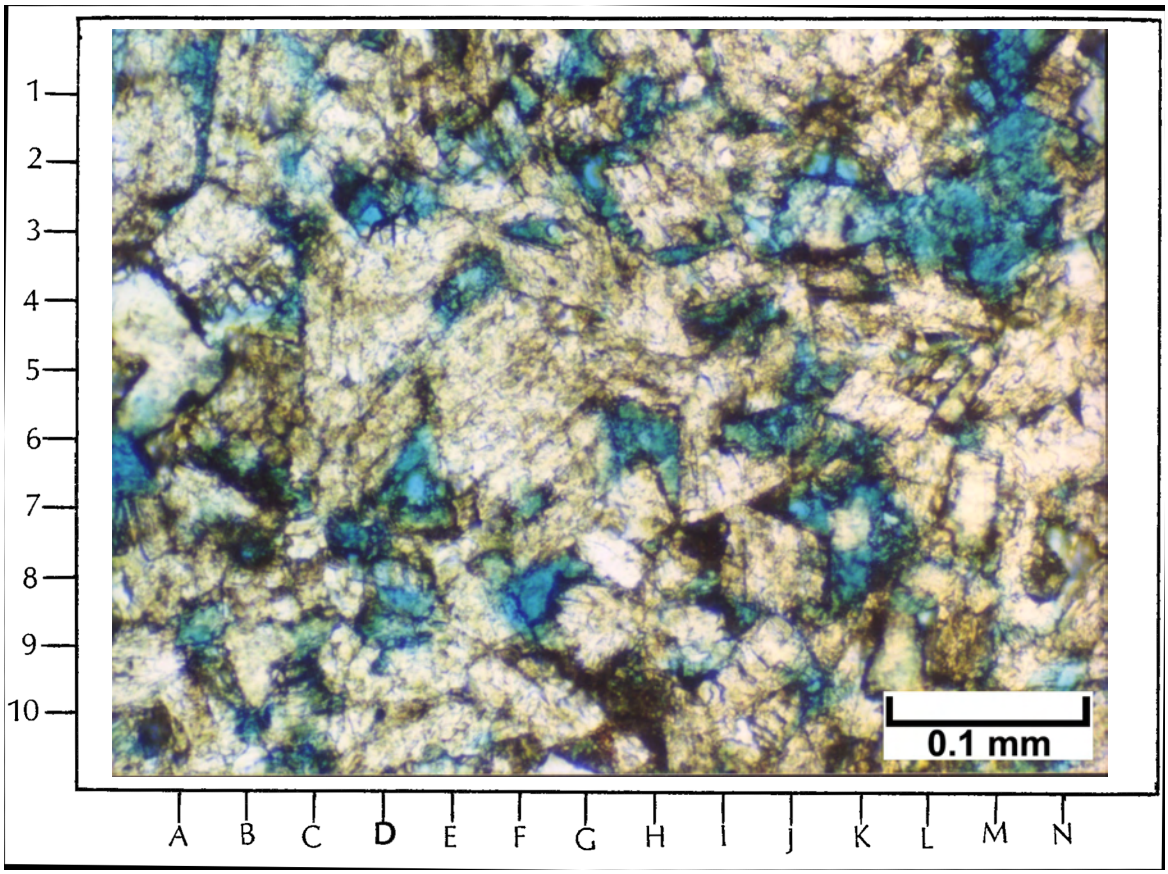
1
2
3
4
5
6
7
8
9
10
A B C D E F G H I J K L M N
0.1 mm

6300.5 feet

Top Photomicrograph

This EF photomicrograph shows an area with a complex network of micro-box-work structure throughout the entire field of view. The yellow areas show cross sections of open pores impregnated with epoxy and lined with some residual oil. The remaining dark areas in this field of view are non-porous dolomite crystal aggregates as well as some late anhydrite pore fillings. In this view, many of the pores appear to be isolated or "blind." Therefore, drainage of oil from this type of pore system may be inefficient.

Bottom Photomicrograph

This Pl view shows the same view as above at the same magnification. Note that it is difficult to resolve the contacts between pores and rock matrix. The brownish areas in this view are composed of dolomite while the white tabular crystals on the right portion of this photomicrograph are composed of anhydrite.

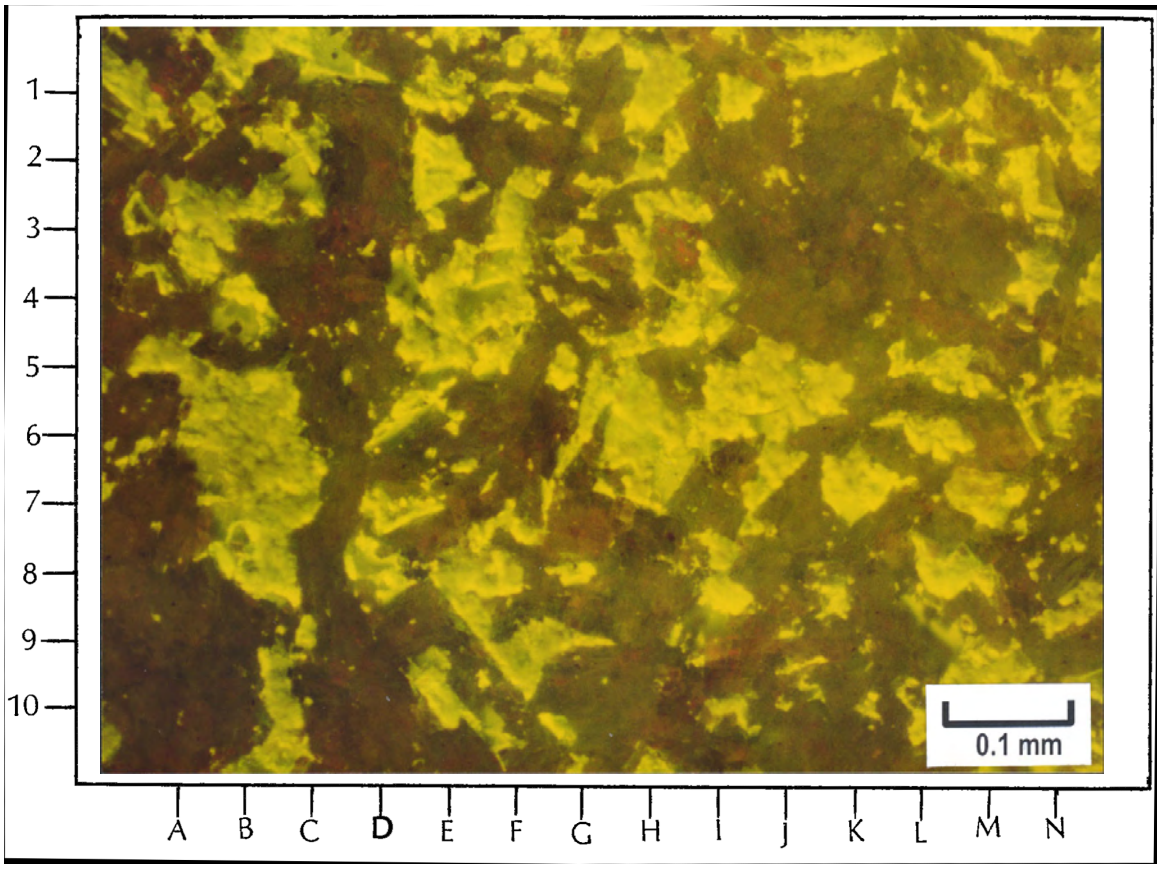
1
2
3
4
5
6
7
8
9
10
A B C D E F G H I J K L M N
0.1 mm

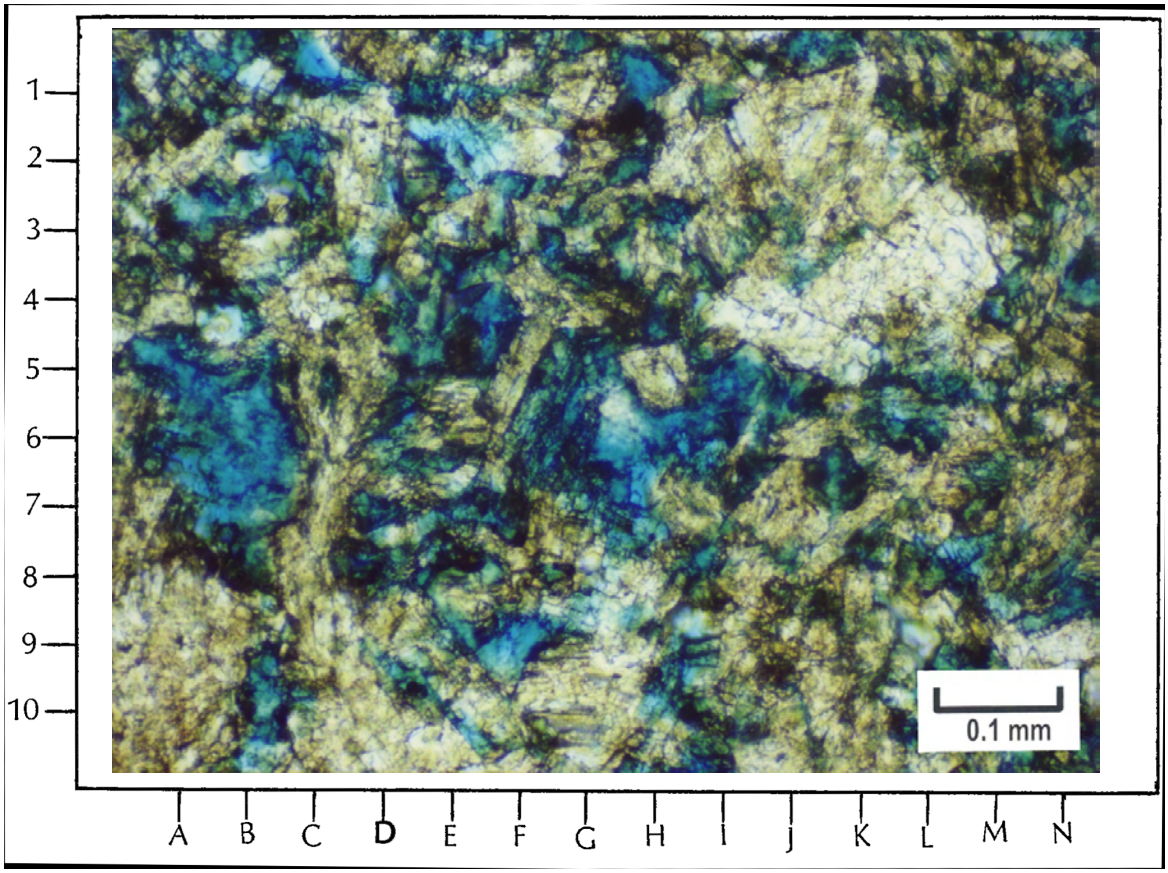
1
2
3
4
5
6
7
8
9
10
A B C D E F G H I J K L M N
0.1 mm

6300.5 feet

Top Photomicrograph

This EF overview of a complex network of micro-box-work structure displays cross sections of open pores impregnated with epoxy and lined with some residual oil. The remaining dark areas in this field of view are non-porous dolomite crystal aggregates as well as some late anhydrite pore fillings. As in the previous set of photomicrographs, many of the pores appear to be isolated or "blind." Thus, many of these pores may not be well connected for good oil drainage.

Bottom Photomicrograph

This Pl view shows the same view as above at the same magnification. The blue areas in this image are pores filled with blue-dyed epoxy. However, the nature of the contacts between the pores and the rock matrix are not easy to see. Dolomite appears as the light brown areas and later anhydrite pore fillings are white.

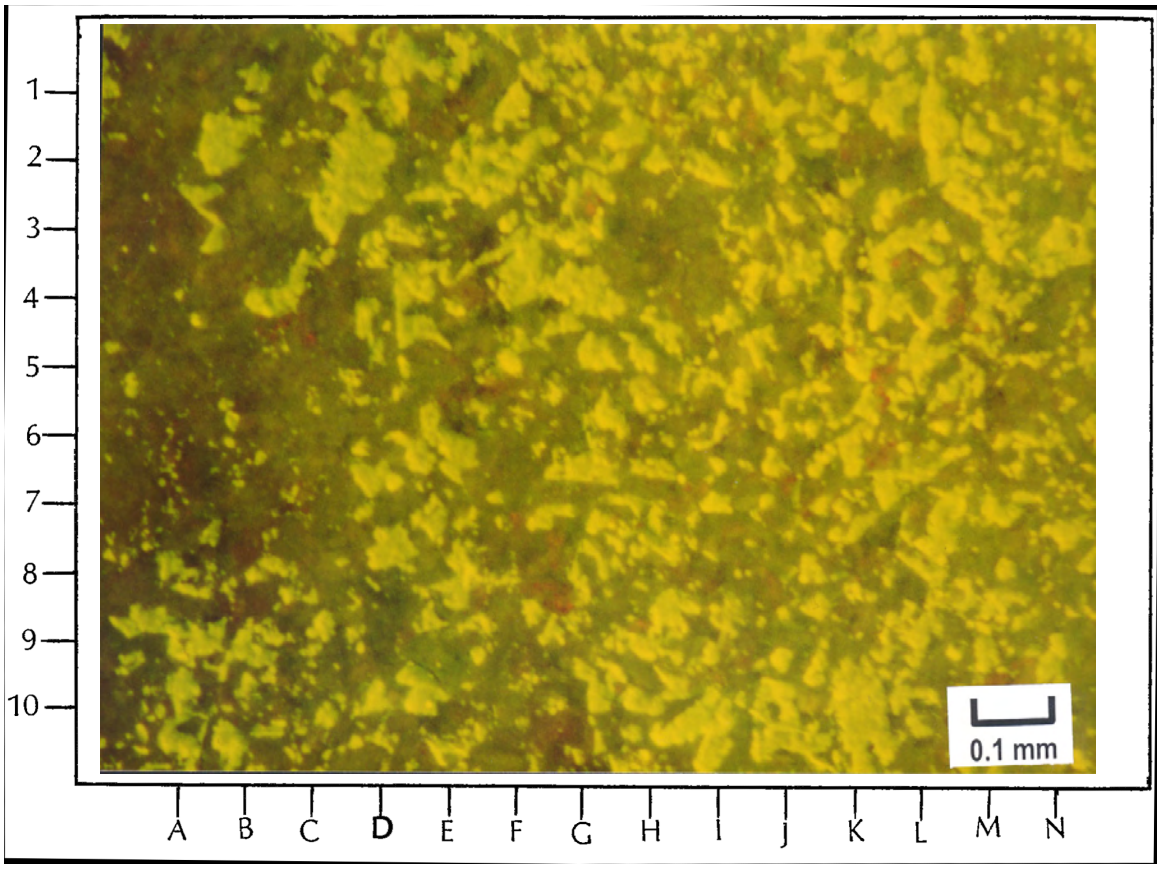
1
2
3
4
5
6
7
8
9
10
A B C D E F G H I J K L M N
0.1 mm

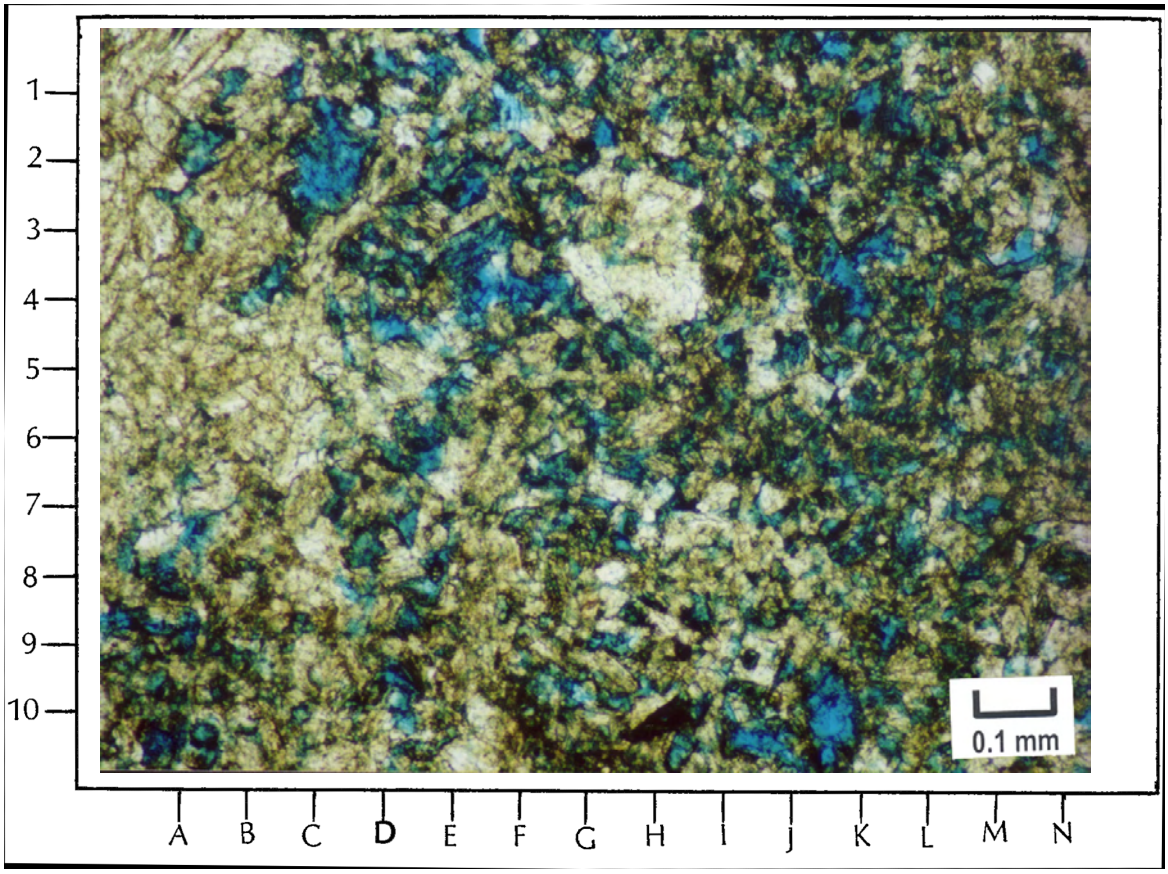
1
2
3
4
5
6
7
8
9
10
A B C D E F G H I J K L M N
0.1 mm

6300.5 feet

Top Photomicrograph

This highly magnified EF view makes it easy to see the highly corroded or scalloped margins of most dolomite crystals. In this view, the dolomite is dark-gray green in color while the pores are greenish yellow. Films of live oil appear as the intense or bright yellow rims along many of the dolomite crystal/pore contacts. The corroded dolomite rhomb contacts indicate that there has been some partial dissolution of dolomite rhombs.

Bottom Photomicrograph

This Pl view shows the same view as above at the same magnification. Note that the outlines of pores are indistinct, despite the impregnation of these pores with blue-dyed epoxy. In addition, it is not possible to see the corroded dolomite rhomb margins with Pl microscopy.

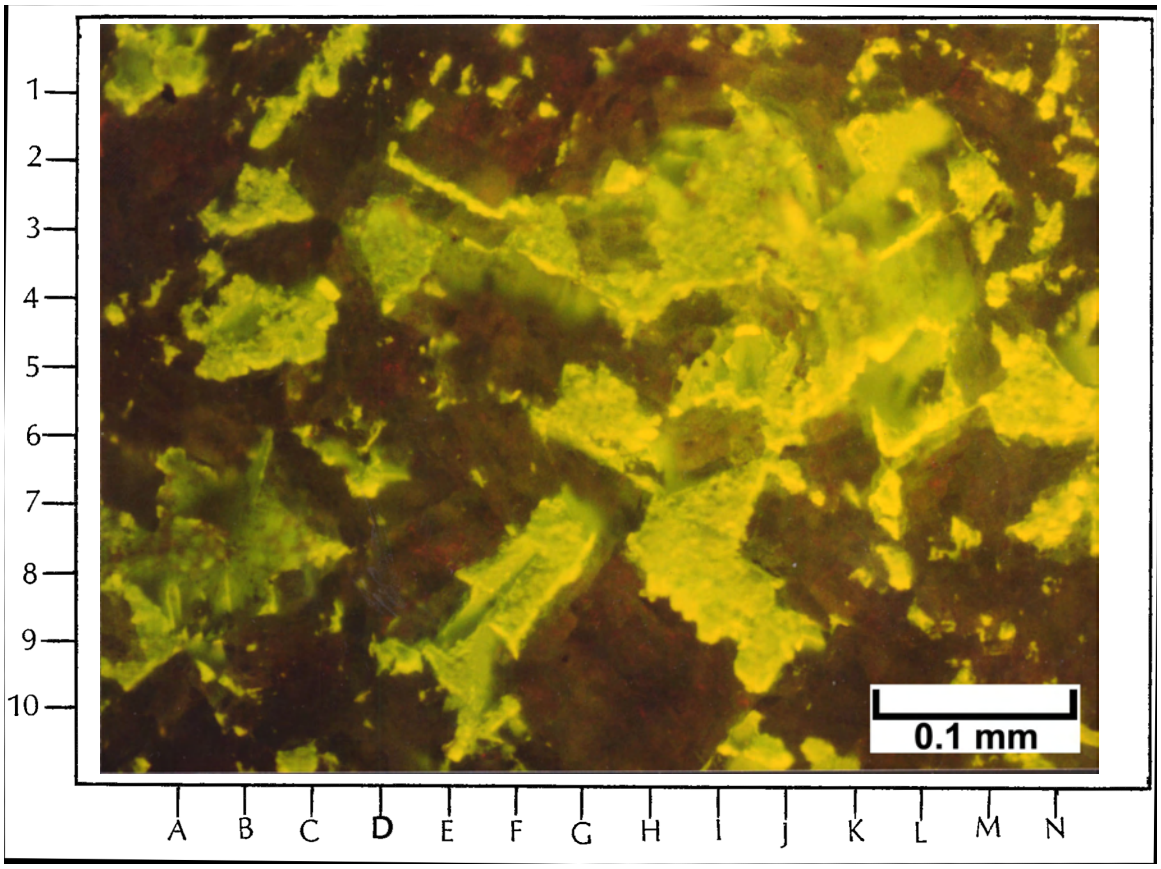
1
2
3
4
5
6
7
8
9
10
A B C D E F G H I J K L M N
0.1 mm

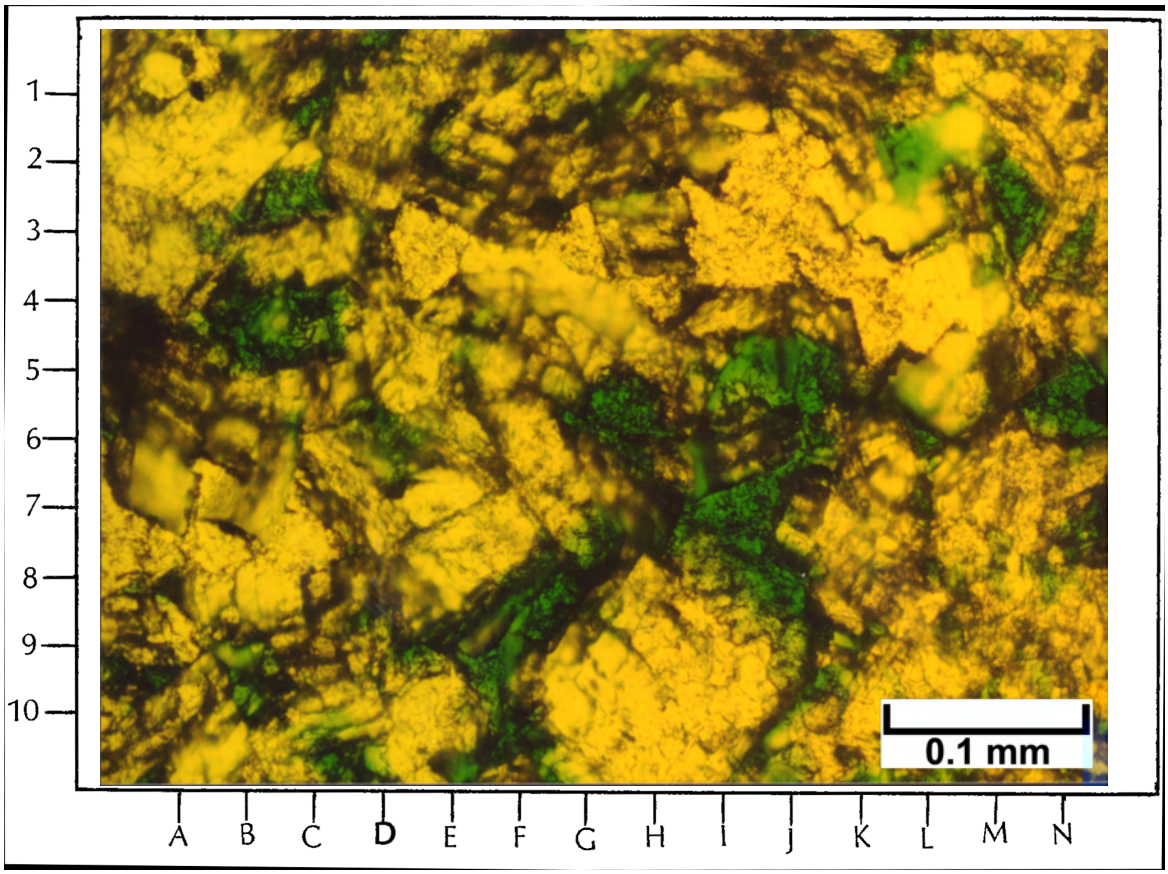
1
2
3
4
5
6
7
8
9
10
A B C D E F G H I J K L M N
0.1 mm